On the preparation and characterisation of MCM-41 supported heterogeneous nickel and molybdenum catalysts

Over de bereiding en karakterisering van MCM-41 gedragen heterogene nikkel- en molybdeenkatalysatoren

(met een samenvatting in het Nederlands)

Proefschrift

ter verkrijging van de graad van doctor aan de Universiteit Utrecht
op gezag van de Rector Magnificus, Prof. Dr. W.H. Gispen,
ingevolge het besluit van het College voor Promoties
in het openbaar te verdedigen op dinsdag 27 mei 2003 des ochtends te 10u30

door

Dennis Lensveld

geboren op 4 mei 1974 te Vlaardingen

Promotores: Prof. Dr. Ir. Krijn de Jong

Prof. Dr. Ir. John Geus

Co-promotor: Dr. Jos van Dillen

Allen verbonden aan de Sectie Anorganische Chemie en Katalyse, onderdeel uitmakende van de Faculteit Scheikunde, Universiteit Utrecht en tevens onderdeel van het Debye Instituut.

Printed by Ponsen & Looijen BV, Wageningen, The Netherlands

ISBN: 90-393-3356-4

Note on referencing: this thesis will also be available on internet, *viz. via* the library page of the University of Utrecht. So, if you refer to this thesis, please (also) provide the appropriate URL as a reference, *i.e.* http://www.library.uu.nl/digiarchief/dip/diss/2003-0325-14324/inhoud.htm

OGENSCHIJNLIJK

Ogenschijnlijk heeft het ene
niets te maken met het ander.

Ogenschijnlijk schuilt er
voordeel in een vaste baan.

Ogenschijnlijk zal er nog
een heleboel verand'ren.

Ogenschijnlijk staan de sterren
hier niet zo ver vandaan.

[uit: *Dag en nacht geopend*, Jules Deelder]

Contents

1

General introduction

The workhorses in various chemical industries are catalysts. Because of their favourable properties heterogeneous catalysts are most frequently used. Heterogeneous catalysts are inorganic solid materials, which contain so-called "active sites" at their surfaces, which are able to affect the kinetics of chemical reactions. Heterogeneous catalysts can be single-phase materials, such as Raney nickel or zeolites, but more often they comprise an inert support material onto which the active phase is dispersed. The active phase generally contains a (transition) metal, which can be present either in the metallic state or in an ionic lattice, for example as an oxide or a sulphide. Since catalysis only takes place at the surface of the active component an important aim of heterogeneous catalysis is to prepare catalysts containing exclusively very small particles / crystallites / clusters of active phase, in order to obtain a high ratio of surface to bulk atoms. Unfortunately, small particles are thermodynamically not stable, due to their relatively large surface energy. As a result these particles will show a tendency to sinter into larger aggregates, especially at elevated temperatures, for example *via* Ostwald ripening or other clustering processes. The role of a support material is to

prevent the occurrence of sintering processes by providing a large surface area onto which the particles of active phase can become anchored. Because of the anchoring process the small particles of active phase become stabilised and will resist sintering much more strongly. Over the years various methods have been developed to anchor catalytically active phases (or precursors thereof) onto a wide variety of support materials. A number of these methods will be addressed in **chapter 2**.

There is a wide variety of support materials onto which active phases can be stabilised. The most common support materials are simple metal oxides, such as aluminas, silicas and titanias, although zirconias and cerias also find application. In addition, carbon support materials are also frequently used. Unfortunately, carbon supports are usually microporous, which is generally disadvantageous for catalytic applications. An exception to this is the evolution of exclusively mesoporous carbon nanofibers, *e.g.* [1]. Recently important developments have been made in the application of active phases onto these carbon nanofibers [2]. Despite these breakthroughs metal oxide supports will remain the most frequently applied support materials. The advantages oxidic supports offer are a.o. easy fine-tuning of a number of physical properties, such as the size of the primary support particles, specific surface area, pore volume and pore size (distribution), as well as chemical properties, such as composition and surface reactivity. Moreover, shaping of the primary support particles into robust bodies of support material is a well-established craft, yielding catalysts suitable for loading into a variety of different reactor designs.

The choice of a suitable support material is often dictated by the process conditions at which a catalyst has to operate. Nevertheless one of the key features of a support material is to exhibit a large specific surface area onto which the catalytically active phase is present with a very high dispersion. As a result, reports in 1992 about the discovery of a new class of silica-based mesoporous materials by researchers of Mobil Company [3, 4] have boosted research into the application of active phases inside the mesopores of these materials. These materials are best known by their abbreviations, *viz.* MCM-41 and MCM-48. MCM denotes Mobil Composition of Matter, whereas the numbers 41 and 48 are merely batch numbers. Research following the development of these MCM-type materials has resulted in the evolution of a large number of other mesoporous materials, exhibiting different pore sizes and geometries as well as specific surface areas, *e.g.* SBA-15 [5], FSM [6, 7], HMS [8], KIT-1 [9, 10] and others. Nevertheless, the development

of dedicated methods for the application of active phases inside the mesopores of these materials has to quite some extent remained illusive.

The best-known mesoporous support material is MCM-41 and the properties of this material will be described in detail in **chapter 2**. Here it suffices to mention that this material displays a honeycomb-like porous structure with pore walls of approximately 1 nm thickness. Due to the very thin pore walls this material displays a rather large instability, a.o. towards steam and basic solutions, but more importantly towards a number of aqueous catalyst precursor solutions, which hampers its application as a support material. Therefore other mesoporous support materials, displaying larger pores and pore walls, such as SBA-15 [5], will probably find more widespread application as a result of a notably higher stability. Nevertheless, from a fundamental point of view MCM-41 is extremely well-suited to serve as a model support material for research aimed at the preparation of heterogeneous catalysts supported by mesoporous materials, because its limited stability necessitates the development of *highly dedicated* alternative catalyst synthesis procedures, which will most probably be suited for *all* (or most of the) mesoporous support materials known to date.

Therefore, the main objective of this thesis is to develop new, *non-destructive* methods for the application of (precursors of) active phases onto mesoporous support materials. To this end all-silica MCM-41 was chosen as a support material and nickel and molybdenum precursors have been applied onto this support, because these elements show attractive catalytic properties (*vide infra*). The studies on catalyst preparation with these elements will be described in **chapters 3 - 5**. Furthermore, a second question that arises is whether the obtained materials are suitable as heterogeneous catalysts, because the very long mesopores (extending over several hundreds of nanometers, see chapter 2) might give rise to the occurrence of internal diffusion limitations of reactants and / or products during catalytic conversions. To study the possible occurrence of this highly unfavourable phenomenon the prepared catalysts have been subjected to a catalytic characterisation in **chapter 6**.

In the first part of **chapter 2** the preparation, characterisation and properties of MCM-41 will be described in detail. Subsequently some selected catalyst preparation procedures and their applicability towards MCM-41 will be addressed. In the next chapters the application of two selected elements, *viz.* nickel and molybdenum, will be dealt with. These metals have been chosen because increasingly severe demands concerning the amount of sulphur in

transportation fuels call for the development of more active hydro-desulphurisation catalysts. Over the years it has been established that catalysts containing molybdenum (or tungsten) and nickel (or cobalt) show the highest activity in the desulphurisation of diesel. The active phase of these types of catalysts is supposed to be composed of small MoS_2 slabs, dispersed over the surface of the support material, containing isolated nickel ions at the edges. Therefore, our aim has been to study methods for the application of these metals inside the mesopores of MCM-41 in order to arrive (eventually) at a new class of highly active hydrotreating catalysts. Moreover, it should be noted that nickel and molybdenum are interesting elements for a large number of other (catalytic) applications as well, including hydrogenations and (selective) oxidations.

For the application of nickel inside the mesopores of MCM-41 use has been made of the favourable properties of an aqueous solution of a chelated nickel precursor complex. In **chapter 3** it will be shown that such a precursor yields Ni(O)/MCM-41 catalysts exhibiting a high dispersion of exclusively small nanoparticles situated inside the mesopores of the support. In **chapters 4 and 5** two new methods for the preparation of MoO_3/MCM-41 catalysts will be presented. With both methods catalysts with high MoO_3 loadings (up to 25 wt%) and dispersions are obtained, whilst the unique textural and structural characteristics of the support material are fully retained. **Chapter 4** discloses the use of a reduced Mo^{3+} precursor, whereas a simpler method, involving a solution of a common molybdenum precursor in hydrochloric acid, is described in **chapter 5**. Finally, thus prepared molybdena catalysts have been studied in the oxidative dehydrogenation of ethane with molecular oxygen. The results of these studies have been compiled in **chapter 6**. The catalytic measurements corroborate the high dispersions of MoO_3 catalysts supported by MCM-41: conversion levels are notably higher than for reference catalysts (MoO_3/Aerosil-200 and bulk MoO_3). In addition transport limitations are shown not to occur.

Literature

[1] K.P. de Jong and J.W. Geus, *Catal. Rev. - Sci. Eng.*, 42, 2000, 482

[2] M.L. Toebes, F.F. Prinsloo, J.H. Bitter, A.J. van Dillen and K.P. de Jong, *Stud. Surf. Sci. Catal.*, 143, 2002, 201

[3] C.T. Kresge, M.E. Leonowicz, W.J. Roth, J.C. Vartuli and J.S. Beck, *Nature*, 359, 1992, 710

[4] J.S. Beck, J.C. Vartuli, W.J. Roth, M.E. Leonowicz, C.T. Kresge, K.D. Schmitt, C.T-W. Chu, D.H. Olson, E.W. Sheppard, S.B. McCullen, J.B. Higgins and J.L. Schlenker, *J. Am. Chem. Soc.*, 114, 1992, 10834

[5] D. Zhao, J. Feng, Q. Huo, N. Melosh, G.H. Fredrickson, B.F. Chmelka and G.D. Stucky, *Science*, 279, 1998, 548

[6] T. Yanagisawa, T. Shimizu, K. Kuroda and C. Kato, *Bull. Chem. Soc. Jpn.*, 63, 1990, 988

[7] S. Inagaki, Y. Fukushima and K. Kuroda, *J.Chem. Soc., Chem. Commun.*, 1993, 680

[8] P.T. Tanev and T.J. Pinnavaia, *Science*, 267, 1995, 865

[9] C.H. Ko and R. Ryoo, *J. Chem. Soc., Chem. Commun.*, 1996, 2467

[10] R . Ryoo, J.M. Kim, C.H. Ko and C.H. Shin, *J.Phys. Chem.*, 100, 1996, 17718

2

MCM-41 and catalyst preparation

MCM-41

The most striking fact about the material MCM-41 is that, although composed of amorphous silica, it displays an ordered structure with uniform mesopores arranged into a hexagonal, honeycomb-like lattice. A nice example of this structure can be seen in figure 1. In this figure one looks directly inside the uniform mesopores, which are separated from each other by thin walls of amorphous silica, approximately 1 - 1.5 nm thick. The mesopores are not necessarily running in a straight way through the silica matrix, but they can be slightly curved, thereby retaining the hexagonal ordering, as can be seen in figure 2. From the micrographs it is apparent that MCM-41 has a very large void fraction, due to the presence of the mesopores, and concomitantly a rather low density. As a result MCM-41 displays a very large specific surface area of approximately 1,000 $m^2 g^{-1}$. This property makes MCM-41 very interesting to be used as a support material for heterogeneous catalysts. Moreover, because MCM-41 exclusively contains mesopores it can both provide access to large molecules and alleviate diffusion problems, which are frequently encountered in microporous materials such as zeolites. It

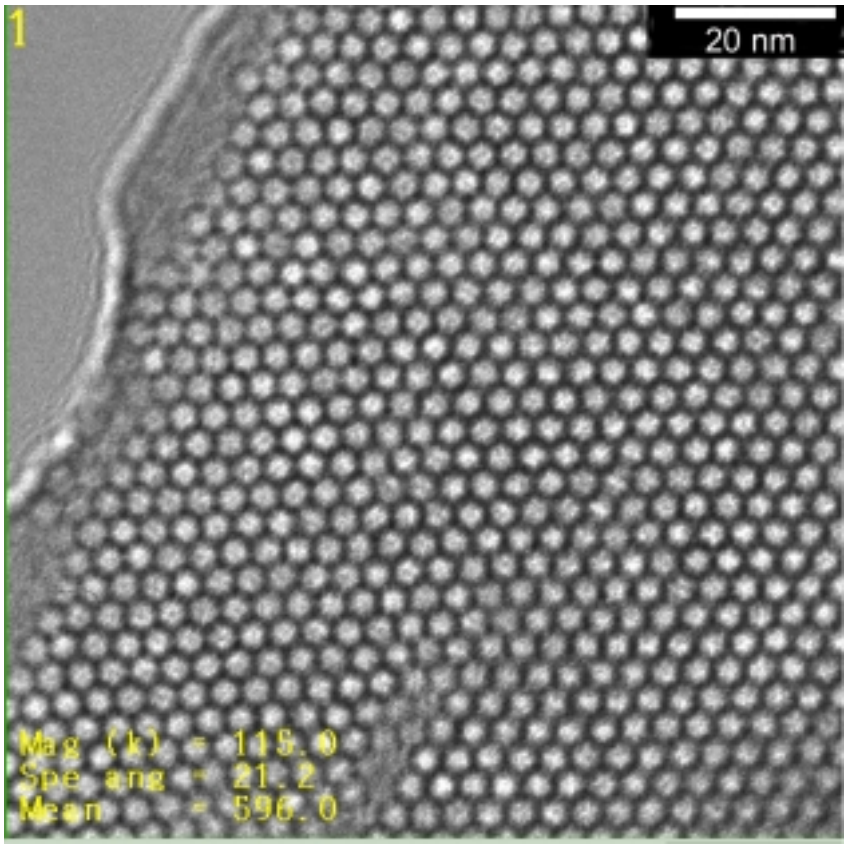

Figure 1: TEM micrograph of MCM-41, allowing the viewer to look directly inside the mesopores. The mesopores are arranged in a honeycomb-like structure, separated by thin, amorphous silica pore walls (black). The pore size of this MCM-41 material is approximately 3 nm in diameter.

should be noted, however, that the one-dimensional nature as well as the relatively large length of the mesopores (usually extending over several hundreds of nanometers) could also give rise to transportation limitations.

Despite the advantages mentioned above there is one eminent drawback associated with MCM-type materials, *viz.* the rather limited stability, which is a result of the very thin, amorphous pore walls. Because of the very large mesopore surface area the pore walls are extremely reactive towards a number of agents, resulting in the collapse of the thin walls upon exposure to these agents. From a viewpoint of application the instability of silica support materials towards steam (either co-fed as a diluent or produced during catalysis), resulting in the chemical evaporation of silica, makes silica-supported catalysts inappropriate for a rather large range of processes. Furthermore, there is a notable instability of MCM-41 towards mineralising agents, *i.e.* hydroxide and fluoride ions, because these agents dissolve silica. As a result the stability of MCM-41 in aqueous solutions is limited to pH

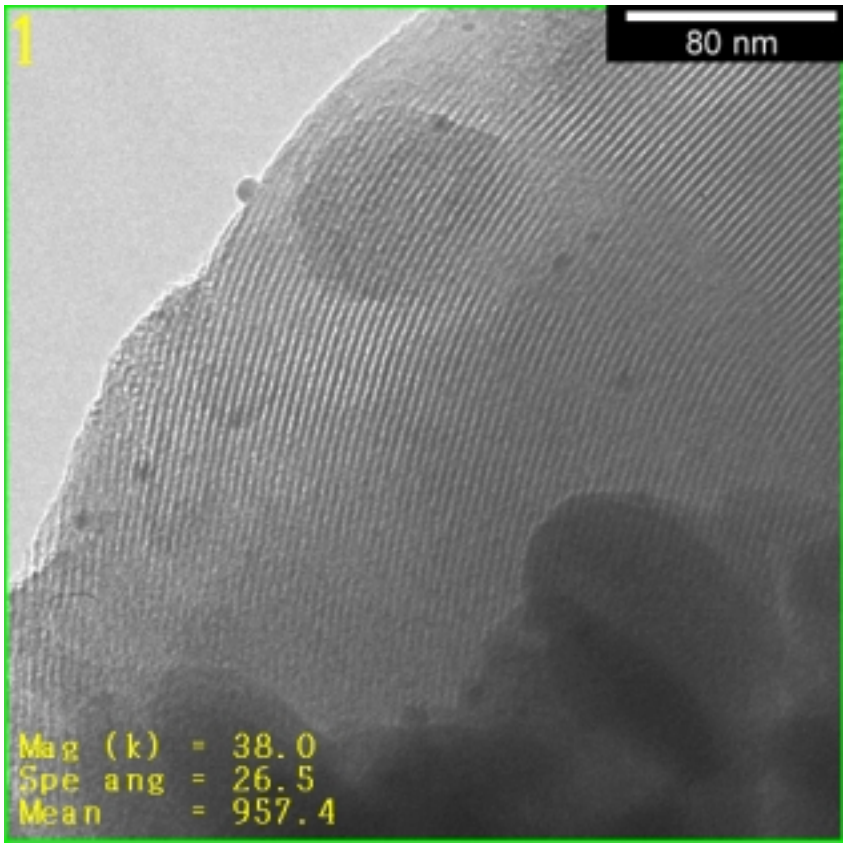

Figure 2: TEM micrograph of MCM-41, showing the slightly curved uniform mesopores running through the silica matrix.

values ≤ 7. Moreover, the chemical affinity of the pore surface towards precursors of catalytically active phases sometimes also results in the collapse of the hexagonal framework structure. An example of this behaviour, which will be dealt with in chapters 4 and 5, is the reaction with aqueous impregnation solutions containing common molybdenum precursors, *viz.* (poly)molybdate anions. Opposed to this behaviour towards molybdenum precursors, the interaction of the MCM-41 pore surface with certain common nickel precursors is relatively weak, resulting in low dispersions of the active phase. Chapter 3 deals with this problem and provides a solution to it.

Synthesis

MCM-41 can be synthesised following a wide variety of preparation procedures. However, there is one thing all these procedures have in common next to the obvious presence of a source of silica, *viz.* a templating agent. A *template* is a structure-directing agent, which is usually a relatively simple molecule or ion, around which a framework is built up. The most

common templates are quaternary ammonium ions with short alkyl chains, which are used for the syntheses of a large number of zeolites. For the synthesis of MCM-41 similar quaternary ammonium ions are frequently used, albeit with one important modification: at least one of the short alkyl chains is replaced by a long alkyl chain, generally a hexadecyl group. This slight modification has an enormous impact on the behaviour of the template in aqueous solutions, however. Due to the large hydrophobic alkyl chain the template ions will aggregate together in order to minimise energetically unfavourable interactions of the apolar alkyl chains with the very polar water solvent molecules. Although unfavourable from an entropic point of view, this is exactly the same behaviour as displayed by soaps upon dissolution in water. The resulting aggregates of ions are denoted *micelles*. It follows that these micelles have a hydrophobic core, containing the large alkyl chains, and a hydrophilic surface, due to the ionic character of the ammonium head groups.

The energetically most favourable form of micelles is spherical, because in this geometry the surface energy is minimised most efficiently. Moreover, this conformation allows the largest number of micelles to be formed out of a certain amount of template, which is attractive considering the entropy of the system. Nevertheless, it is observed that at increasing amounts of template in water a different micelle geometry evolves: the spherical micelles gradually transform into long tubes, often denoted as rod-like micelles. Increasing the template concentration even further results in aggregation of the rod-like micelles into a hexagonal *liquid crystalline structure*, resembling the MCM-41 structure. If the template concentration is increased further this hexagonal liquid crystalline phase first transforms into a cubic liquid crystalline phase and eventually, at the highest template concentrations, into a lamellar liquid crystalline phase, *e.g.* [1 - 3]. The cubic liquid crystalline phase resembles the structure of mesoporous MCM-48, whereas the lamellar phase is the structural analogue of MCM-50 (an unstable material, which consists of platelets of amorphous silica). Because of the resemblances between the liquid crystalline phases and the MCM structures it is often assumed that the liquid crystalline structures are the actual templates of MCM-41 and MCM-48. In the case of MCM-48 this is indeed the most likely templating mechanism (*e.g.* [1, 4]). However, in a large number of studies that were devoted to the elucidation of the mechanism of MCM-41 formation the hexagonal liquid crystalline phase was initially not observed in the synthesis gels, although MCM-41 was formed, *e.g.* [5, 6]. These findings imply that another mechanism can be operative as well in the

formation of MCM-41. In this alternative mechanism the rod-like micelles assemble not prior to but during the generation of the MCM-41 structure. A convincing explanation for this behaviour is that the aggregation of the rod-like micelles into a liquid crystalline structure is thought to be energetically unfavourable, due to the electrostatic repulsions between the positively charged surfaces of the micelles (electrical charges are a result of the presence of the ionic head groups). During synthesis of MCM-41 the electrostatic repulsions decrease as a result of the formation of a monolayer of silica around the micelles, thereby facilitating the subsequent aggregation of the micelles into close-packed hexagonal structures.

Next to a structure-directing agent and water as a solvent two more ingredients are required for the synthesis of MCM-41: a source of silica and a mineralising agent. Various sources of silica can be used for syntheses, *viz.* water glass, amorphous silica and Kanemite (a layered silicate structure consisting of anionic silica sheets with charge-compensating sodium ions present in the interlayers). Furthermore, organic silicon alkoxides are also frequently used. For the dissolution of the various silica sources a so-called "mineralising agent" is used. For this purpose sodium hydroxide or a concentrated ammonia solution are frequently used, although HF also finds application, despite the hazards associated with its use. Upon dissolution of silica by the mineralising agent small silicon oxy-anions are produced. In the presence of the rod-like template micelles the silicate anions diffuse towards the surfaces of the micelles as a result of electrostatic attractions. Therefore the concentration of silicate anions at the surface of the micelles rapidly increases, as do the electrostatic repulsions between the individual silicate ions. In order to alleviate these repulsive interactions the silicate ions start to condense with each other, thereby forming a monolayer of amorphous silica around the micelles. Charge compensation of the ionic headgroups of the template is still brought about by deprotonated silanol groups of the silica monolayer. At this stage the silica "coated" micelles can start to cluster together by condensation reactions between the silica layers of individual micelles, thus generating the MCM-41 framework. As a result of these processes the pore walls of MCM-41 are amorphous and only 2-3 monolayers thick [5].

The processes described above can take place over a wide range of synthesis conditions, including gel composition, pH, timescale, temperature and pressure. However, once MCM-41 has been formed its pores are filled with template and in order to obtain a completely mesoporous support material the micelles must be removed. The most elegant solution to this

demand is removal by means of (repeated) washing with (slightly acidified) mixtures of organic solvent and water, resulting in extraction of the template. The resulting solutions, containing the template, can be evaporated to dryness, which leads to recovery of the template. If the synthesis conditions were relatively mild the template will not have decomposed and can be re-used for a next synthesis. A simpler method for template removal is calcination. During this process template is decomposed into CO_2, some NO_x and steam. Although MCM-41 is unstable with respect to steam, the quantities of steam produced during this process are too small to do any damage to the MCM-41 framework structure.

Some modifications to the synthesis procedure described above are possible. The first possibility is the incorporation of hetero-elements inside the pore walls of the MCM-41 structure. The most frequently incorporated elements are aluminium and titanium. The presence of aluminium inside the pore walls generates an excess negative framework charge (as in zeolites and amorphous silica-aluminas). When this charge is compensated by protons the resulting material is weakly Brønsted acidic. Compared to all-silica MCM-41 the physical properties of materials containing aluminium are generally a bit less well-developed and dealumination can take place during template removal (especially in the presence of steam during calcination). Incorporation of titanium inside the pore walls results in materials displaying interesting oxidation properties. A second adaptation that can be made to MCM-41 is "engineering" of the pore size. The most frequently used template for the synthesis of MCM-41 is hexadecyl (=cetyl) trimethyl ammonium bromide (or chloride), *i.e.* a template with an alkyl chain containing sixteen $-CH_2-$ moieties. This template yields MCM-41 with a uniform pore size of approximately 2.7 nm (*vide infra*). Using templates with longer or shorter alkyl chains the pore size can be influenced. Nevertheless, due to the limited range of alkylammonium ions suitable for the preparation of MCM-41 the pore size can be adjusted to a small extent only [1, 7 - 10]. A more dramatic increase of pore size can be accomplished by the addition of so-called "auxiliary organics" to the synthesis gel, *e.g.* 1,3,5-trimethylbenzene (mesitylene) [1, 8, 9]. These organic molecules, which must be apolar, do not dissolve in water, but instead they are absorbed in the hydrophobic core of the template micelles. Due to this absorption the micelles swell, thus increasing the average size of the mesopores in MCM-41 up to values of approximately 8-10 nm in diameter.

Finally, it should be mentioned that a wide variety of preparation methods for MCM-41 have been reported and details of the presented methods often dictate reproducibility and stability of the prepared MCM-41

material to a large extent. A paper by Grün *et al.* is accepted to describe a "fool proof" method for the synthesis of MCM-41 [11]. Nevertheless, the MCM-41 materials for our research have been prepared following the method of Cheng *et al.* [12], which also yields (all-silica) MCM-41 material of good quality and reproducibility.

Characterisation

Although a variety of techniques exist for the characterisation of heterogeneous catalysts and support materials, MCM-41 is most frequently studied with nitrogen physisorption and x-ray diffraction. Therefore, only these two techniques will be dealt with here.

First of all, the application of x-ray diffraction for the characterisation of a basically amorphous material appears to be rather useless, since x-ray diffraction is always used to attain information on crystalline materials. Nevertheless, the prerequisite for x-ray diffraction is that the materials studied display long-range structural ordering and it can be seen in figure 1 that MCM-41 presents a well-ordered lattice. Moreover, because of the geometry of its lattice MCM-41 can be indexed with a hexagonal unit cell, with a = b and c = ∞. Because the parameters a and b are in the order of nanometers instead of tenths of nanometers, as usually encountered in crystals, x-rays are diffracted over small angles only. Therefore, characterisation of MCM-41 with x-ray diffraction yields a diffractogram with a limited number of reflections, all situated at low angles. A representative example can be seen in figure 3.

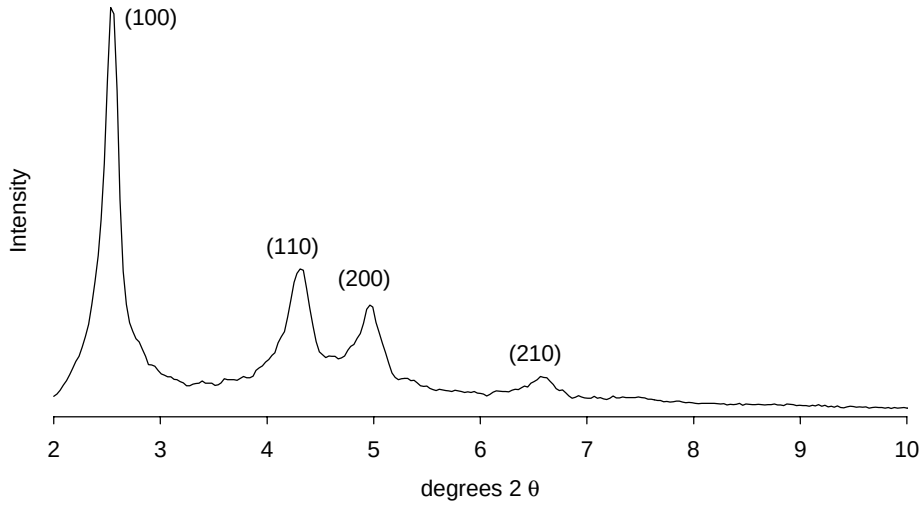

Figure 3: X-ray diffractogram of MCM-41 showing four reflections, which can be assigned to the hexagonal lattice of the mesoporous material. The (100), (110) and (200) reflections are well-resolved. (Radiation used: Co $K\alpha_1$, with λ = 0.1788970 nm).

Generally only three diffractions are well-resolved, corresponding to the (100), (110) and (200) reflections. A fourth diffraction peak with a notably lower intensity, corresponding to the (210) reflection, is sometimes also present. When an MCM-41 material of exceptionally good quality has been obtained a fifth diffraction peak, corresponding to the (300) reflection, is also observed [3]. From the reflection angles the size of the hexagonal unit cell of MCM-41 can be calculated (*i.e.* the parameters a and b). With these values and the pore diameter (determined with nitrogen physisorption, *vide infra*) the thickness of the silica pore walls can easily be calculated. The value thus obtained is a good measure for the quality (stability) of the MCM-41 support material. Ideally the thickness of the pore walls should be close to 1.5 nm, but values as low as 0.8 nm have been reported.

Nitrogen physisorption probes the textural properties of materials, *i.e.* surface area, pore volume, pore size (distribution) and pore geometry. Moreover, the technique also discloses to what extent the measured surface area is associated with micro-, meso- and / or macropores. A typical nitrogen isotherm for MCM-41 is shown in figure 4. Both the adsorption (straight line) and desorption (dotted line) curves are shown. Five distinct regions can be discerned in this graph. At very low relative pressures (p / p_0) a very large amount of nitrogen becomes physisorbed (region I). Nitrogen physisorption at these low pressures is usually assigned to condensation of nitrogen inside the micropores of a material. However, as outlined before, MCM-41 is a completely mesoporous material and does not contain any micropores. Therefore, the process taking place in region I is monolayer adsorption of nitrogen on the surface of MCM-41 (both on the external surface and inside the mesopores). Because the surface area is very high the concomitant monolayer adsorption requires a large amount of nitrogen. Upon monolayer adsorption multilayers of nitrogen start to develop at higher relative pressures of nitrogen (region II). Also in this case both the external surface area and the mesopores contribute to the physisorption process. Therefore, the data collected in this part of the isotherm are used for the calculation of the surface area of the material with the method developed by Brunauer, Emmett and Teller (BET-method). The thus calculated surface area amounts to approximately 1,000 $m^2 g^{-1}$ for the all-silica MCM-41 materials used in the research described here.

At a relative nitrogen pressure of approximately 0.37 a sudden steep increase of the amount of adsorbed nitrogen is observed (region III). This steep increase is caused by capillary condensation of nitrogen inside the mesopores, *i.e.* the mesopores of MCM-41 become suddenly filled by liquid

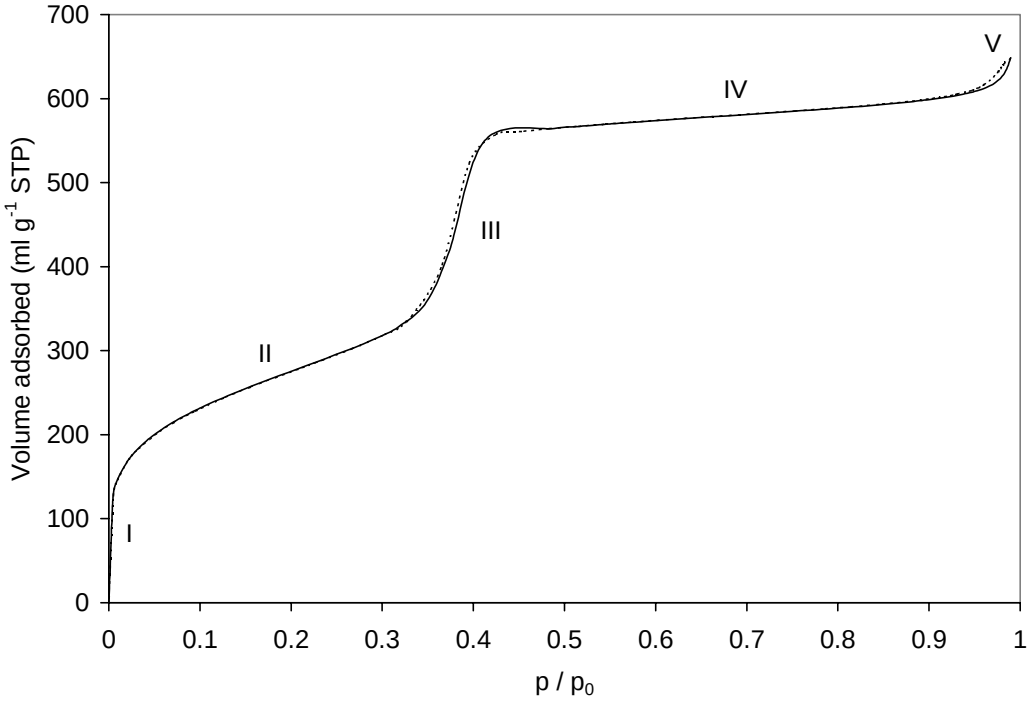

Figure 4: Nitrogen isotherm for all-silica MCM-41. The straight line is the adsorption curve and the dotted line is the desorption curve. (Measurement performed at -196°C).

nitrogen, since the meniscus of the liquid nitrogen film inside the mesopores becomes thermodynamically unstable at this pressure. The Kelvin equation relates the pore diameter of a material with the relative pressure at which capillary condensation occurs. Because filling of the mesopores takes place over a relatively small range of relative pressures (*i.e.* $p / p_0 \approx 0.34\text{-}0.40$) the pores associated with this process must all be nearly equal in size (which is indeed the case, as is apparent from figure 1). A further indication for this statement is the fact that the desorption curve almost completely coincides with the adsorption isotherm in this pressure range, giving a very narrow hysteresis loop (*i.e.* the difference between the adsorption and desorption curves). Moreover, the shapes of the curves and the hysteresis loop are very characteristic for cylindrical mesopores, which indeed constitute the MCM-41 structure (see figure 1).

When the mesopores have become completely filled with nitrogen only the external surface of MCM-41 remains accessible for nitrogen adsorption. Therefore region IV is associated with multilayer adsorption of nitrogen at the external surface of MCM-41. The very shallow slope of this region indicates that the external surface area of MCM-41 is rather small. Indeed, Voegtlin *et al.* determined the surface area of MCM-41 with the mesopores completely filled (with template) and a value of approximately only 10 $m^2 g^{-1}$ was reported

[13]. Finally, at relative pressures close to 1 the nitrogen uptake by the sample increases again and a small hysteresis loop evolves upon the subsequent desorption of nitrogen (region V). These features can be assigned to condensation of nitrogen within the interstitial voids between the MCM-41 particles.

From the adsorption and desorption curves pore size distributions can be calculated according to the method of Barrett, Joyner and Halenda (BJH-method) This method is very appropriate to study changes of pore diameters upon catalyst preparation. In the recent literature, however, there is a debate about the accuracy of the absolute values derived for the pore diameter. The pore size distribution plots calculated from the isotherm in figure 4 are shown in figure 5. Note that the horizontal axis, displaying the pore diameter, is logarithmic. A very narrow pore size distribution, centred around 2.7 nm, is obtained for MCM-41. Almost similar results are obtained for adsorption and desorption data. Moreover, larger mesopores (*i.e.* pores between 2 and 50 nm) and macropores (> 50 nm) are not present in the prepared MCM-41 material. Also, the presence of large micropores can quite probably be excluded. However, a proper determination of micropores calls either for more sensitive equipment or a closer analysis of the physisorption data with the t-plot method.

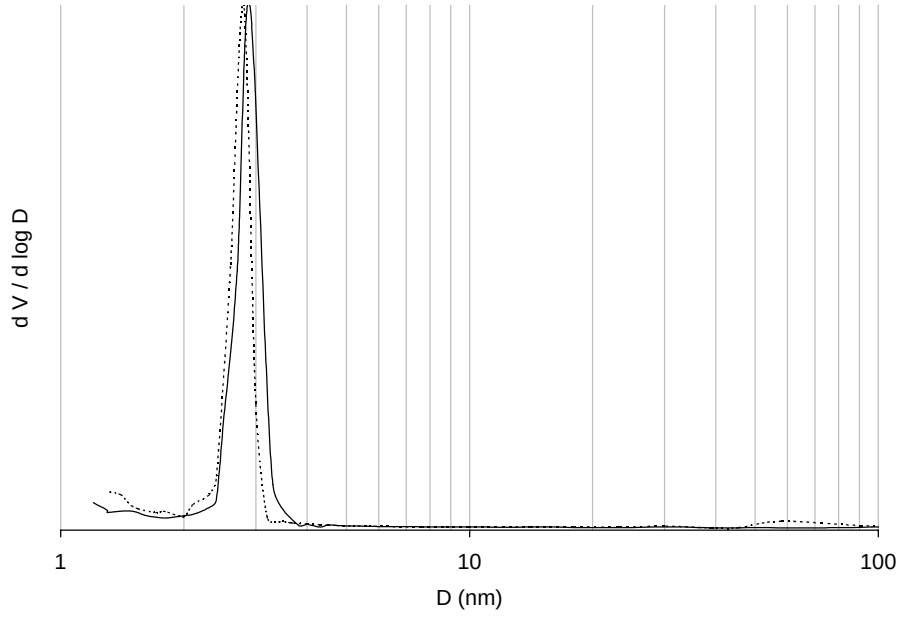

Figure 5: Pore size distribution plots of MCM-41, calculated from the isotherm shown in figure 4. The straight line presents adsorption data and the dotted line presents desorption data. Note that the horizontal axis, representing the pore diameter, is logarithmic.

With the t-plot method the *volume* of nitrogen adsorbed inside micropores can be determined and as a result a value for the micropore surface area can be calculated. However, due to geometrical constraints (*i.e.* the formation of layers of nitrogen molecules inside micropores deviates strongly from ideal packing) a thus calculated surface area must be considered as an *apparent* micropore surface area, since the *true* micropore surface area will be larger. Nevertheless, when the *volume* of nitrogen adsorbed inside micropores is known a value can be calculated for the total *surface area* in both meso- and macropores and on the external surface. To this purpose the t-plot is used. The t-plot for our MCM-41 material is given in figure 6. A limited number of data points are used to construct a curve. Ideally, a straight line can be fitted through the first few points of this curve. Fortunately, this is also the case for MCM-41. This line (in grey) is also included in figure 6 and extrapolated to t = 0. The intercept of this line with the y-axis yields the volume of nitrogen adsorbed inside micropores. It is seen that in this case a negative micropore volume is obtained, which makes no sense from a physical point of view. However, in view of the limited amount of data points and the rather large error margin of the technique, *viz.* approximately 5 percent, the obtained value (-0.006 ml g^{-1}) is satisfactory, since it is very close to the expected micropore volume (*viz.* 0 ml g^{-1}). Moreover, the absolute value of the micropore volume is very small compared to the total pore volume, which is generally close to a value of 1 ml g^{-1} for MCM-41 powder (in this case: 0.97 ml g^{-1}).

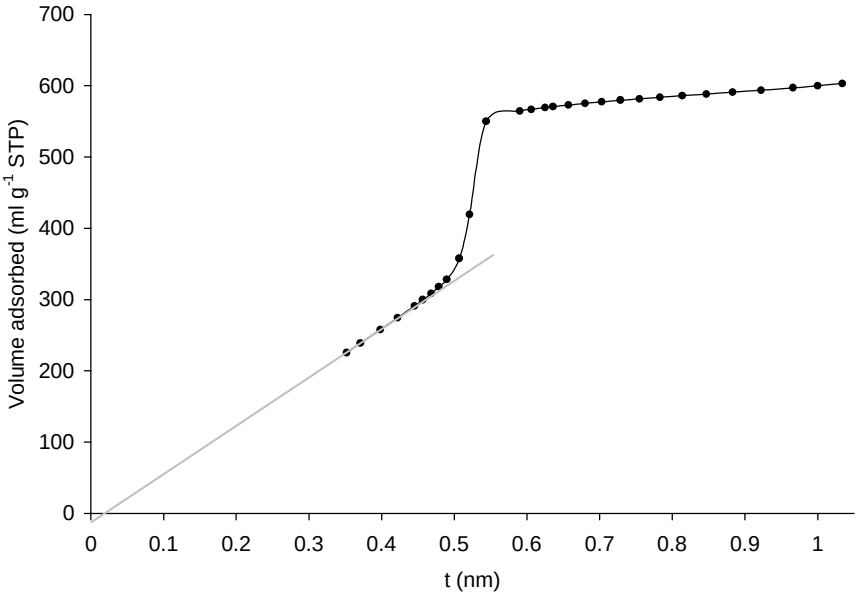

Figure 6: A representative t-plot of MCM-41. Black dots are data points. The grey line has been fitted through the first few data points and extrapolated to t = 0.

In addition, the slope of the straight line fitted through the data points yields a value for the surface area excluding the amount of nitrogen physisorbed inside micropores. This value is often referred to as "external surface area", but this term is misleading, since the thus calculated surface area must be attributed not only to the external surface area, but also to the surface area inside meso- and macropores. When a material does not contain micropores, as is the case with MCM-41, the value for the surface area calculated with the t-plot should be very close to the value calculated with the BET-method, as is the case for the material described here (S_{BET} = 996 m^2 g^{-1} and S_t = 989 m^2 g^{-1}). Unfortunately, the t-plot value is not often included in publications on MCM-41 or related mesoporous materials. Since the t-plot is generally not included either it is not clear whether reported BET surface areas should be attributed solely to the surface area inside the mesopores and on the external surface of MCM-41 or whether micropores are present as well (*e.g.* as a result of a failed attempt to prepare MCM-41 supported heterogeneous catalysts). A result of this omission can be that large BET surface areas are erroneously interpreted as a prove of high quality of mesoporous supports or catalysts, whereas in fact (partial) collapse of the structure might have occurred. In chapter 4 we will show that this is the case for the preparation of MCM-41 supported molybdenum catalysts with an aqueous ammonium heptamolybdate solution as precursor (a method that is nevertheless very frequently described in literature). Therefore we strongly advise to include information obtained from t-plots in future communications on mesoporous materials and catalysts.

Catalyst preparation

The first "modern" heterogeneous catalysts, developed in the second half of the 19th century, were supported by such "natural" support materials as pumice (highly porous volcanic deposits) and Kieselguhr ("Rhine-sand", composed of the inorganic, silica-based skeletons of tiny sea-creatures called diatoms). Since then a number of methods have evolved for the application of active phases on these and newer types of support materials. Here a short overview of some selected application processes, which have been studied thoroughly in our department, will be given. The applicability of these methods with respect to mesoporous MCM-41 will also be addressed shortly. For a more detailed overview of catalyst preparation techniques one is referred to the more specific literature on this topic, *e.g.* [14, 15].

Impregnation

The most frequently applied preparation method for heterogeneous catalysts is impregnation. The major advantage of this method is its simplicity. During impregnation a suitable support material is contacted with a solution containing a precursor of the active phase. Upon drying of the support material after impregnation solvent (usually water) is evaporated and as a result the precursor of the active phase adheres to the surface of the support. Prior to impregnation support materials are frequently shaped into robust bodies, which facilitates their handling. Because of the shaping process voids are generated between the primary particles of support material and upon impregnation these voids (also denoted as "pores") are filled with precursor solution. Generally, there are two different methods of impregnation. In "wet" impregnation the amount of precursor solution added to the support material exceeds the pore volume. Although this is the simplest impregnation method it can result in the deposition of a vast amount of precursor material at the exterior parts of the support bodies during drying and the resulting heterogeneous catalysts display an egg-shell distribution of the active component. Nevertheless such a distribution might be beneficial from an application point of view, since it alleviates the need of reactant penetration deep inside the catalyst bodies, thus improving the catalytic process. When the catalyst bodies are subject to a lot of friction during operation, causing abrasion of the outer parts, other types of distribution of the active phase are necessary, *e.g.* homogeneous, egg-white or egg-yolk. For this purpose another type of impregnation is usually required, *viz.* incipient wetness impregnation. This method is also referred to as "dry" impregnation, since during the impregnation process the amount of precursor solution added to the support material equals the pore volume. As a result the support bodies appear to be dry, even after admission of the precursor solution. After the impregnation process, be it wet or dry, the impregnated support material needs to be dried in order to allow the precursor compound to be converted into a catalytically more suitable chemical phase. Although drying of an impregnated support material appears to be very simple it should be noted that the conditions during drying can adversely influence the distribution of the precursor compound over the support material. This behaviour is caused by solvent flows inside the pores of the support material during drying. As a result of these flows the precursor material is entrained through the pores, which can lead to inhomogeneous distributions after drying. To prevent redistribution of the precursor during drying special measures have to be

taken, *e.g.* by carefully controlling the drying rate of the impregnated bodies [16]. Another option to overcome redistribution of precursor compound during drying involves the use of chelated precursor complexes, *e.g.* [17]. After drying the precursor of the active phase is usually converted into a phase (more closely) resembling the catalytically active phase, *e.g.* by calcination, yielding a catalyst in the oxidic state. A subsequent reduction treatment can be used to convert the catalyst into the metallic state.

Since MCM-41 offers a relatively large pore volume, impregnation appears to be a suitable method for the application of precursors of active phase(s) inside the mesopores. However, care should be taken to avoid redistribution of precursors during drying after impregnation. In view of the above-described processes incipient wetness impregnation is the most suitable impregnation procedure, since this procedure offers the advantage (at least in theory) that the precursor compound is deposited completely inside the pores of the support material. A point of concern is the stability of the MCM-41 support towards the impregnated precursors. Limited stability will have to result in the selection of alternative precursor compounds. A question that remains, however, is whether impregnation with alternative precursors is still viable from a practical point of view.

Precipitation

Homogeneous Deposition Precipitation (HDP)

Another method of catalyst preparation involves the precipitation of a precursor of the active phase onto the surface of a support material. Over the years various precipitation processes have been developed. The most illustrious method probably is *Homogeneous Deposition Precipitation* (HDP), also referred to as precipitation from homogeneous solution, *e.g.* [15, 18]. For HDP a suitable, *powdered* support material is suspended into a solution containing precursor ions of the catalytically active phase. During the HDP process the pH of the thus generated suspension is homogeneously raised, resulting in the precipitation of the precursor ions. Key feature of this process is that precipitation of the precursor ions does not occur in the bulk of the solution, but on the surfaces of the suspended powdered support. *I.e.* the powdered support material acts as a source of nuclei onto which the precursor ions precipitate once the pH has reached a critical value. This critical value generally is the pH level corresponding to the solubility level of the metal hydroxide that is formed out of the precursor ions and OH^-. In the

absence of a support (*i.e.* nuclei) precipitation of the precursor ions would occur at a higher pH level, corresponding to the supersolubility level of the metal hydroxide. In conclusion, the presence of a powdered support material allows for the deposition of precursor ions at its surface during precipitation from a homogeneous solution. However, it should be noted that the support material is not just an inert phase offering a sufficient number of sites necessary for precipitation, since the surface chemistry of the support material and the resulting interactions with the precipitating, partly hydrolysed species sometimes also play a major role. These interactions strongly depend on the temperature at which the process is executed. At low temperatures (*i.e.* generally below 40°C) the reaction between the precipitating precursor ions and the support is generally restricted to the surface of the support. As a result the interface between the precipitating metal hydroxide and a silica support material rearranges into a very thin metal silicate sheet during the precipitation process. Hydroxide ions (presumably) play an active role in this transformation. At higher precipitation temperatures (*i.e.* up to 90°C) the reaction between the support material and the precipitating agens is not restricted to the formation of an interface structure and as a result mixed bulk structures are (also) formed: layered structures, denoted as metal hydro- or phyllo-silicates, which closely resemble clay-like materials. Detailed studies of the formation processes and resulting materials have been made by Burattin *et al.* [19, 20].

It should be mentioned that there are various methods to increase the pH during catalyst preparation with HDP. The simplest option is the controlled addition of a diluted solution containing sodium or potassium hydroxide, although diluted ammonia solutions are also frequently used. An alternative approach to increase the pH during HDP is the use of urea ($CO(NH_2)_2$) or a derivation of it, *viz.* potassium isocyanate (KCNO). At temperatures exceeding 70°C urea decomposes in water according to the following reaction equations:

$$CO(NH_2)_2 \rightarrow NH_4^+ + CNO^- \quad (1)$$

$$CNO^- + 3\ H_2O \rightarrow NH_4^+ + CO_2 + 2\ OH^- \quad (2)$$

Nevertheless, HDP with urea is usually carried out at a temperature of 90°C. Isocyanate ions decompose at a notably lower temperature, *viz.* 40°C. As a result of reaction (2) hydroxyl ions are generated, thus enabling the precipitation of metal hydroxide onto the support material. Because the

decomposition processes take place in solution the hydroxide ions are generated truly homogeneously.

Precipitation after impregnation

Although the above-described HDP process is very suitable for the deposition of metal ions onto powdered "common" support materials it poses the drawback that after the deposition process the resulting powder still needs to be shaped into catalyst bodies. Moreover, with porous support materials precipitation of metal hydroxide is very likely to occur to a very large extent onto the external support surface during HDP. To overcome both problems alternative precipitation processes have been invented, which rely on the precipitation of metal ions inside the pores of (bodies of porous) support materials. Knijff was the first to impregnate solutions containing both metal ions and a precipitating agent (urea or a nitrite salt) [21, 22]. Upon heating of the impregnated support bodies precipitation of metal hydroxide occurred inside the pores of the support material, due to the decomposition of precipitating agent at elevated temperatures.

Another method for the precipitation of metals inside the pores of support bodies, involving oxalate precursors, was also developed by Knijff [21, 23]. Generally oxalates display a very limited solubility. By impregnating solutions containing both metal ions and oxalate ions, Knijff was able to precipitate mixed oxalates (containing both nickel and magnesium) with a high dispersion inside the pores of both silica and α-alumina. Upon calcination the organic oxalate ligands are removed and a mixed nickel-magnesium oxide is obtained. Both co-impregnation and sequential impregnation were used for catalyst preparation. In the case of co-impregnation care should be taken to avoid precipitation of mixed oxalate prior to impregnation.

Finally, De Jong combined impregnation and precipitation to obtain highly dispersed molybdena catalysts supported by porous silica bodies [24]. Solutions containing molybdate ions and hydrazine were either impregnated successively or mixed and co-impregnated. The role of hydrazine was to reduce molybdate ions to trivalent molybdenum precursor ions, which subsequently precipitated as $Mo(OH)_3$, according to the following reaction equation:

$$4\ MoO_4^{2-} + 3\ N_2H_4 + 4\ H_2O \rightarrow 4\ Mo(OH)_3 + 3\ N_2 + 8\ OH^- \qquad (3)$$

Co-precipitation

A final method for the preparation of heterogeneous catalysts *via* precipitation involves *co-precipitation* of both a support material and a(n) (precursor of the) active phase. The precipitation of bulk mixed nickel-magnesium oxalate, as described in the previous section, yielding magnesia-supported nickel catalysts, is an example. It should be noted, though, that catalysts prepared *via* co-precipitation sometimes display structures deviating from common supported heterogeneous catalysts, as clay-like compounds can be formed. Examples of these kinds of materials are smectites and hydrotalcites. A first step in the preparation of silica-based, cationic smectite clays involves the gelation of a starting solution containing the metal ions of interest. Subsequent decomposition of urea at 90°C results in the formation of the desired clay structures [25]. In addition, these materials can also be obtained by hydrothermal preparation [26]. Hydrotalcites, on the other hand, are anionic clays, generally composed of magnesium- and aluminium-containing hydroxide sheets displaying the Brucite-structure [27, 28]. Hydrotalcite syntheses generally comprise the addition of a slightly acidic solution containing magnesium and aluminium ions to a sodium hydroxide solution, resulting in the immediate formation of a precipitate, followed by an aging period (at temperatures ranging from room temperature to hydrothermal conditions).

MCM-41 and catalyst preparation via precipitation

From the above discussion on precipitation processes it is clear that the processes of HDP and impregnation-precipitation both rely on the addition or generation of hydroxyl ions for the precipitation of metal ions onto support materials. As stated in the section on MCM-41, this material is highly unstable towards mineralising agents, such as hydroxide ions. Therefore, it is highly questionable whether HDP or impregnation-precipitation would give satisfactory results when applied for the preparation of catalysts supported by MCM-41. Most likely these methods will result in (partial) dissolution of the thin, amorphous silica mesopore walls, leading to structural collapse of the unique support structure and thus to the disappearance of its favourable properties. Moreover, HDP would also pose the problem of reactant diffusion into the mesopores of MCM-41 during the precipitation process.

The third method for catalyst preparation *via* precipitation, *i.e.* co-precipitation, is sometimes used for the preparation of MCM-41 supported

heterogeneous catalysts. In this case the process is usually referred to as *in-situ* incorporation, since metal ions are incorporated into the silica pore walls during the synthesis of MCM-41. This process is basically the same as for the incorporation of aluminium or titanium into the pore walls of the MCM-41 structure, as described above in the section on the synthesis of MCM-41. Although this method is viable for the incorporation of aluminium and titanium the results for a number of other elements are rather disappointing. An explanation for this finding can be that the presence of metal ions during synthesis of MCM-41 changes the chemistry of the synthesis gel in such a way that the precipitation of an ordered mesoporous material is no longer kinetically favoured. Another explanation is that incorporation of hetero-elements inside the pore walls decreases the stability of these walls to such an extent that structural collapse of the framework occurs upon removal of template. Nevertheless, whatever the exact cause of the instability, this method is not at all useful for the application of nickel inside the mesopores of MCM-41 [29]. For the application of molybdenum some satisfying results have been obtained, albeit at rather low Mo loadings. A detailed overview of the incorporation of molybdenum onto MCM-41 *via* co-precipitation will be given in the introductory section of chapter 4.

Other preparation methods

The methods described above are most frequently used for the preparation of heterogeneous catalysts, including catalysts supported by MCM-41. Nevertheless, a wide variety of alternative processes for the application of metals onto support materials have been developed over the years and these processes have also been applied to MCM-41 and related mesoporous supports. Here a short overview of methods will be given as well as the relation of these processes with MCM-41. If applicable, detailed examples will be given in the introductory sections of chapters 3 and 4.

A very simple method for catalyst preparation relates to the *spreading* behaviour of certain metal oxides, *viz.* MoO_3 and V_2O_5, over the surface of a support material when a physical mixture of metal oxide and support material is annealed at elevated temperatures for a sufficient long period of time. Unfortunately the interactions of these metal oxides with silica support materials are rather weak, resulting in either low dispersions or low loadings of thus prepared catalysts. The very large surface area of MCM-41 alleviates these constraints to some extent.

Chemical Vapour Deposition (CVD) relies on the adsorption of a volatile metal precursor compound onto the surface of a support material. Upon interaction the precursor compound usually decomposes, resulting in the deposition of the selected element onto the support surface. CVD has been applied for the deposition of molybdenum onto MCM-41 *via* $Mo(CO)_6$, but the Mo loadings thus obtained are very disappointing.

Another, very common procedure for the application of metal ions onto a support material is *ion-exchange*. This method implies that a support material has an excess negative framework charge in order to adsorb the metal cations. Unfortunately, in order to generate sufficient excess negative charge on the framework of MCM-41 it is necessary to incorporate aluminium ions inside the pore walls during synthesis, resulting in a decreased stability of the support material (*vide supra*). During ion-exchange simple charge-compensating cations, such as alkali metal ions, ammonium ions or protons are replaced by the metal ions of interest, a process which is generally entropy-driven. However, it should be noted that ion-exchange is generally diffusion-limited and as a result rather long equilibration times are required. Moreover, metal loadings are generally limited. Ion-exchange has been used to apply nickel inside the mesopores of MCM-41.

Finally, (organo)metallic precursors can also be applied for the preparation of supported heterogeneous catalysts, *via* the processes of grafting or tethering. During grafting a precursor complex reacts chemically with a hydroxyl group at the surface of a support material. As a result a covalent bond is formed between the metal ion / atom and the support material. Tethering involves the use of both a metal complex and a so-called "spacer". The spacer, which is generally a small organic linking agent reacts with a hydroxyl group of the support surface and subsequently a metal ion / atom becomes complexed to the other end of the spacer. As a result, tethering yields heterogeneous catalysts containing metal complexes suitable for homogeneous catalysis. Therefore, thus produced catalysts are referred to as heterogenised homogeneous catalysts. Decomposition of the complexes grafted or tethered to the support material results in truly heterogeneous catalysts. Nevertheless, this method of catalyst preparation is generally rather laborious and expensive and as a result it does not find widespread application for the preparation of heterogeneous catalysts. Nevertheless, in literature a few examples can be found for the application of molybdenum onto MCM-41 *via* grafting.

Acknowledgements

Gerbrand Mesu is kindly thanked for the preparation of the MCM-41 material shown in this chapter. John Raaymakers and Marjan Versluijs-Helder are thanked for their efforts during the characterisation of the MCM-41 material with nitrogen physisorption and x-ray diffraction, respectively. Sandra Kemp is acknowledged for making the beautiful TEM micrographs. Marjolein Toebes is thanked for writing an interesting and helpful essay on the preparation and characterisation of MCM materials.

Literature

[1] J.S. Beck, J.C. Vartuli, W.J. Roth, M.E. Leonowicz, C.T. Kresge, K.D. Schmitt, C.T-W. Chu, D.H. Olson, E.W. Sheppard, S.B. McCullen, J.B. Higgins and J.L. Schlenker, *J. Am. Chem. Soc.*, 114, 1992, 10834

[2] G.D. Stucky, A. Monnier, F. Schüth, Q. Huo, D. Margolese, D. Kumar, M. Krishnamurty, P.Petroff, A. Firouzi, M. Janicke and B.F. Chmelka, *Mol. Cryst. Liq. Cryst.*, 240, 1994, 187

[3] Q. Huo, D.I. Margolese and G.D. Stucky, *Chem. Mater.*, 8, 1996, 1147

[4] J.C. Vartuli, K.D. Schmitt, C.T. Kresge, W.J. Roth, M.E. Leonowicz, S.B. McCullen, S.D. Hellring, J.S. Beck, J.L. Schlenker, D.H. Olson and E.W. Sheppard, *Chem. Mater.*, 6, 1994, 2317

[5] C-Y. Chen, S.L. Burkett, H-X Li and M.E. Davis, *Micropor. Mater.*, 2, 1993, 27

[6] A. Monnier, F. Schüth, Q. Huo, D. Kumar, D. Margolese, R.S. Maxwell, G.D. Stucky, M. Krishnamurty, P.Petroff, A. Firouzi, M. Janicke and B.F. Chmelka, *Science*, 261, 1993, 1299

[7] J.S. Beck, J.C. Vartuli, G.J. Kennedy, C.T. Kresge, W.J. Roth and S.E. Schramm, *Chem. Mater.*, 9, 1994, 1816

[8] N.K. Raman, M.T. Anderson and C.J. Brinker, *Chem. Mater.*, 8, 1996, 1682

[9] O. Franke, J. Rathousky, G. Schulz-Ekloff and A. Zukal, *Stud. Surf. Sci. Catal.*, 91, 1995, 309

[10] F.P. Matthae, D. Genske, C. Minchev and H. Lechert, *Stud. Surf. Sci. Catal.*, 117, 1998, 223

[11] M. Grün, I. Lauer, K.K. Unger, *Adv. Mater.*, 9, 1997, 254

[12] C.-F. Cheng, D.H. Park and J. Klinowski, *J. Chem. Soc., Faraday Trans.*, 93, 1997, 193

[13] A.C. Voegtlin, A. Matijasic, J. Patarin, C. Sauerland, Y. Grillet and L. Huve, *Micropor. Mater.*, 10, 1997, 137

[14] K.P. de Jong, *Current Opinions in Solid State & Materials Science*, 4, 1999, 55

[15] K.P. de Jong and A.J. van Dillen, in: *HeteroGEneoUS Catalysis (K.P. de Jong and A.J. van Dillen, Editors)*, published by the Department of Inorganic Chemistry and Catalysis, Utrecht University, Utrecht, The Netherlands, 1998, chapter 2

[16] L.M. Knijff, *Ph.D. Thesis*, Utrecht University, The Netherlands, 1993, chapters 2 and 3

[17] A.J. van Dillen, R.J.A.M. Terörde, D.J. Lensveld, J.W. Geus and K.P. de Jong, *J. Catal.*, 2003, in press

[18] A.J. van Dillen, J.W. Geus, L.A.M. Hermans and J. van der Meijden, in: *Proc. Int. Congr. Catal. (G.C. Bond, P.B. Wells and F.C. Tompkins, Editors)*, published by The Chemical Society, Letchworth, England, volume 2, 1977, 677

[19] P. Burattin, M. Che and C. Louis, *J. Phys. Chem. B*, 102, 1998, 2722

[20] P. Burattin, M. Che and C. Louis, *J. Phys. Chem. B*, 103, 1999, 6171

[21] L.M. Knijff, P.H. Bolt, R. van Yperen, A.J. van Dillen and J.W. Geus, *Stud. Surf. Sci. Catal.*, 63, 1991, 165

[22] L.M. Knijff, *Ph.D. Thesis*, Utrecht University, The Netherlands, 1993, chapter 5

[23] L.M. Knijff, *Ph.D. Thesis*, Utrecht University, The Netherlands, 1993, chapters 6 and 7

[24] K.P. de Jong, *Stud. Surf. Sci. Catal.*, 63, 1991, 19

[25] R.J.M.J. Vogels, *Ph.D. Thesis*, Utrecht University, The Netherlands, 1996

[26] J.T. Kloprogge, *Ph.D. Thesis*, Utrecht University, The Netherlands, 1992

[27] M.K. Titulaer, *Ph.D. Thesis*, Utrecht University, The Netherlands, 1993

[28] J.C.A.A. Roelofs, *Ph.D. Thesis*, Utrecht University, The Netherlands, 2001; available at http://www.library.uu.nl/digiarchief/dip/diss/1977553/inhoud.htm

[29] U. Junges, S. Disser, G. Schmid and F. Schüth, *Stud. Surf. Sci. Catal.*, 117, 1998, 391

3

The preparation of MCM-41 supported nickel catalysts with a chelated nickel citrate precursor

Abstract

Incipient wetness impregnation with a chelating nickel citrate precursor yields MCM-41 supported nickel catalysts with a high dispersion of nickel (oxide) nanoclusters inside the mesopores. Impregnation with a common nickel nitrate precursor solution resulted in the formation of a bimodal particle size distribution of nickel (oxide), with very large particles situated outside the mesopores. The interactions of nickel nitrate with the silica pore surface are too weak to provide sufficient anchoring of the nickel ions during drying (entrainment with solvent flow) and calcination (sintering). Solutions of nickel citrate, on the other hand, display an increase of viscosity upon drying and as a result a thin, amorphous film of precursor material, strongly adhering to the pore surface, is formed. Upon calcination this film decomposes and an MCM-41 supported nickel catalyst combining both an unprecedented high loading and dispersion of the active phase is obtained. For both methods neither pore-blocking nor structural collapse of the support structure occurred.

Parts of this chapter have been published as D.J. Lensveld, J.G. Mesu, A.J. van Dillen and K.P. de Jong, *Micropor. Mesopor. Mater.*, 44-45, 2001, 401 and *ibid.*, *Stud. Surf. Sci. Catal.*, 143, 2002, 647.

Introduction

Highly active heterogeneous catalysts often call for the use of high surface area support materials onto which active phase(s) can be deposited. In this respect MCM-type [1, 2] and related mesoporous materials display interesting textural properties, combining both high surface areas and high porosities. Since the first discovery of MCM-41 efforts have been undertaken to apply metals inside the mesopores, in order to prepare silica-based heterogeneous catalysts with unprecedented high surface areas and unique structure. However, in order to exploit the favourable properties of MCM-41 and related mesoporous materials dedicated catalyst synthesis procedures need to be developed. In this chapter a new procedure for the application of nickel nanoparticles inside the mesopores is presented.

In the open literature only a small number of publications have dealt with the application of nickel onto mesoporous support materials. The most frequently applied method to prepare nickel catalysts supported by mesoporous materials is incipient wetness impregnation with simple nickel precursor salts, such as nickel nitrate [3 - 9] and nickel chloride [6]. Ziolek *et al.* showed that the hexagonal structure of aluminium-containing MCM-41 was preserved upon impregnation with nickel nitrate (nickel loading was 5 wt%) [3]. Only catalyst preparation *via* impregnation with nickel nitrate has resulted in catalysts with nickel loadings exceeding 5 wt% [4, 5]. Unfortunately, already at nickel oxide loadings as low as 6-10 wt% the use of this precursor results in the appearance of intense NiO reflections in XRD after calcination, indicating the formation of large nickel oxide particles. Moreover, a rather large decrease of surface area and pore volume was observed, both with MCM-41 [4, 5] and KIT-1 [5].

Two other methods for the incorporation of nickel inside the pores of mesoporous supports are "*in-situ* synthesis" [6] and ion-exchange [6, 10 - 12]. During *in-situ* synthesis a nickel precursor salt is present in the MCM-41 synthesis gel. However, this is not a very successful method for the preparation of MCM-41 supported nickel catalysts, as Junges *et al.* showed that already at loadings exceeding 1.5 wt% the distinct capillary condensation step in the nitrogen isotherms disappeared [6]. Hartmann *et al.* used aqueous nickel chloride solutions to prepare both all-silica and aluminium-containing MCM-41 supported nickel catalysts *via* ion-exchange [10 - 12]. Unfortunately, apart from electron spin resonance during catalysis experiments no physical characterisations of the prepared materials were provided.

Here the use of an aqueous solution containing a chelated nickel precursor for the preparation of MCM-41 supported heterogeneous nickel catalysts *via* incipient wetness impregnation is disclosed. It is shown that the unique properties of this type of precursor solution during drying result in the formation of catalysts combining both unprecedented high nickel loadings and dispersions.

Experimental

Support synthesis

All-silica MCM-41 was prepared following a slightly adapted literature procedure [13]. Template (cetyltrimethylammoniumbromide, Acros, 99+%) was dissolved in demineralised water. To the resulting solution a mineralising agent (tetraethylammoniumhydroxide, Acros, 20 wt% in water) and finally silica (Aerosil 380, Degussa) were added. The molar composition of the resulting gel was 1 SiO_2 : 0.27 CTABr : 0.19 TEAOH : 40 H_2O. The highly viscous gel was stirred for one day at room temperature, after which it was transferred to a teflon-lined autoclave. This autoclave was placed in an oven and the synthesis gel was aged at 150°C under autogeneous pressure for 2-3 days. After the hydrothermal treatment the product was worked up by repeated washing with demineralised water and filtration, after which it was dried in air for 12 hours at 120°C (heating rate = 1°C min^{-1}). Template was removed by calcination in air for 6 hours at 550°C (heating rate = 1°C min^{-1}).

Catalyst preparation

Nickel catalysts were prepared by incipient wetness impregnation of the powdered MCM-41 support with solutions of nickel citrate. To prepare these solutions a suspension of nickel carbonate (Baker Analyzed Reagent) in demineralised water was made and after heating to 100°C citric acid (Merck, p.a.) was added until a clear solution had formed (molar ratio $NiCO_3$: citric acid ≈ 3 : 2). After impregnation the samples were dried for 12 hours at 120°C and calcined for 4 hours at 450°C (heating rates = 1°C min^{-1}), both in air.

As a reference a catalyst was made by incipient wetness impregnation with a solution of nickel nitrate (Riedel-de-Haën, extra pure) in demineralised water. This catalyst was dried and calcined similar to the citrate catalyst. For both catalysts the loadings were 10 wt% Ni, calculated as:

$$\{g_{Ni} / (g_{Ni} + g_{MCM\text{-}41})\} * 100\% = 10\%.$$

To study the conversion of the resulting nickel oxide catalysts to their metallic counterparts a reduction treatment was performed: a small amount (± 0.2 g) of catalyst sample was pelletised, placed in a fixed bed reactor and hydrogen was passed through the catalyst bed at a rate of 50 ml min^{-1} at 650°C. Next the reactor was cooled to room temperature and the catalyst sample was subjected to a gentle passivation treatment, by injecting small amounts of air with a syringe into the gas stream (argon). No heat release was measured during this treatment.

Characterisation techniques

Nitrogen physisorption

Nitrogen physisorption was performed at -196°C with a Micromeritics ASAP 2400 apparatus. Prior to the measurements the powdered samples were degassed for 24 hours at 300°C *in vacuo*. Surface areas, pore volumes and pore size distributions were determined with standard BET and BJH theory respectively.

XRD

X-ray diffraction patterns were collected on an Enraf Nonius PDS 120 powder diffraction system equipped with a position-sensitive detector, using Co $K\alpha_1$ radiation with a wavelength of 0.1788970 nm.

TEM

Electron microscopy was performed with a Philips CM 200 transmission electron microscope equipped with a field emission gun and operated at 200 keV. For the measurements sample material was ultrasonically dispersed in ethanol and a drop of the resulting, highly diluted suspension was applied onto a holey carbon film supported on a copper grid.

TPR

TPR experiments were performed with a TPDRO 1100 apparatus from Thermo Quest CE Instruments. For the TPR measurements the calcined catalyst samples were pelletised, ground and sieved. Sieve fractions of ∅

425-850 μm were placed in a fixed bed reactor and used for analysis. A flow containing 5 % hydrogen and 95 % argon (Hoek Loos) was passed downward through the catalyst bed at a rate of 20 ml min^{-1} (STP). The heating rate was 10°C min^{-1}. After water removal from the outcoming flow (molsieves) the hydrogen consumption was measured using a tungsten thermal conductivity detector.

XPS

XPS spectra were measured using a VG Escalab 200 MK spectrometer equipped with an Al Kα source and a hemispherical analyser connected to a five-channel detector. Measurements were done at 20 eV pass energy. Energy correction was performed by using the Si 2p peak of SiO_2 at 103.3 eV as a reference. Calcined catalyst samples were ground and pressed into an indium foil attached to the sample holder. The XPS spectra have been fitted with a VGS program fit routine. A Shirley background subtraction was applied and Gauss-Lorentz curves were used.

Results

The textural characteristics of the MCM-41 support material and the nickel catalysts were determined with nitrogen physisorption. Representative isotherms of the materials obtained are given in figure 1. All samples show a characteristic capillary condensation pore-filling step at a relative pressure of approximately 0.37, which is indicative of the filling of the uniform mesopores of the support. The surface areas and pore volumes of the materials are listed in table 1. The high values for S_{BET} and pore volumes of the nickel catalysts indicate that no pore blocking has occurred after catalyst preparation with both precursors. This assessment is also apparent from the pore size distributions, which are presented in figure 2, since no shrinkage of the average pore diameter is observed, nor a broadening of the pore size distribution.

The structural integrity of the nickel catalysts, as well as the support material, was determined with x-ray diffraction. The results are given in figure 3. At least three well-resolved diffractions are visible, indicating that an MCM-41 support material with long-range hexagonal ordering had been prepared. Moreover, the structural integrity of the support material is retained upon catalyst preparation with both nickel precursors.

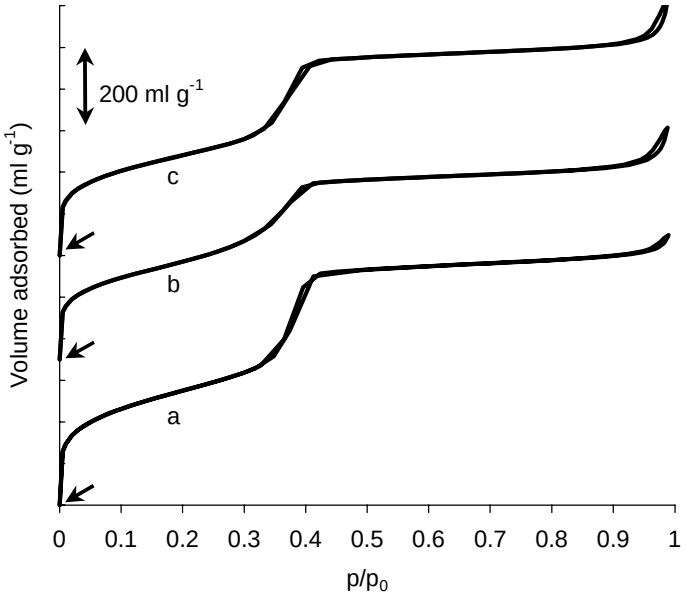

Figure 1: Nitrogen isotherms of the parent MCM-41 support material and MCM-41 supported nickel oxide catalysts. a = parent MCM-41, b = catalyst *ex* citrate, c = catalyst *ex* nitrate. The arrows indicate the "onset" of each isotherm.

Table 1: Textural characteristics of parent MCM-41 and MCM-41 supported nickel catalysts.

	S_{BET} (m^2 g^{-1})	pore volume (ml g^{-1})
parent MCM-41	1,000	0.98
catalyst *ex* citrate	860	0.84
catalyst *ex* nitrate	870	0.92

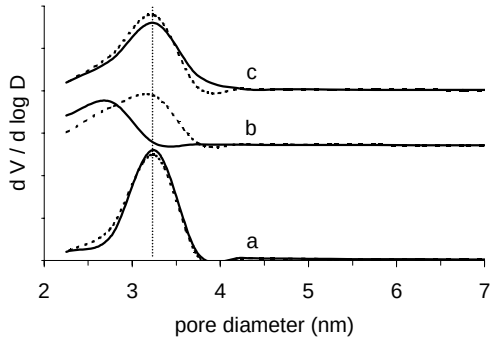

Figure 2: Pore size distributions of parent MCM-41 and MCM-41 supported nickel oxide catalysts. a = parent MCM-41, b = catalyst *ex* citrate, c = catalyst *ex* nitrate. Solid lines = adsorption data, dotted lines = desorption data.

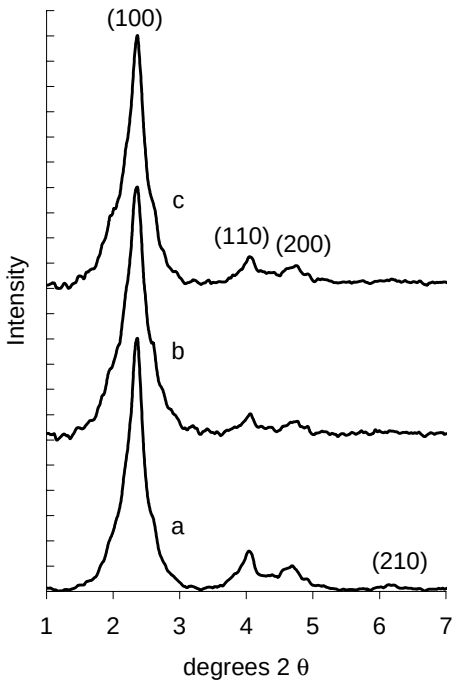

Figure 3: X-ray diffractograms of parent MCM-41 and MCM-41 supported nickel oxide catalysts. a = parent MCM-41, b = catalyst *ex* citrate, c = catalyst *ex* nitrate.

Both x-ray diffraction and transmission electron microscopy were used to determine the (approximate) particle size (distributions) for the catalysts *ex* citrate and *ex* nitrate. For the catalyst *ex* nitrate sharp reflections, assignable to NiO, were observed with x-ray diffraction (figure 4, upper line), indicating the presence of large nickel oxide crystallites. However, the onsets of the peaks are very broadened, which means that very small crystallites must be present as well. A completely different diffractogram was obtained for the catalyst *ex* citrate (figure 4, lower line): NiO reflections were almost absent, the ones remaining having very low intensities and being very broad. As a result the nickel oxide particles present on this catalyst must, without exception, be very small: *i.e.* << 10 nm. An estimation of the external surface area of the MCM-41 support material of less than 10 m^2 g^{-1} by Voegtlin *et al.* [14] learns that these nickel oxide nanoparticles have to be accommodated inside the mesopores of the support to prevent extensive sintering during calcination.

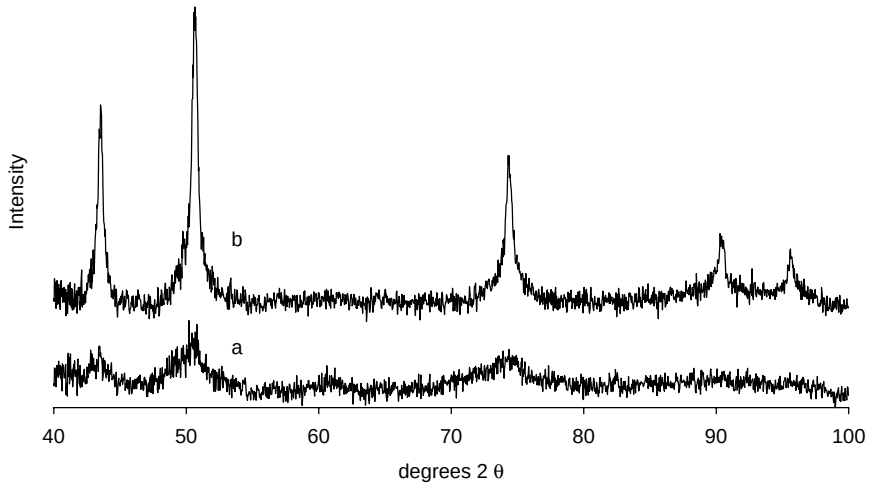

Figure 4: X-ray diffractograms of the catalysts, showing reflections characteristic of NiO. a = catalyst *ex* citrate, b = catalyst *ex* nitrate.

These assumptions were corroborated by transmission electron microscopy, as can be seen in figures 5 - 7. The catalyst *ex* nitrate displays very large nickel oxide particles (figure 5) as well as nanoparticles that are confined inside the mesopores of the support (figure 6). For the catalyst *ex* citrate only very small nanoparticles are observed, which are situated inside the mesopores of the support material (figure 7).

Reduction plots of the calcined catalysts are given in figure 8. To enable comparison a reduction plot of bulk nickel oxide, obtained from nickel

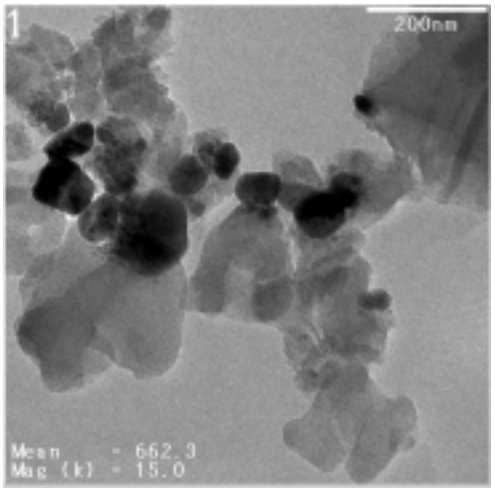

Figure 5: Transmission electron micrograph of the catalyst *ex* nitrate showing very large nickel oxide particles outside the mesopores of MCM-41.

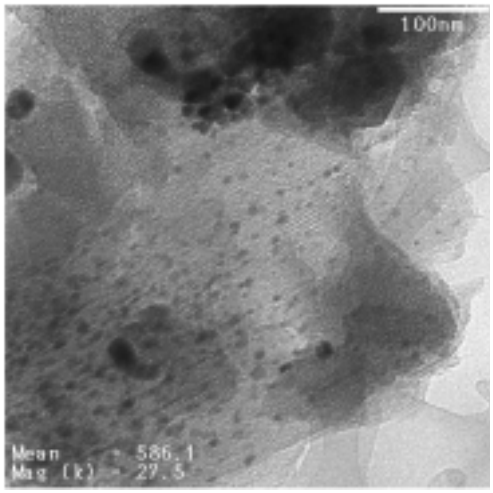

Figure 6: Transmission electron micrograph of the catalyst *ex* nitrate showing small nickel oxide nanoparticles confined inside the mesopores of MCM-41.

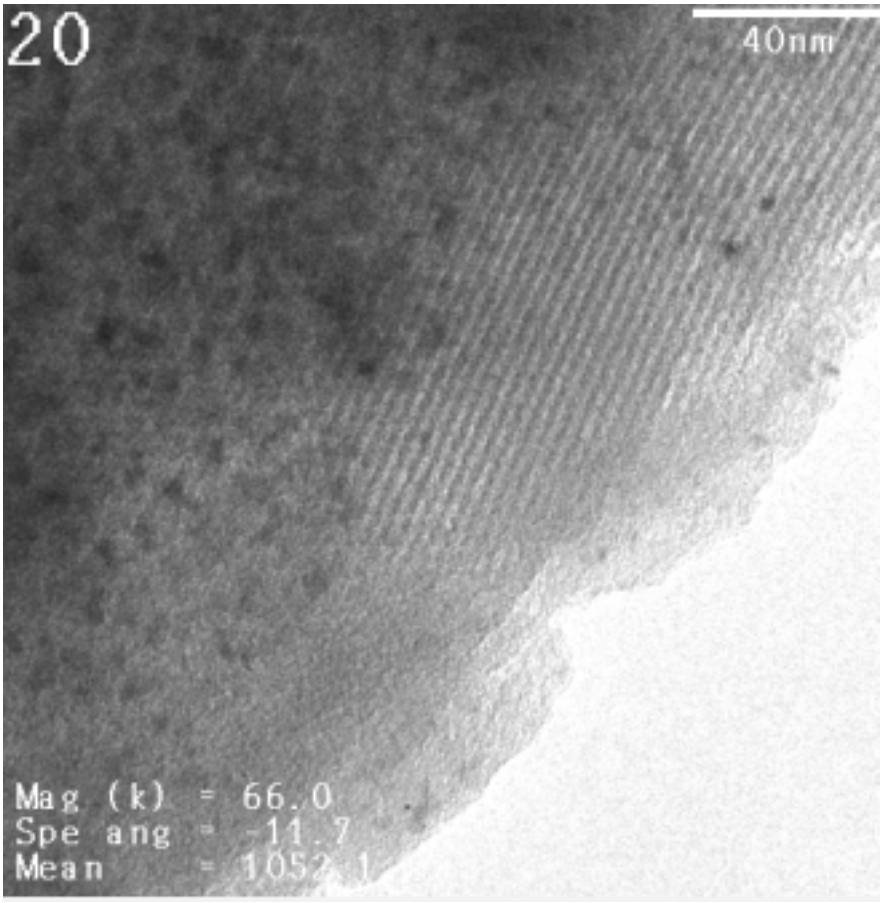

Figure 7: Transmission electron micrograph of the catalyst *ex* citrate showing exclusively small nickel oxide particles which are confined inside the mesopores of the MCM-41 support material. These mesopores are also clearly visible in this image.

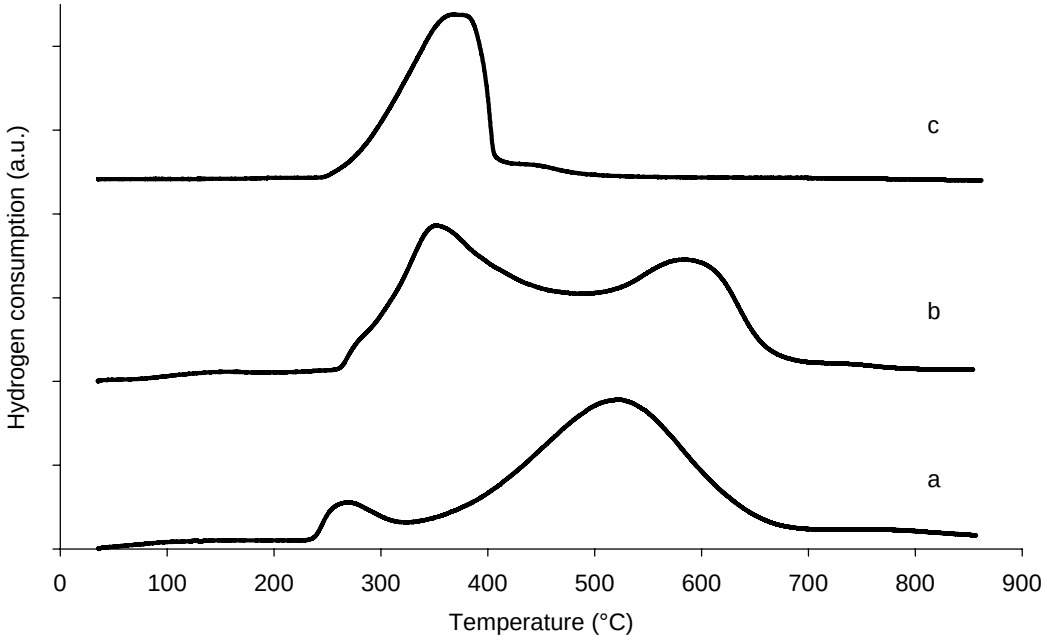

Figure 8: TPR patterns of nickel oxide, bulk and supported by MCM-41. a = catalyst *ex* citrate, b = catalyst *ex* nitrate, c = bulk NiO.

nitrate by calcination, is also included. Bulk NiO is reduced in one step, the onset temperature being 250°C. Both catalysts display two reduction stages. The first reduction stage coincides with (the onset of) reduction of bulk NiO. This stage is limited with the catalyst *ex* citrate. For both catalysts a substantial amount of nickel oxide is reduced at relatively high temperatures (*i.e.* exceeding 400°C).

XPS was used to attain information about the nickel oxide dispersion of the catalysts. From the results the atomic Ni:Si ratio was calculated for both catalysts. This ratio was found to be lowest for the catalyst *ex* nitrate (Ni:Si = 0.05), indicating a low dispersion of nickel oxide particles. For the catalyst *ex* citrate the higher Ni:Si ratio (0.09) implies a higher dispersion of small nickel oxide particles over the support surface.

The results that have been obtained with the catalysts after reduction and passivation are the same as those after calcination, *i.e.* the textural and structural properties of the support material have been completely retained after the treatments (as determined with nitrogen physisorption, x-ray diffraction and transmission electron microscopy). Information concerning the metallic nickel particles has been obtained with x-ray diffraction and transmission electron microscopy. Diffractograms of the catalysts after passivation are shown in figure 9. The observed features are exactly the same as for the oxidic systems (figure 4): only very broad and low diffractions

are visible for the catalyst *ex* citrate, whereas sharp, intense peaks with a broad onset are observed for the catalyst *ex* nitrate. Consequently, the nickel particles of the catalyst *ex* citrate have resisted sintering during the reduction treatment, thereby conserving the high dispersion of the catalyst. These results were confirmed by transmission electron microscopy measurements (not shown): only very small nickel nanoparticles situated inside the mesopores were found for the catalyst *ex* citrate.

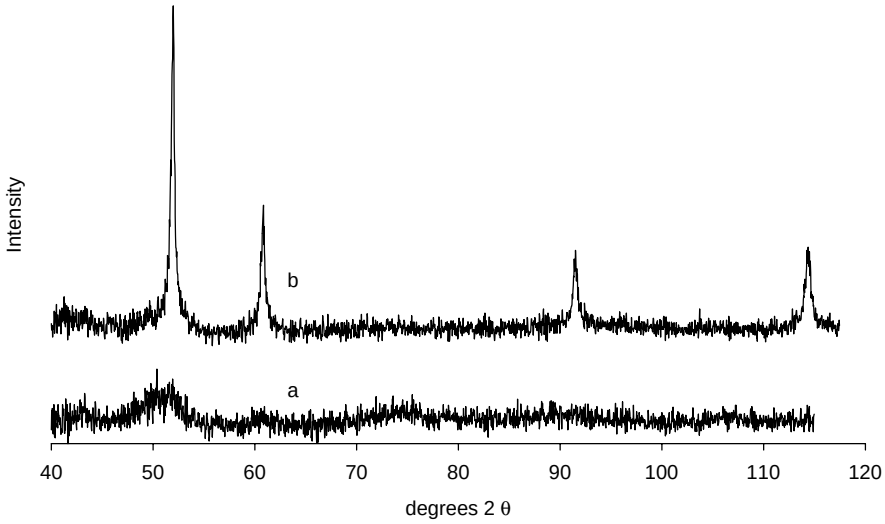

Figure 9: X-ray diffractograms of the catalysts after isothermal reduction at 650°C showing diffractions originating from metallic nickel. a = catalyst *ex* citrate, b = catalyst *ex* nitrate.

Discussion

Several characterisation techniques indicate that the characteristic features of the MCM-41 support material have been retained after application of nickel with two different precursor solutions. Surface areas and pore volumes have remained very high after nickel incorporation, indicating the absence of mesopore blocking for both systems. TEM as well as XRD measurements provide explanations for this finding. First of all, very large nickel oxide particles have been found for the catalyst *ex* nitrate, which have to be situated at or next to the external surface of the support material. Growth of these very large particles inside the mesopores of the support material is very unlikely, because TEM as well as XRD (figure 3) indicate that the characteristic, hexagonal structure of the support material is retained after nickel application, thus indicating framework stability. Growth inside the MCM-41 particles would have resulted in extensive damage of the framework and broadening of the pore size distribution, which is not observed. Therefore,

these large nickel oxide particles likely have been formed by a different mechanism. The most probable explanation is that after incipient wetness impregnation a large amount of the nickel ions has been entrained out of the mesopores with the solvent flow during the drying treatment. As a result, large nickel nitrate crystallites have precipitated at or next to the external surface during drying, thus giving rise to the formation of the very large nickel oxide crystallites of this catalyst during calcination. However, also a significant quantity of nickel ions has been retained inside the mesopores after drying, giving rise to the formation of very small nickel oxide particles inside the mesoporous support structure. Therefore, due to the limited interaction between nickel ions and the silica pore walls during the mild catalyst preparation process a catalyst with a very broad particle size distribution is obtained, consequently exhibiting a relatively low dispersion of nickel (oxide).

For matter of completeness it should be mentioned that recent research by Van der Lee *et al.* alludes to the possibility of the occurrence of dispersion decreases during the *calcination* treatment of supported heterogeneous catalysts *ex* nitrate [15]. Therefore, it is recommended to extend research on MCM-41 catalysts *ex* nitrate further to investigate whether unfavourable processes during calcination also take place with this mesoporous material. Such a study would reveal to what extent a calcination treatment adds to the observed low disperions of the resulting catalysts, next to the adverse processes occurring during drying.

When a chelated nickel citrate precursor is used for catalyst preparation strikingly different results are obtained. Only very small nickel oxide nanoparticles can be observed after calcination, which are situated inside the mesopores of the support material. As a result the nickel oxide dispersion of this catalyst is higher than in the case of a nitrate precursor. The explanation for these observations can be found in the behaviour of the impregnated solution, containing the chelating citrate precursor, during drying and subsequent calcination. The viscosity of such a solution is higher than that of a nickel nitrate solution with the same nickel content. Moreover, upon solvent removal during drying the viscosity of the solution with chelated complex rapidly increases, contrary to the behaviour of a nickel nitrate solution. As a result, the solvent flow out of the mesopores during drying will be much less or even absent for a solution with chelated precursor compound. Furthermore, due to the high viscosity of the impregnated solution diffusion of the chelated complexes inside the mesopores is very much hindered during drying, which results in a homogeneous distribution of precursor compound in the mesopores, where it interacts with silanol groups

at the pore surface *via* hydrogen bonding. After drying the chelated nickel precursor is therefore expected to have formed a thin film on the pore surface of the support. Because of the hydrogen bonding this film is tightly adhered to the pore surface. Upon calcination of the thus immobilised catalyst precursor the thin film of nickel citrate breaks up and decomposes due to the combustion of the organic ligand. The resulting catalyst contains only very small nickel oxide nanoparticles situated inside the mesopores. Moreover, the pore volume for this catalyst decreases much more than for the catalyst *ex* nitrate, indicating that a significantly larger amount of nickel oxide must be present inside the mesopores.

It is remarkable, though, that the textural and structural properties of the support material have been completely retained after calcination of the thin film of nickel citrate precursor, since a rather large adiabatic rise in temperature is generally observed during the combustion of these types of precursor materials. This sudden rise in temperature might very well have damaged the structure of MCM-41. Nevertheless, XRD learns that the structural order of the mesoporous support material is retained and TEM (figure 7) and nitrogen physisorption clearly show the presence of the 2.7 nm mesopores after calcination. Furthermore, these characterisation techniques do not provide evidence for the formation of additional pores, nor for a decrease of long-range order of the materials, indicating that the support structure has not been damaged during the combustion of the organic part of the precursor.

The nickel oxide dispersion of the prepared catalysts was probed further with XPS. Because of the high porosity of MCM-41 the penetration depth with XPS is in the order of 5 - 10 nanometers (equivalent to 2 - 4 cylindrical pores). Therefore not only the external surface of the catalysts is probed, but also the pores near the external surface. The small value of the Ni:Si ratio for the catalyst *ex* nitrate (0.05) reflects the large average particle size of NiO, located at the external surface. With the catalyst *ex* citrate a notably higher Ni:Si ratio (0.09) is obtained, which is close to the calculated bulk ratio of 0.114. This finding indicates first of all that the dispersion of nickel oxide is distinctly higher after catalyst preparation with a film-forming chelating ligand. Moreover, it can be concluded that the small nickel oxide nanoparticles situated inside the mesopores are fully "transparent" for the x-rays penetrating the catalyst material. Secondly, the Ni:Si ratio for the catalyst *ex* citrate is lower than the calculated bulk value, which is an indication that only a small amount of nickel is probed and that a considerable amount of nickel is present

deep inside the MCM-41 mesopores, implying that nickel deposition has not been restricted to the outer parts of the support material.

TPR analysis was used to attain information about the reducibility of the nickel oxide phase(s) of the calcined catalysts. In the case of the catalyst *ex* nitrate two large reduction stages are observed. The large low-temperature reduction stage coincides with the reduction of bulk NiO, indicating the presence of nickel oxide with a bulk character. Clearly, the large NiO particles previously detected with the other characterisation techniques are responsible for this reduction stage. Accordingly, the second reduction stage is associated with the presence of very small nickel oxide particles. The high temperature of reduction for the catalyst *ex* citrate again demonstrates that this catalyst mainly contains small nickel oxide particles, which was already apparent from the other characterisation techniques. Nevertheless, the very small low-temperature reduction peak might point to the presence of some slightly enlarged particles too, which were not observed with the other characterisation techniques, although the presence of some Ni^{3+} can not be ruled out either.

Finally, isothermal (650°C) reduction experiments of the catalysts showed that the nickel oxide nanoparticles of the catalyst *ex* citrate could be converted gently into metallic nickel nanoparticles without damaging the structure of the support material. This finding indicates that despite the intimate interaction between precursor and support material no "mutual" surface compound, exhibiting a nickel phyllo- or hydro-silicate structure, had formed after calcination, since reduction of these kinds of compounds would result in extensive restructuring of the support material. However, there is a sufficiently large interaction between nickel and the support material to prevent sintering of the active phase during the reduction treatment. Therefore, after reduction the resulting nickel nanoparticles are still confined inside the mesopores of MCM-41, thereby retaining the high dispersion of nickel that had been achieved during the catalyst preparation procedure.

Various research efforts over the years have demonstrated that solutions of chelated metal ions provide excellent precursors for the preparation of heterogeneous catalysts by means of incipient wetness impregnation, *e.g.* [16]. The film-forming abilities of these precursors on a support material, notably during drying after impregnation, result in homogeneous distributions of active phase over catalyst support bodies. Moreover, the resulting catalysts after calcination (and reduction) contain only very small particles of metal (oxide) supported by such common "flat" support materials as SiO_2, α- and γ-Al_2O_3, TiO_2 and ZrO_2. Also the dispersions of the

active phases thus obtained are very high. The results described in this chapter indicate that the use of chelated metal precursors for the preparation of heterogeneous catalysts can suitably be extended to mesoporous support materials. The mechanisms underlying the fundamental processes occurring during catalyst preparation appear to be the same for both types of support material. Moreover, the used preparation method with nickel citrate can be considered as a "mild" technique for the preparation of catalysts supported by a mesoporous host material, exhibiting a high dispersion of active phase, since the support structure is fully preserved during catalyst preparation. Therefore no limitations appear to exist to apply a wide variety of other elements into the pores of several types of mesoporous support materials, with retention of the unique textural and structural properties of the support materials. Catalysts thus prepared will feature very high dispersions of active phase as well as very small particles with sizes even smaller than on conventional support materials (due to the limiting size of the pores of mesoporous support materials).

Conclusions

For the preparation of nickel catalysts supported by mesoporous MCM-41 material the choice of nickel precursor was found to significantly influence the characteristics of the resulting catalysts. With a weakly interacting nickel precursor (nickel nitrate) a very broad particle size distribution was obtained, with both very large nickel particles situated outside the mesopores of the support and very small nickel nanoparticles inside the mesopores. The very weak interaction between nickel ions and the silica pore surface is thought to cause a considerable amount of these ions to be entrained with the solvent flow during drying after incipient wetness impregnation, giving rise to a decreased dispersion of thus prepared catalysts. In addition, calcination might also have an (additional) adverse effect (sintering).

Impregnation with a solution of chelated nickel citrate precursor results in catalysts with only very small nickel oxide nanoparticles confined inside the mesopores of MCM-41. Upon reduction the high dispersion is retained. The viscosity of the impregnation solution during drying prevents transport of precursor complexes out of the mesopores, thus giving rise to the formation of a thin film of nickel citrate that is tightly bound to the surface of the mesopores. Combustion of the precursor film during calcination results in a high dispersion of nickel oxide nanoparticles over the support material.

Therefore it is concluded, in contrast to Cui *et al.* [4], that it is not the nickel oxide phase by itself that determines the ultimate catalyst dispersion, but the precursor of this phase, notably its behaviour during drying and calcination.

Nickel loadings of thus prepared mesoporous catalysts are relatively high, *viz.* 10 wt%, and the favourable and unique structural and textural properties of MCM-41 are completely retained upon catalyst preparation. A comparison with results obtained with ordinary support materials in the past indicates that no fundamental differences during catalyst preparation are apparent, which offers a possibility for the future application of a wide variety of other elements inside the pores of mesoporous materials with chelated precursor complexes.

Acknowledgements

Gerbrand Mesu is kindly thanked for all the valuable contributions he has made to the research described in this chapter and the very pleasant co-operation. Adri van Laak, Alwies van der Heijden, Joke Ferwerda and Mayken Wadman are also thanked for their enthusiastic participation in the research. Leon Coulier (Eindhoven Technical University) is kindly acknowledged for performing the XPS analyses of the catalysts. John Raaymakers is kindly thanked for nitrogen physisorption as well as TPR measurements. Fred Broersma is thanked for thermogravimetrical analyses. Cor van der Spek and Sandra Kemp are acknowledged for making TEM micrographs of the catalysts. Ries Janssen is also thanked for TEM characterisations and valuable discussions.

Literature

[1] C.T. Kresge, M.E. Leonowicz, W.J. Roth, J.C. Vartuli and J.S. Beck, *Nature*, 359, 1992, 710

[2] J.S. Beck, J.C. Vartuli, W.J. Roth, M.E. Leonowicz, C.T. Kresge, K.D. Schmitt, C.T-W. Chu, D.H. Olson, E.W. Sheppard, S.B. McCullen, J.B. Higgins and J.L. Schlenker, *J. Am. Chem. Soc.*, 114, 1992, 10834

[3] M. Ziolek, I. Nowak, P. Decyk and J. Kujawa, *Stud. Surf. Sci. Catal.*, 117, 1998, 509

[4] J. Cui, Y.-H. Yue, W.-Y. Dong and Z. Gao, *Stud. Surf. Sci. Catal.*, 105, 1997, 687

[5] Y. Yue, Y. Sun and Z. Gao, *Catal. Lett.*, 47, 1997, 167

[6] U. Junges, S. Disser, G. Schmid and F. Schüth, *Stud. Surf. Sci. Catal.*, 117, 1998, 391

[7] T. Halachev, R. Nava and L. Dimitrov, *Appl. Catal. A*, 169, 1998, 111

[8] A. Corma, A. Martínez, V. Martínez-Soria and J.B. Montón, *J. Catal.*, 153, 1995, 25

[9] T. Klimova, J. Ramírez, M. Calderón and J.M. Domínguez, *Stud. Surf. Sci. Catal.*, 117, 1998, 493

[10] M. Hartmann, A. Pöppl and L. Kevan, *J. Phys. Chem.*, 99, 1995, 17494

[11] M. Hartmann, A. Pöppl and L. Kevan, *J. Phys. Chem.*, 100, 1996, 9906

[12] M. Hartmann, A. Pöppl and L. Kevan, *Stud. Surf. Sci. Catal.*, 101, 1996, 801

[13] C.-F. Cheng, D.H. Park and J. Klinowski, *J. Chem. Soc., Faraday Trans.*, 93, 1997, 193

[14] A.C. Voegtlin, A. Matijasic, J. Patarin, C. Sauerland, Y. Grillet and L. Huve, *Micropor. Mater.*, 10, 1997, 137

[15] M.K. van der Lee, A.J. van Dillen and K.P. de Jong, *manuscript in preparation*

[16] A.J. van Dillen, R.J.A.M. Terörde, D.J. Lensveld, J.W. Geus and K.P. de Jong, *J. Catal.*, 2003, in press

4

The preparation of MCM-41 supported molybdenum catalysts with Mo^{3+} as precursor

Abstract

MoO_3 was applied onto all-silica MCM-41 *via* an incipient wetness impregnation procedure with a reduced molybdenum precursor complex, *viz.* Mo^{3+}, followed by drying and calcination. The impregnating solution containing the trivalent molybdenum precursor complex was obtained by electrochemical reduction of a suspension of Mo^{6+} (*ex* ammonium heptamolybdate, AHM) in a 1 : 1 mixture of hydrochloric acid and water. As a reference MCM-41 was impregnated with an aqueous AHM solution.

Combined characterisation results (N_2 physisorption, XRD) indicate that the favourable structural and textural properties of MCM-41 have been completely retained after catalyst preparation with Mo^{3+}. Moreover, no molybdena particles were detected (TEM, XRD) and a slight decrease of the mesopore diameter was observed, indicating the formation of a layer of MoO_3 inside the mesopores. A high dispersion of MoO_3 was corroborated by EDX. No chloride was retained after calcination. In contrast, impregnation with AHM led to a complete destruction of the MCM-41 support material.

Introduction

Since the first discovery of MCM-41 in 1991 [1, 2] and the subsequent evolution of related materials a lot of attention has been paid to the application of catalytically active phases inside the (uniform) mesopores. One element that has attracted special attention in this respect is molybdenum. Because of increasingly severe legislation concerning the specifications of sulphur in transportation fuels the development of new, molybdenum- or tungsten-based hydrotreating catalysts is currently of utmost importance. Therefore several researchers have tried to take advantage of the unique textural properties of (ordered) mesoporous materials (high surface area and accessibility) to enhance the dispersion of the catalytically active cobalt- or nickel-promoted MoS_2-phase and thus also increasing catalytic activity. For these and other reasons a lot of efforts have been undertaken so far to introduce molybdenum inside the mesopores of MCM-41 and related materials. Unfortunately, information concerning the stability of the support after introduction of molybdenum precursors and the resulting catalysts has been rather shallow.

In general, the methods to prepare molybdenum-loaded mesoporous catalysts can be divided into four groups: 1. Incorporation during synthesis, 2. Solid state dispersion (*i.e.* "spreading"), 3. Impregnation with (suitable) precursor solution and 4. More "exotic" preparation techniques. These methods will all be shortly reviewed here.

Incorporation during synthesis has been described by several authors [3 - 12]. The method most widely employed incorporates molybdate anions into the framework under alkaline conditions during ambient or hydrothermal synthesis [3 - 7]. Usually only very low loadings of molybdenum can be achieved in this way, *i.e.* below 0.2% Mo [3 - 6], the exception being Cho *et al.* who managed to prepare stable Mo-MCM-41 catalysts (as determined with XRD and nitrogen physisorption) with Mo loadings up to 10 wt% [7]. However, the presented nitrogen isotherms indicate that a second pore system, containing slit-shaped pores, might be present in the support and catalysts. Other groups mentioned a rather low thermostability for thus-prepared catalysts (*i.e.* structural collapse below 400°C [3]) and surface concentrations of molybdenum (XPS) far higher than the bulk concentration (ICP), indicating phase segregation during synthesis and the subsequent deposition of Mo onto the external surface of the support material [4].

Therefore a different approach towards Mo-MCM-41 catalysts was undertaken by Piquemal *et al.* [8, 9] and Zhang *et al.* [10], who synthesised their catalysts under acidic or neutral conditions. It was beautifully explained

by Piquemal *et al.* that incorporation of molybdate species inside the silica framework is most efficient when "molybdate" is present as small, low-condensed oxo-peroxo species or alternatively as oxo or polyoxo species, with the preference for the oxo-peroxo species [8, 9]. For the oxo-peroxo method the amounts of molybdenum incorporated inside the silica walls are so high that the Si/Mo ratio of the produced catalysts is lower than the corresponding value of the synthesis gel, whereas these values are approximately the same for the oxo or polyoxo method. These results were corroborated by Zhang *et al.* [10] who also found that more molybdenum was incorporated in the framework when an acidic synthesis route was followed, as compared to a neutrally templated pathway. Much less satisfying results concerning molybdenum incorporation were obtained when syntheses were performed under alkaline conditions [8]. Besides the issue of molybdenum incorporation it was shown by Piquemal *et al.* [9] that Mo-MCM-41 showed a better structural order (XRD, TEM) when prepared by the oxo-peroxo route, whereas both oxo-peroxo and oxo or polyoxo routes yielded materials with high nitrogen adsorption capacities, indicating good textural properties. It should be noted here that all mentioned "acidic" syntheses were performed at room temperature in order to allow for the formation of the desired molybdenum species. This "low temperature" synthesis method might also explain the somewhat smaller pore sizes of the Mo-MCM-41 samples compared to the samples obtained after hydrothermal synthesis.

Since molybdenum incorporated during synthesis is situated inside the silica walls of the MCM-41 framework these materials are frequently used for oxidation catalysis [3, 5 - 7, 9, 10]. However, because of the framework incorporation it is impossible, without destroying the mesoporous structure, to convert incorporated molybdenum into other molybdenum phases (such as MoO_3 or MoS_2) which possess other interesting catalytic properties. Therefore a lot of research has also been devoted to the application of molybdenum onto instead of within the pore walls.

One of these methods relates to the spreading behaviour of MoO_3 in contact with an oxidic support at elevated temperatures. At temperatures of approximately 450°C or higher, MoO_3, in contact with the support, tends to migrate into the pores, to react with surface hydroxyl groups and to form molybdenum (sub-)oxide monolayers or isolated (poly-)molybdate species on the surface of the support. Although this method is most successful for alumina type of supports satisfying results have also been reported for siliceous MCM-41 and related mesoporous supports [4, 13 - 16]. It was found that upon application of MoO_3 the structural order of the MCM-41 support was

retained [4, 13]. A high dispersion of MoO_3 inside the mesopores of the supports was inferred from the absence of diffractions originating from crystalline molybdenum species in XRD analyses [4, 13 - 15]. However, the MoO_3 loadings at which the diffraction lines appeared were different for the various publications. Wong *et al.* mentioned that at MoO_3 loadings of 9 wt% no molybdenum oxide diffractions could be observed [13]. Cui *et al.* [14] and Yue *et al.* [15] reported that even up to MoO_3 loadings as high as 20 wt% no MoO_3 diffractions were observed on MCM-41 [14] and KIT-1 [15] mesoporous supports respectively. However, in contrast with these observations, Djajanti and Howe noted the incomplete dispersion of MoO_3 at a loading as low as 7.5 wt% [4]. This is quite strange because the conditions during catalyst preparation were almost similar in all these cases: 6 hours at 460°C for Cui *et al.* [14] and Yue *et al.* [15] and 8 hours at 450°C for Djajanti and Howe [4], all with MoO_3 as starting material.

When the textural properties of catalysts prepared by solid state dispersion are considered it is seen that for MCM-41 support materials the high surface areas and pore volumes are completely retained upon application of MoO_3 loadings as high as 9 [13] or 10 wt% [14], indicating coverage of the pore walls by a (non-complete) monolayer of molybdenum oxide. At higher loadings the decrease of surface area and pore volume is higher than expected on the basis of the calculated density increase of the materials [14]. This finding indicates that at MoO_3 loadings exceeding 10 wt% narrowing of the mesopores by the formation of molybdenum oxide multilayers or, alternatively, pore-blocking occurs, indicating that the dispersion of the active phase is lowered as well as its accessibility. For KIT-1 supported catalysts this decrease of surface area and pore volume at higher MoO_3 loadings is even more pronounced [15].

A third way of catalyst preparation involves the application of a wide variety of inorganic or organometallic molybdenum complexes, which can be grafted or adsorbed onto the mesopore surface of the support materials. Here we will limit ourselves to those cases where the prepared catalysts are to be used as heterogeneous catalysts. For a description of the preparation and application of organometallic complexes tethered to the surface of a mesoporous material and which are to be used as heterogenised homogeneous catalysts the reader is referred to the more specific literature on this topic, *e.g.* [17]. Two examples involving the use of an organometallic precursor will be described here, though. The first method relates to the surface adsorption and subsequent decomposition of molybdenum

hexacarbonyl. Furthermore a short overview of the grafting of various molybdenum complexes with different nuclearities will be given.

The adsorption of $Mo(CO)_6$ onto the pore surface of a mesoporous support can be accomplished by means of either chemical vapour deposition (CVD) [4, 18] or adsorption from solution [19, 20]. Upon heating of the thus loaded support material the carbonyl compound decomposes and molybdenum is deposited on the pore surface. The oxidation state of molybdenum after dissociation of the complex depends on the chemical nature of the support material: *e.g.* for SiO_2 the average calculated valency is in the range of +0.20 to +0.25, whereas it amounts to + 1.66 for γ-Al_2O_3 and +1.5 for ZrO_2 [19]. After $Mo(CO)_6$ adsorption onto silica there is only a weak interaction with the surface which results in a delayed decomposition of the carbonyl compound with respect to other oxidic support materials [19]. An implication of this decreased interaction with silica is a relatively high activation energy for carbonyl decomposition, which means that the carbonyl ligands are removed at temperatures at which the rate of sublimation of the $Mo(CO)_6$ complex from the support surface is so high, that only about 25% of the initially present molybdenum is deposited, resulting in very low molybdenum loadings of approximately 0.50 wt% [19]. The limited interaction of $Mo(CO)_6$ with the silica surface and the concomitant low catalyst loadings can be explained by the cation field strength of the support material. It was found that the activation energy for the dissociation of the first CO ligand was linearly dependent on the field strength of the surface cations of various oxidic support materials, being the highest for SiO_2 [19]. As a consequence the decomposition mechanisms of $Mo(CO)_6$ over various supports are also different, but the implications of these differences will not be addressed further here. However, it was recognised by Djajanti and Howe [4, 18] that incorporating hetero-atoms such as Al and Na inside the MCM-41 structure significantly influences the $Mo(CO)_6$ uptake by the support material, *i.e.* much higher amounts of $Mo(CO)_6$ are adsorbed and more molybdenum is retained on the support after thermal treatment. Nevertheless, the molybdenum loadings thus obtained are still very low: 0.1 wt% for SiO_2-MCM-41 compared to 0.5 wt% for Al-MCM-41 (Si/Al = 7) and 1 wt% for Na-Al-MCM-41 [18]. However, it was found that upon repeated adsorption and activation more molybdenum can be deposited, *viz.* 2.7 wt% for Na-Al-MCM-41 [18]. Also Landau *et al.* used $Mo(CO)_6$ as a precursor for the preparation of MCM-41 supported molybdena catalysts [20]. To this end an $Mo(CO)_6$ in decalin solution was added to the support material and subsequently treated

ultrasonically under oxidising conditions. As a result MoO_3/MCM-41 catalysts with MoO_3 loadings as high as 65 wt% were claimed to be obtained.

Grafting of a number of molybdenum complexes onto the pore surface of mesoporous supports has been described by several authors [4, 17, 21, 22]. Zama *et al.* showed that the nuclearity of the complex (*i.e.* the number of molybdenum centres in one complex moiety) can play an essential role in directing the catalytic performance of the resulting heterogeneous catalyst [21]. The catalytic reaction studied was the metathesis of propene over an FSM-16 supported molybdenum catalyst. It was found that a dinuclear precursor complex ($Mo_2(OAc)_4$) yielded the highest TOF for the catalytic reaction. A trinuclear precursor complex ($[Mo_3O(CCH_3)(OAc)_6(CH_3OH)_3]Cl$) showed only a moderate activity, whereas the activity of tetranuclear ($[Rh(C_5H_5)]_4Mo_4O_{16}$) and heptanuclear ($(NH_4)_7Mo_7O_{24}$) precursor complexes was negligible. It should be noted that in order to obtain the catalytically active phase out of the precursor complexes an activation procedure had to be performed. It was shown that the activation should be brought about with great care since catalytic activity was highly dependent on the activation temperature. At too low temperatures the ligands were not sufficiently removed, thereby blocking the active sites for the reactant. On the other hand, at too high temperatures polynuclear molybdate species or highly dispersed MoO_3 particles are formed, which are inactive for metathesis due to the absence of Mo-Mo bonds. So, for this specific reaction optimum catalytic activity is achieved by combining the most appropriate catalyst precursor with a suitable activation procedure. Unfortunately, no information about the structural and / or textural properties of the support material after complex grafting and / or activation procedure was provided by the authors.

Another important feature of molybdena catalysts is surface coverage. It was shown by Shannon *et al.* that the oxidative dehydrogenation of methanol over molybdenum catalysts supported on MCM-41 was strongly influenced by the nature of the molybdate species present, and therefore also on the catalyst loading [22]. At low loadings (*i.e.* 1.43 wt% MoO_3) isolated molybdenum-oxo species were present at the support surface, whereas at higher loadings (*i.e.* 9.05 wt% MoO_3) polymeric molybdate species are present as well. In order to achieve high dispersions of molybdate, catalyst preparation was performed by diffusion of a molybdenum-metallocene complex ($Mo(C_5H_5)_2Cl_2$) from a chloroform solution. The grafted molybdocene complex, which was bonded to the surface by reaction with two silanol groups, was converted into molybdate by calcination, resulting in isolated molybdate moieties at low loadings. During these procedures the structural

order of the MCM-41 support material was retained, as shown by x-ray diffraction.

A final method of catalyst preparation with complexes involves grafting of $MoCl_5$ onto MCM-41 [4]. During this process the all-silica MCM-41 support behaves like a common silica gel, *i.e.* only a limited amount of molybdenum is incorporated: 1 - 3%, as determined with XPS. No details concerning support stability were mentioned for this method.

From the above described synthesis procedures for molybdenum catalysts supported by mesoporous materials it is clear that these procedures have various limitations, originating from the practical operations and / or as a result of the rather low loadings of the catalysts. Therefore, the most frequently used catalyst preparation method for molybdenum loaded mesoporous materials involves contacting the support with a solution containing inorganic molybdate salts; a process commonly referred to as (incipient wetness) impregnation. During this process a relatively simple, inorganic molybdenum precursor compound is admitted inside the mesopores, which is converted into MoO_3 upon subsequent calcination. The precursor material that is most commonly used is ammonium heptamolybdate (AHM), which is easily dissolved in water. The reason that this precursor compound is so frequently used is because results obtained in the preparation of hydrotreating catalysts with AHM are very satisfactory. However, hydrotreating catalysts are usually supported by various types of alumina and it should be noted here that the interactions between alumina and MoO_3 and its precursors are remarkably different than for silica or silica-based materials (see *e.g.* [23]). Since mesoporous support materials are generally silica-based, the results obtained after catalyst preparation *via* impregnation with AHM are generally much less satisfactory (*vide infra*). Here a short overview of the publications dealing with the application of molybdenum inside the pores of various mesoporous supports *via* impregnation will be given first. Since the interaction between alumina and molybdenum precursors is far more favourable than with silica-based materials, publications concerning support systems which are a physical mixture of alumina and a mesoporous material will not be dealt with here [24 - 26].

As stated above, by far the most common precursor for the application of molybdenum inside mesoporous supports is AHM [4 - 6, 27 - 34]. Only Kostova *et al.* used a different, Keggin-type precursor for the impregnation of zirconium-substituted HMS supports, *viz.* 12-phosphomolybdic acid [35]. Unfortunately, the amount of details relating to the characterisation of the structural stability of thus obtained catalysts is generally very shallow [4, 5, 28

- 31] and often restricted to only a BET surface area or a diffractogram, without further discussion. However, exceptions are also encountered in the literature. Both Wang *et al.* [32] and Kostova *et al.* [35] ascribe an observed decrease of surface area and pore volume after impregnation with AHM to the occurrence of pore blocking (next to the increase in density of the materials because of the molybdena loading, 20 and 18 wt%, respectively). Klimova *et al.* [33] who applied molybdena (12 wt%) on both all-silica and titanium-modified MCM-41 attribute decreases in surface area and pore volume to plugging at the pore openings as well, although they also allude to the possibility of (partial) destruction of the support material, since a significant decrease of structural integrity of the support materials is observed with x-ray diffraction. This observation is also made by Rana and Viswanathan [6], in combination with a decrease in pore size and pore volume (already at MoO_3 loadings as low as 0.10%), although they do not ascribe these results to destruction of the MCM-41 support material, but to a coverage of the pore walls by molybdenum species.

A comprehensive study on MCM-41 supported heterogeneous catalysts, including molybdena catalysts prepared *via* impregnation with AHM, by Wong *et al.* [13] clearly showed that the all-silica MCM-41 support material was not stable towards an AHM-impregnation procedure. X-ray diffractograms showed that the unique structure of MCM-41 almost completely disappeared, whereas nitrogen isotherms indicated a severe loss of capillary condensation in the initially present uniform mesopores. Moreover, a large decrease of surface area and pore volume was observed for thus prepared catalysts. Even worse results were obtained after impregnation with a sodium molybdate solution. Therefore it is concluded that this method is not a viable one for the preparation of molybdenum catalysts supported by (all-silica) mesoporous materials, because a (nearly) complete destruction of the mesoporous support structure occurs during molybdenum application. These findings were to a large extent corroborated by the work of Cheng *et al.* [34], in which AHM was applied to a number of MCM-41 materials with different Si:Al ratios. For materials with a low to medium aluminium content exactly the same results were obtained as those reported by Wong *et al.*, *viz.* a tremendous decrease of surface area, pore volume and pore diameter, along with the disappearance of the capillary condensation pore filling step in the nitrogen isotherms (MoO_3 loading = 9 wt%). Only for a material with a relatively high aluminium content (*i.e.* Si:Al = 27) the textural properties of the mesoporous support material are fully retained at this molybdena loading. Nevertheless, at higher loadings the decrease of surface area is no longer

compensated by the weight loading of the materials and rather large decreases of surface area, pore volume and pore diameter are observed again. Next to a partial destruction of the support material the dispersion of molybdena also decreases, since crystallites of MoO_3 are observed with x-ray diffraction.

Summarising, it can be concluded that there are several methods for the application of molybdenum inside the pores of mesoporous support materials, each with its *pros* and *cons*. Incipient wetness impregnation with AHM is the most frequently used technique, although the results obtained with this method are quite disappointing. Nevertheless, impregnation remains a very attractive method for the preparation of heterogeneous catalysts. Therefore we have explored a novel way for the deposition of molybdenum inside the mesopores of MCM-41 *via* incipient wetness impregnation. With our method the favourable textural and structural properties of the support material are fully preserved, even at molybdena loadings as high as 25 wt%.

Reviewing the literature we recognised that there clearly is a highly unfavourable interaction between (hepta)molybdate precursor ions and pore wall silica, which results in the destruction of the unique support structure. Therefore our research focused on the development of an incipient wetness impregnation procedure with a suitable, alternative molybdenum precursor. Previous research in our group revealed that unfavourable interactions between molybdate and vanadate precursors and "ordinary" silica support materials are common [23]. Catalyst preparation with these precursors results in the formation of large crystallites of the active phase over the support surface, with a concomitant low dispersion and catalytic activity. In order to overcome these problems the dissolved molybdate (or vanadate) precursors were reduced to effectuate their application on silica supports. Two methods were followed to bring about the conversion of molybdate (vanadate) to lower valency species, *viz. pre*-reduction [36 - 38] and *in-situ* reduction [39]. During *pre*-reduction molybdate was converted into Mo^{3+}-chloride complexes by an electrolysis process. Since Mo^{3+} is stable only in acidic media a diluted (6 mol l^{-1}) HCl solution was used. After preparation of this Mo^{3+}-solution silica was suspended in it and the pH of the solution was slowly raised by continuous injection of a diluted basic solution. As a result molybdenum was precipitated on the silica surface as $Mo(OH)_3$ by means of the so-called Homogeneous Deposition Precipitation (HDP) process, first developed by Geus and Van Dillen [40]. After calcination a well-dispersed catalyst was obtained with molybdena homogeneously distributed over the support

surface. For the *in-situ* reduction method both molybdate and hydrazine (the reductant) were admitted in the pores of pre-shaped silica catalyst support bodies, either by consecutive or co-impregnation of pH-adjusted solutions. During the resulting deposition precipitation process $Mo(OH)_3$ precipitated on the support surface due to the following reaction:

$$4\ MoO_4^{2-} + 3\ N_2H_4 + 4\ H_2O \rightarrow 4\ Mo(OH)_3 + 3\ N_2 + 8\ OH^-$$

The characteristics of thus prepared catalysts were dependent on a number of parameters and will not be discussed here. Nevertheless, both preparation methods yielded suitable, silica-supported molybdena catalysts.

In view of these results we decided to explore the possibility to extend the use of reduced molybdenum complexes as precursors for the preparation of heterogeneous molybdena catalysts to silica-based mesoporous support materials; notably MCM-41. However, we realised that the above described methods of homogeneous deposition precipitation (*pre*-reduction) and *in-situ* reduction would most likely not be applicable to mesoporous MCM-41, because both methods rely on either the addition or the generation of hydroxide ions. Since it is well known that MCM-41 and related materials are unstable with respect to mineralising agents (such as OH^-), we took another approach and impregnated acidic Mo^{3+}-solutions, prepared by the *pre*-reduction method, onto all-silica MCM-41. The resulting molybdena catalysts show both unprecedented high MoO_3 loadings and dispersions, in combination with the complete preservation of the unique structural and textural properties of the support material.

Experimental

Support synthesis

All-silica MCM-41 was prepared following a slightly adapted literature procedure [41]. First a synthesis gel was made starting from pyrogenic silica (Aerosil 380, Degussa), cetyltrimethylammoniumbromide (CTABr, Acros, 99+%), tetraethylammoniumhydroxide-solution (TEAOH, 20 wt% in water, Acros) and demineralised water. The TEAOH-solution was diluted with demineralised water and CTABr was dissolved at ambient temperature. Subsequently SiO_2 was added over a period of about one hour and the resulting synthesis gel was aged at room temperature for 24 hours under stirring. The molar composition was 1 SiO_2 : 0.27 CTABr : 0.19 TEAOH : 40

H_2O. This gel was transferred to a teflon-lined autoclave and treated hydrothermally at a temperature of 150°C for 2-3 days.

The resulting white product was washed with demineralised water and filtered numerous times, dried (12 hours, 120°C, ramp = 1°C min^{-1}) and calcined (6 hours, 550°C, ramp = 1°C min^{-1}); all in air.

Mo^{3+}-solution

100 ml of a 1 : 1 mixture of demineralised water and hydrochloric acid (37%, Merck, *p.a.*) was added to a suitable ammonium precursor salt, *i.e.* ammonium heptamolybdate (AHM, Acros, *p.a.*) (alternatively MoO_3, H_2MoO_4 or $MoO_3 \cdot xH_2O$ can be used). Typically 6.5 - 41 g of AHM, depending on MoO_3 loading, was used. The resulting suspension was flushed for a sufficiently long period of time with nitrogen in order to remove oxygen. Into this suspension a porous ceramic compartment containing a platinum anode was immersed. The anodic compartment was also filled with the 1 : 1 mixture of demineralised water and concentrated hydrochloric acid. Into the cathodic compartment a platinum gauze electrode was immersed, as well as a pH-electrode and a nitrogen inlet tube. Before and during the electrolysis process the electrolysis cell was sufficiently shielded from air and nitrogen was led through the reaction mixture in order to prevent re-oxidation of the formed trivalent molybdenum species. For the electrochemical reduction of molybdenum a potential difference of 3 Volts was applied over the electrodes for a sufficiently long period of time (2 hours - approximately 1 day, depending on the MoO_3 loading of the resulting catalyst). During the electrolysis process the initially present suspension turned into an intensely red solution. For further experimental details we refer to the work of Vogt [38, 42].

Catalyst preparation

Mo^{3+}-solutions were impregnated onto the MCM-41 support by means of the incipient wetness technique. Prior to impregnation the powdered support material (typically 1 gram) was degassed for at least 15 minutes in vacuum. The impregnations were also carried out under static vacuum. Catalyst loadings were 5, 10, 15, 20 and 25 % MoO_3 by weight. As a reference material a 20 wt% MoO_3/MCM-41 catalyst prepared by impregnation with AHM was used. After impregnation the catalyst samples were dried at 120°C for 12 hours and calcined at 450°C for 6 hours, all in air (heating rates: 1°C min^{-1}). MoO_3 loadings of the catalysts were corroborated

with x-ray fluorescence spectroscopy (XRF) and inductively coupled plasma spectroscopy (ICP).

Characterisation techniques

Nitrogen physisorption

Textural analyses of the samples were performed on a Micromeritics ASAP 2400 apparatus. Measurements were carried out at -196°C. Prior to analysis the samples were outgassed *in vacuo* at 300°C. Surface areas were calculated using standard BET and t-plot theory; pore volumes and pore size (distributions) were calculated according to BJH theory.

XRD

The structural order of the MCM-41 support material and catalyst samples, as well as the presence or absence of crystalline molybdenum phases were determined with a Philips PW 1820 powder diffraction system using Cu Kα radiation and an Enraf Nonius PDS 120 powder diffraction system using Co Kα_1 radiation, respectively.

TEM / EDX

Electron microscopy and EDX analyses were performed with Philips CM200 and Tecnai 20F transmission electron microscopes equipped with a FEG operated at 200 keV. For the measurements sample material was applied onto a holey carbon film supported by a copper grid. The EDX facility was not calibrated, implying that the obtained results are *semi*-quantitative.

XPS

X-ray photo-electron spectroscopy was used to assess whether chlorine was still present on the catalyst samples after calcination. The XPS data were obtained with a Vacuum Generators XPS system using a CLAM-2 hemispherical analyser for electron detection. Non-monochromatic Al K$_\alpha$ x-ray radiation was used for generating the photo-electrons at an anode current of 20 mA at 10 keV. The pass energy of the analyser was set at 50 eV. The survey scan was taken with a pass energy of 100 eV.

Results and Discussion

Support stability

From the x-ray diffraction patterns, shown in figure 1, it can be seen that an MCM-41 support material with excellent ordering was prepared. Four distinct major diffraction peaks are visible, which can be assigned to the (100), (110), (200) and (210) reflections of the hexagonal MCM-41 framework structure. After incipient wetness impregnation with a solution of trivalent molybdenum in hydrochloric acid and subsequent calcination procedure at least three of the diffraction peaks are fully retained as can be seen in the patterns of the calcined samples, albeit with a slightly lower intensity. This intensity decrease can however be explained by the deposition of molybdena inside the mesopores, leading to a decreased density difference between the pores and the pore walls. Because of this smaller density difference

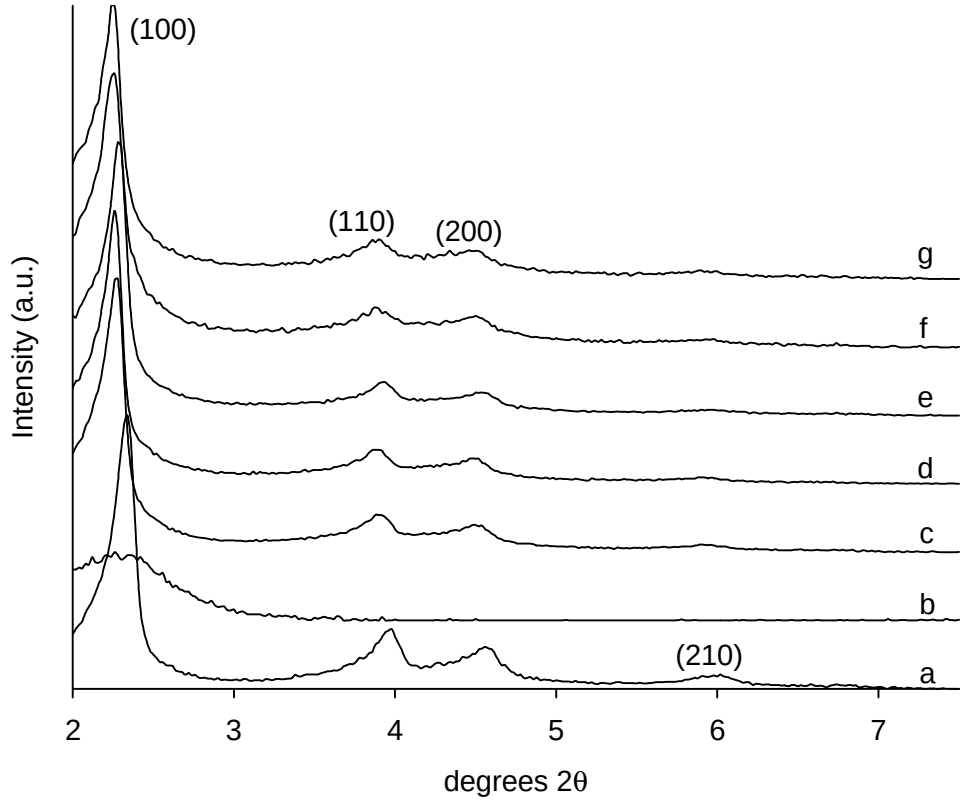

Figure 1: X-ray diffraction patterns showing the diffractions arising from the hexagonal structure of the MCM-41 support material. a = parent MCM-41 (calcined), b = 20 wt% MoO_3 *ex* AHM, c = 5 wt% MoO_3 *ex* Mo^{3+}, d = 10 wt% MoO_3 *ex* Mo^{3+}, e = 15 wt% MoO_3 *ex* Mo^{3+}, f = 20 wt% MoO_3 *ex* Mo^{3+}, g = 25 wt% MoO_3 *ex* Mo^{3+}.

compared to the parent MCM-41 the diffraction intensities are somewhat lower. The conservation of the framework structure after molybdenum application is also apparent from electron microscopic investigations on the calcined samples, as can be seen in figure 2. The hexagonal arrangement of the uniform mesopores as well as the mesopores themselves are clearly visible. On the other hand, when AHM was admitted inside the mesopores as molybdenum precursor the structural characteristics of the support were completely lost, as can also be seen in figure 1 (pattern b). This structural collapse of mesoporous supports when contacted with a solution containing (poly)molybdate anions has also been described previously by a number of other authors [13, 33, 34]. The explanation for the structural instability towards molybdate is that these molybdate anions (or poly-anions) are far too reactive towards silica, which results in attack of the support pore walls during impregnation (and subsequent drying and calcination procedure), leading to the destruction of the mesoporous structure. During this process the formation of (an) x-ray amorphous phase(s) occurs, the majority of which will resemble amorphous silica. However, the chemical nature of another significant part of the resulting material will presumably be close to that of silicomolybdic acid or analogous compounds.

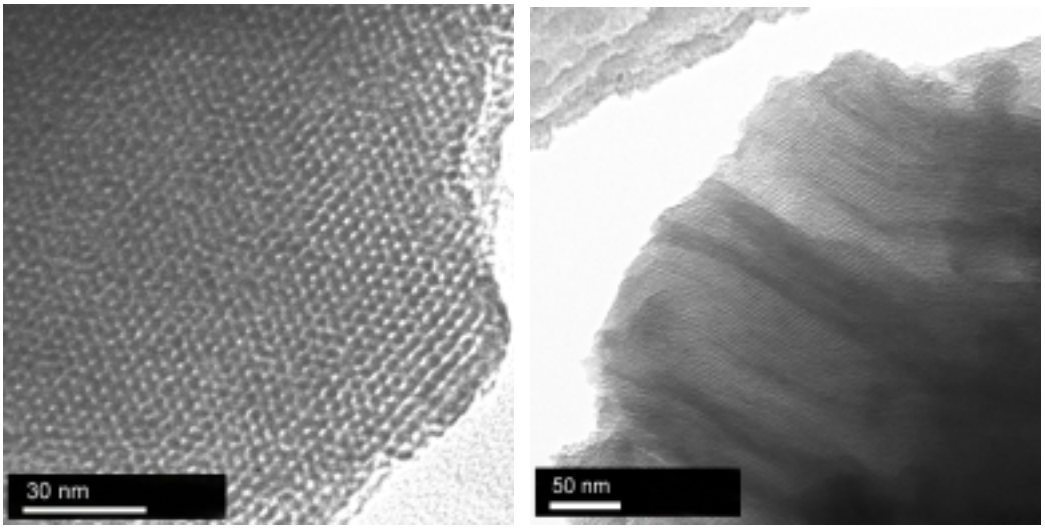

Figure 2: Transmission electron micrographs showing the MCM-41 material after application of molybdenum from a solution with trivalent precursor. The mesopores, which are well-retained upon catalyst preparation, are clearly visible.

The textural properties of the parent MCM-41 support material and the resulting molybdenum-loaded catalysts were studied with nitrogen physisorption. The isotherms, measured at -196°C, are presented in figure 3. It is seen that the parent MCM-41 shows a very distinct capillary condensation pore filling step at a p / p_0 value of approximately 0.35 and that this capillary condensation is retained after application of molybdenum *via* impregnation with a trivalent precursor, albeit at slightly lower p / p_0. From the isotherms the surface areas according to the BET-method were calculated and these values are given in table 1. However, a drawback of the BET-method is that micropores that might be present also add to the surface area. Therefore, we also used the slope of the t-plot to determine the surface area in pores with a diameter exceeding 2 nm, as described before [43]. These surface areas are also included in table 1. From a comparison of the two differently calculated surface areas it is immediately clear that the BET-method gives misleading results, as is evident from the data on the AHM-impregnated catalyst. The t-plot surface area of this catalyst is considerably lower than the BET surface

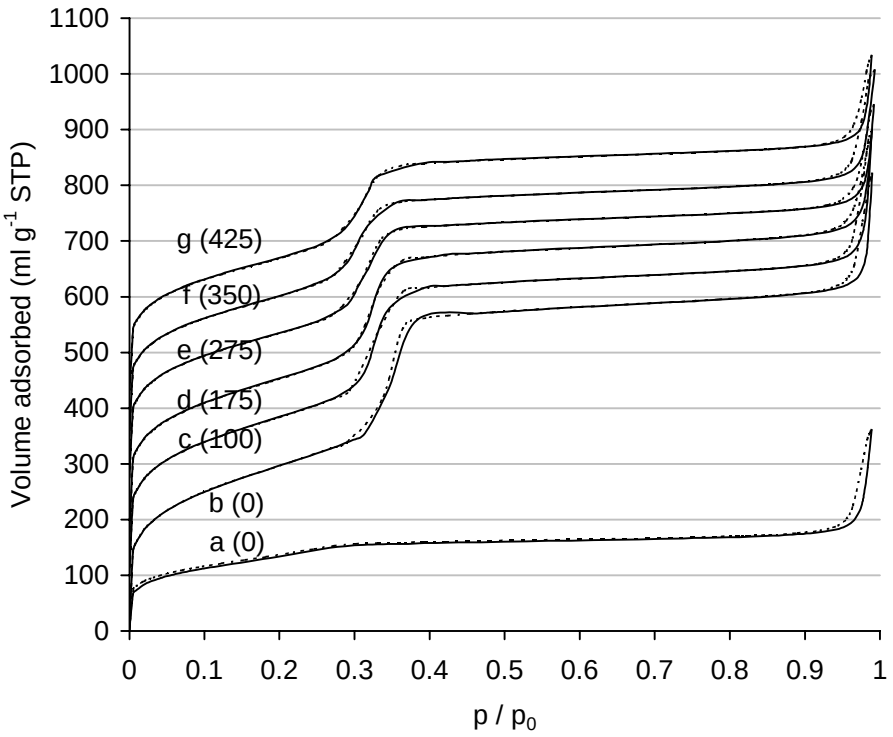

Figure 3: Nitrogen physisorption isotherms. The isotherms have been shifted with respect to each other for clarity reasons; the start of each isotherm is indicated by the value in parentheses. a = 20 wt% MoO_3 *ex* AHM (0), b = parent MCM-41 (0), c = 5 wt% MoO_3 *ex* Mo^{3+} (100), d = 10 wt% MoO_3 *ex* Mo^{3+} (175), e = 15 wt% MoO_3 *ex* Mo^{3+} (275), f = 20 wt% MoO_3 *ex* Mo^{3+} (350), g = 25 wt% MoO_3 *ex* Mo^{3+} (425). Solid lines = adsorption data, dotted lines = desorption data.

Table 1: Textural properties of parent MCM-41 and catalyst samples.

sample	BET surface area ($m^2\ g^{-1}$)	t-plot surface area [a] ($m^2\ g^{-1}$)	pore volume ($ml\ g^{-1}$)	average pore diameter (nm)
parent MCM-41	1,076	1,079	1.24	2.70
5 wt% MoO_3 *ex* Mo^{3+}	1,037	1,013	1.20	2.60
10 wt% MoO_3 *ex* Mo^{3+}	1,016	980	1.06	2.55
15 wt% MoO_3 *ex* Mo^{3+}	944	907	1.00	2.50
20 wt% MoO_3 *ex* Mo^{3+}	918	895	0.98	2.45
25 wt% MoO_3 *ex* Mo^{3+}	889	860	0.91	2.40
20 wt% MoO_3 *ex* AHM	487	35	0.54	mp [b]

[a] surface area in pores larger than 2 nm [43]

[b] mp = micropores (see figure 4)

area, in contrast with the other samples. During the discussion of the x-ray diffraction data it was shown that impregnation with AHM led to a complete destruction of the support structure. Moreover, from the pore size distribution plot of the AHM-impregnated catalyst (figure 4, line b) it is also evident that most mesopores have disappeared and that a broad pore size distribution, including micropores, has been obtained instead. These findings, combined with the absence of capillary condensation in the isotherm, demonstrate that the MCM-41 support material is not stable with respect to heptamolybdate precursor anions and that the catalysts obtained with this precursor are of a very poor quality. However, when only the BET surface area of this catalyst would have been considered one might erroneously be tempted to think that catalyst preparation had been rather successful. Therefore we would like to stress the importance of the need to expand the amount of details related to the textural properties beyond merely the BET surface area in future publications on this topic.

When the t-plot surface areas of the catalyst samples and the parent support material are compared it is seen that only a relatively small decrease of surface area occurs when MCM-41 is impregnated with a Mo^{3+} precursor solution (table 1). This decrease can however be fully ascribed to the effect of molybdena weight loading. The same trend is observed for the pore volumes of the samples, as can also be seen in table 1. The BJH pore size distributions of the parent MCM-41 support material and the catalysts are shown in figure 4. It is seen that the parent MCM-41 has a sharp pore size distribution and that this sharp distribution is preserved upon application of molybdenum *via* Mo^{3+}. However, a small decrease of pore diameter is observed after loading of the MCM-41 support, indicating that molybdena is situated inside the pores after catalyst synthesis. Nevertheless, it should be

stressed again here that no pore plugging occurs. The average pore diameters of the samples are also listed in table 1.

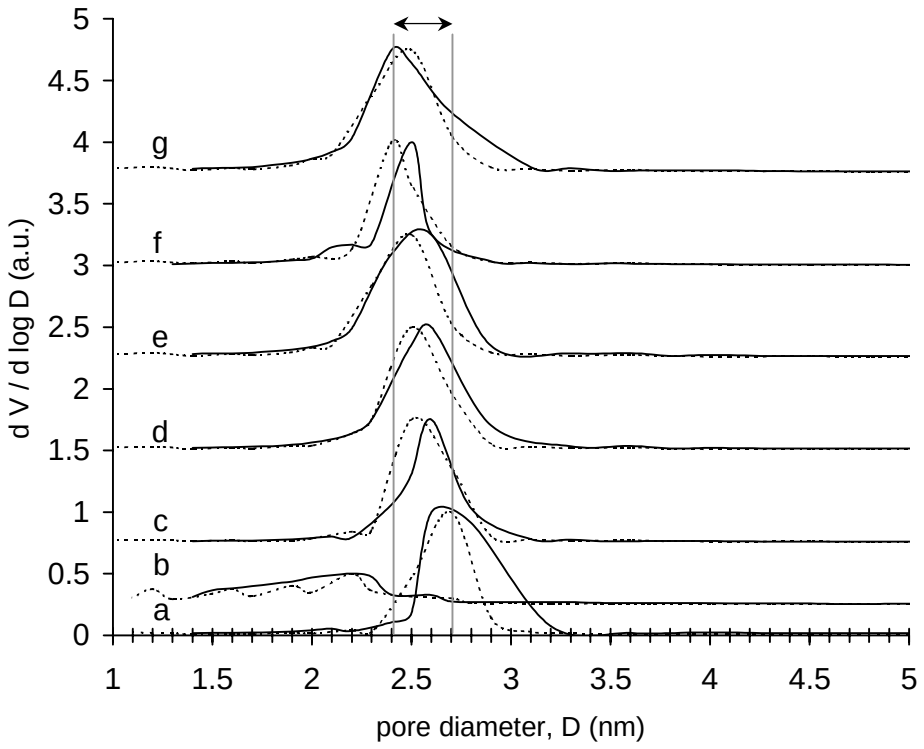

Figure 4: Pore size distributions. a = parent MCM-41, b = 20 wt% MoO_3 *ex* AHM, c = 5 wt% MoO_3 *ex* Mo^{3+}, d = 10 wt% MoO_3 *ex* Mo^{3+}, e = 15 wt% MoO_3 *ex* Mo^{3+}, f = 20 wt% MoO_3 *ex* Mo^{3+}, g = 25 wt% MoO_3 *ex* Mo^{3+}. Solid lines = adsorption data, dotted lines = desorption data. (Data have been normalised).

These findings regarding the structural and textural characteristics of the MCM-41 support material indicate that MCM-41 shows a high structural stability towards trivalent molybdenum precursors in hydrochloric acid and that its favourable textural properties (mesoporosity and good accessibility) have been retained. After the catalyst synthesis procedure molybdena is present inside the mesopores. In contrast to these findings, impregnation with AHM results in a non-ordered material containing micropores.

<u>Mo^{3+}-solution</u>

The chemical nature of the impregnated Mo^{3+}-solution was found to influence the results of the catalyst preparation experiments significantly. When a solution of hydrochloric acid was used satisfying results were obtained (*vide supra*). Both the structural integrity and the excellent textural properties of the MCM-41 support material are retained upon impregnation,

drying and calcination. Moreover, a high molybdena dispersion is obtained. Nevertheless, hydrochloric acid has some less favourable properties, such as its corrosivity and volatility. Moreover, chlorine might be retained on the catalysts after preparation, acting as a potential poison during catalytic applications.

Therefore the experiments were also performed with an electrolysis solution consisting of a 1 : 1 mixture of sulphuric acid and demineralised water. Unfortunately, less satisfactory results were obtained (not shown here). The ordering of the support material had declined after calcination and also the surface areas calculated by both the BET- and t-plot methods had decreased significantly. Nitrogen physisorption indicated that part of the mesopores of the MCM-41 support had been retained (capillary condensation step and pore size distributions), but that a considerable amount of micropores had been generated as well. These combined characterisation results indicate that the support structure had been severely damaged by the catalyst preparation process. An explanation for these findings is that the ability of sulphate anions to form stable molybdenum(III) complexes is far less than for chloride anions. As a result the dissolved Mo^{3+}-ions can conceivably be re-oxidised by water and / or atmospheric oxygen after impregnation and during drying and the early stages of calcination (when still some water is present inside the mesopores). The molybdenum species thus generated react with the very thin all-silica pore walls of MCM-41, thereby provoking a partial collapse of the support material. In contrast, chloride ions have far stronger complex-forming properties which enhance the stability of the molybdenum(III) complexes and prevent their re-oxidation. As a result the favourable features of the support material are conserved during the catalyst synthesis processes. Nevertheless, it should be noted here that the properties of catalysts obtained with the Mo^{3+}-solutions in sulphuric acid were still much better than those of catalysts prepared by impregnation with aqueous AHM-solutions.

Finally, the catalysts obtained with Mo^{3+} in hydrochloric acid solution were tested for the presence of chlorine after calcination. Two different methods were used. Photo-electron spectra (not shown) of calcined catalysts, obtained with XPS, contained no peaks that could be assigned to chlorine. Nevertheless, XPS is a surface sensitive technique and as a result the presence of traces of chlorine deep inside the mesopores could not be excluded. Therefore, a bulk analysis of the catalysts was also performed. In order to analyse the MoO_3 loadings with ICP the catalyst samples had to be dissolved. To the resulting solutions a silver nitrate solution was added. The

presence of chloride anions in the solution would have resulted in the precipitation of AgCl. No precipitate was observed, however.

Molybdenum dispersion

The various characterisation techniques indicate that after catalyst preparation with Mo^{3+} in hydrochloric acid solution molybdena is well dispersed over the MCM-41 support material. Even at the highest loadings (*i.e.* 25 wt% MoO_3) the absence of MoO_3 reflections, or any other reflections of molybdenum phases for that matter, in XRD indicates that no large molybdena particles have formed and that molybdena is likely to have well spread over the surface of the support. This is rather surprising, since the dispersive ability of molybdena on silica support materials is generally very low, resulting in the formation of large crystallites of MoO_3 after thermal treatment. However, also with TEM analyses no large particles on or next to the support material could be detected. Since the external surface area of MCM-41 amounts to approximately only 10 m^2 g^{-1} [44] well-dispersed molybdena can only to a very small extent be situated at the external surface and therefore has to be incorporated inside the mesopores. Because of the low dispersive ability on silica the aggregation of molybdena into nanoparticles inside the support mesopores is expected. Nevertheless, textural analysis learns that upon molybdenum application the pore diameter has only slightly decreased from 2.7 nm to about 2.4 nm (figure 4 and table 1) and pore volumes remain invariably high (table 1), *i.e.* pore plugging does not occur. From these results it is evident that molybdena must be present as a well-spread (incomplete) layer inside the mesopores of the support. Apparently, despite the normally encountered weak interaction between MoO_3 and SiO_2, the surface area of MCM-41 is sufficiently large to accommodate a well-dispersed layer of molybdena, even at loadings as high as 25 wt% MoO_3.

It should be mentioned here that the amounts of molybdena applied onto the support material are insufficient to bring about the formation of complete monolayers inside the mesopores. Nevertheless, a small decrease of pore diameter is observed at increasing molybdena loadings. The explanation for this finding must be that there is an enrichment of molybdena near the openings of the mesopores. Most likely this enrichment originates from the processes occurring during drying of the catalysts. During drying water evaporates at the openings of the mesopores. As a result a flow of impregnated solution from deep within the pores to the pore openings is generated. Although part of the impregnated molybdenum precursor

complexes will remain inside the mesopores because of interactions with the silica pore wall surfaces, another part will be entrained with the solvent flow to the openings of the mesopores, where the evaporation process takes place. Due to the evaporation process and the resulting flow of impregnate the concentration of molybdenum precursor near the pore openings steadily increases and as a result the highest concentration of precursor material inside the support material after drying will also be situated near the pore openings. During calcination precursor material is converted into molybdena, which is to some extent able to disperse itself over the support surface by spreading. Unfortunately, spreading of MoO_3 over silica support materials is not a very efficient process and as a result (part of) the initial enrichment of molybdenum at the pore openings after drying is still observed after calcination. EDX studies on the 20 wt% catalyst support this conclusion. In figure 5 some representative micrographs of the catalyst are presented. For EDX analyses the electron beam was focused to a small spot. The positions where the catalyst was studied are indicated by the black and white circles. From the resulting EDX-spectra (not shown) two conclusions can be drawn:

1. Despite intensity differences the bulk Si : Mo ratio was found to be constant (spots 2-4), indicating that darker spots in the bright-field TEM images are not caused by MoO_3 particles, but that the electron beam has been travelling through a thicker part of the specimen.
2. In both examples shown the Si : Mo ratio in spot 1 was approximately 50% lower than in the other spots, indicating that a larger amount of MoO_3 is present at the outer regions of the mesopores, as was already suggested in the discussion above.

Finally, macroscopically a uniform distribution of molybdena over the MCM-41 support material was observed qualitatively with EDX analysis. The results revealed that segregation of molybdena over the support material had not occurred to a large extent, as molybdenum was found to be distributed nearly homogeneously over all the MCM-41 particles that were studied. Some examples can be seen in figure 6. This (nearly) homogeneous molybdenum distribution is another indication that the molybdena dispersion over the support material is high, thus inferring that incipient wetness impregnation is a very suitable method for the preparation of molybdena catalysts supported by a mesoporous material, despite the slightly increased concentration of precursor material near the pore openings after drying.

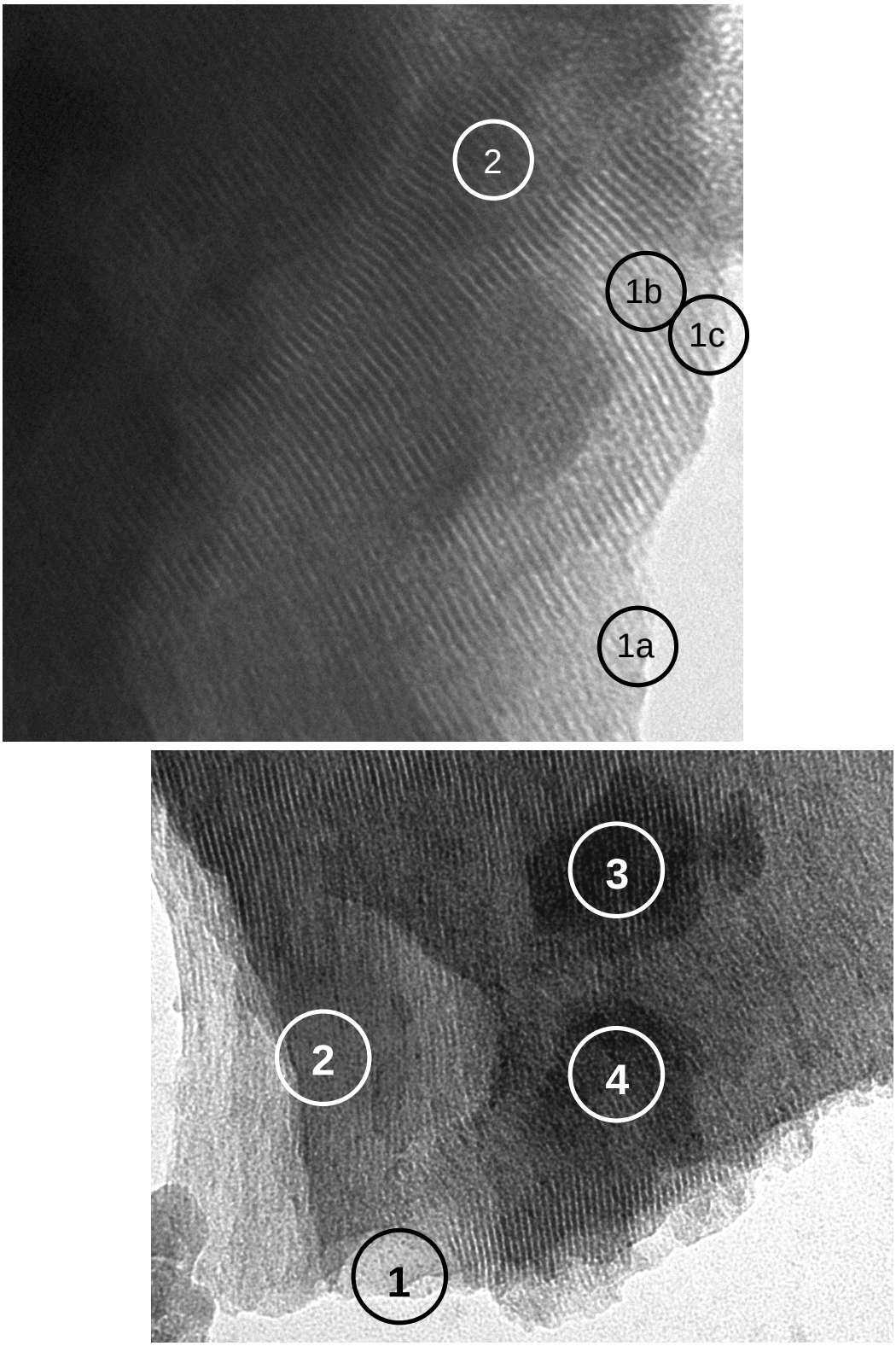

Figure 5: Transmission electron micrographs of the 20 wt% catalyst *ex* Mo^{3+}, showing the MCM-41 mesopores as well as the spots used for EDX analyses. In both cases the Si : Mo ratio in spot 1 was only 50% of the value in the other spots.

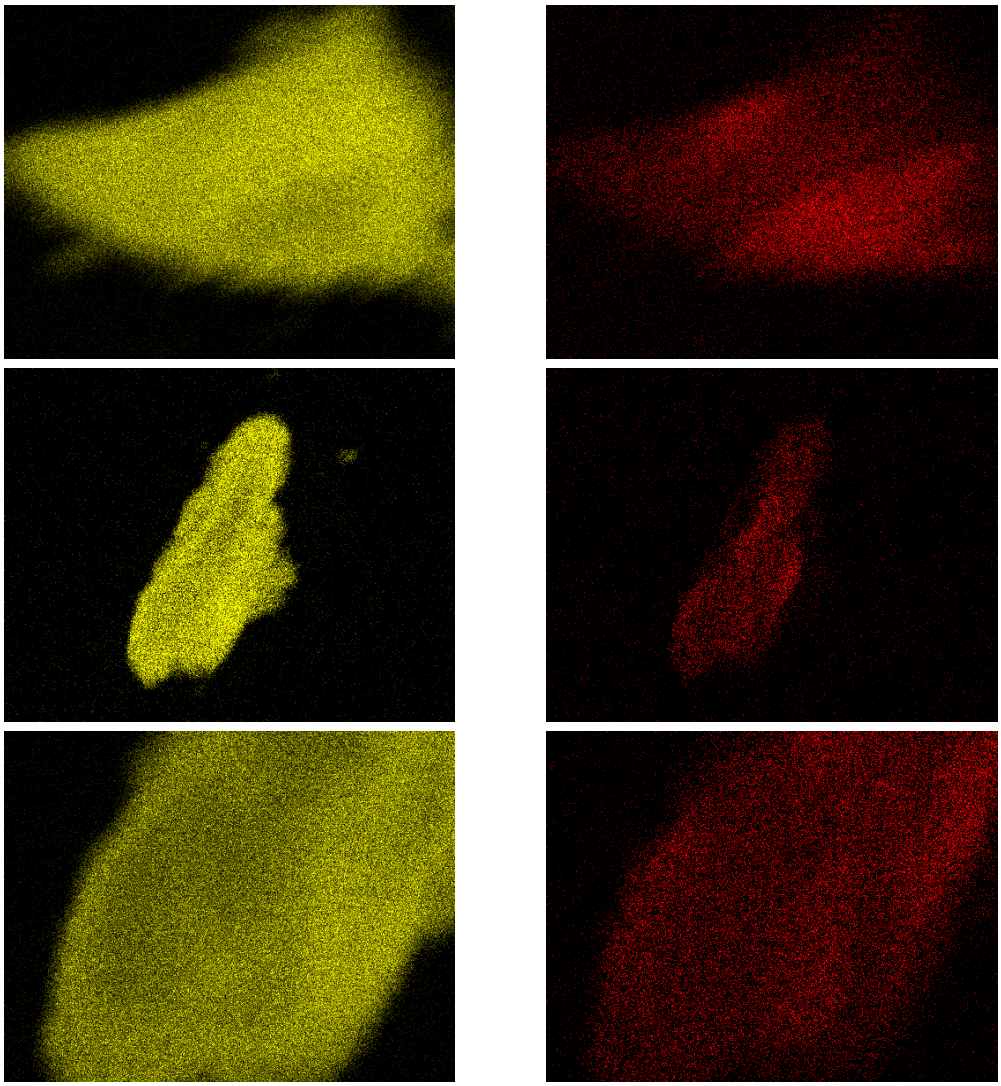

Figure 6: Micrographs showing the elemental mapping of some catalyst particles, obtained with EDX. Photographs on the left = Si K edge, photographs on the right = Mo K edge.

Conclusions

Heterogeneous MCM-41 supported molybdena catalysts have been synthesised *via* a new incipient wetness impregnation procedure. We have shown that the choice of molybdenum precursor is of eminent importance in order to fully retain the unique structural and textural properties of the all-silica mesoporous support material. Impregnation with a common ammonium heptamolybdate precursor solution, a method which is commonly applied in literature, results in a complete destruction of the support material. Our newly developed preparation method, described in this chapter, overcomes this major problem by *pre*-reducing the molybdate precursor solution *via* an electrochemical process. When the resulting precursor solution, containing

Mo^{3+}-chloride complexes, is impregnated onto the all-silica support material no unfavourable interactions between the silica pore walls and the molybdenum precursor complexes occur. As a result the molybdena catalysts obtained after drying and calcination have retained their structural integrity and display all the interesting properties of the parent support material, *viz.* a high surface area, mesoporosity and accessibility. Moreover, we have been able for the first time to prepare MoO_3/MCM-41 catalysts with unprecedented high loadings (*viz.* 25 wt%) ánd dispersions *via* the attractive method of incipient wetness impregnation.

It was shown that the acid used to stabilise the generated Mo^{3+}-ions during electrolysis significantly influenced the properties of the prepared catalysts. A comparison between hydrochloric and sulphuric acid learnt that chloride is a much better counter-anion for Mo^{3+} than sulphate, since the bonds between Mo^{3+} and chloride anions are sufficiently strong to form molybdenum(III) complexes which are stable enough to withstand re-oxidation during the catalyst preparation process. With sulphate anions this is not the case and as a result MCM-41 supported molybdena catalysts prepared with a Mo^{3+}-solution in (diluted) sulphuric acid are of a poorer quality, albeit still much better than catalysts prepared by AHM-impregnation. It was found for the catalysts prepared with the Mo^{3+}-solutions in hydrochloric acid that no chlorine was present after calcination.

Several characterisation techniques indicate that catalysts prepared *via* the "Mo^{3+} in HCl" -method exhibit a very high dispersion of molybdena, which appears to be distributed almost homogeneously over the support material and which has to be situated to a very large extent inside the mesopores of the MCM-41 support material. Textural analysis indicates that pore plugging does not occur, but that molybdena is deposited as a thin layer inside the mesopores resulting in only a slight decrease of pore diameter, even for MoO_3 loadings as high as 25 wt%. However, there is a slightly increased concentration of molybdena near the openings of the mesopores, resulting from the processes occurring during drying of the catalysts. From a catalytic point of view this enrichment at the pore openings might prove to be not a disadvantage, since the situation of part of the active phase close to the openings of the mesopores might alleviate the occurrence of diffusion limitations during catalytic conversions. Nevertheless, our findings contradict the normally observed behaviour for molybdena catalysts supported by silica, where the dispersion of the active phase is generally low. Two independent phenomena account for the more favourable features of our MCM-41 supported molybdena catalysts. First of all, the Mo^{3+} precursor does not only

prevent destruction of the ordered support structure, but probably also gives rise to attractive electrostatic interactions with the support during impregnation and drying [23]. Secondly, unlike other silica support materials the unique structure of the MCM-41 support material offers a very large surface area onto which MoO_3, generated during calcination, can become dispersed.

Acknowledgements

Jeannette Smulders is kindly thanked for her enthusiastic and highly appreciated collaboration in the described research. Birgit Wieczorek and Marcel Peterse are also thanked for their efforts during the first explorative experiments. Ad Mens and John Raaymakers are kindly acknowledged for nitrogen physisorption measurements. Ad Mens is also thanked for XPS analyses of the catalysts. Sandra Kemp, Professor Geus and Hans Meeldijk are kindly thanked for characterisation of the catalysts with TEM / EDX. Marjan Versluijs-Helder is thanked for XRD characterisations. The Catalysts Division of Akzo Nobel Amsterdam is acknowledged for performing XRF measurements.

Literature

[1] C.T. Kresge, M.E. Leonowicz, W.J. Roth, J.C. Vartuli and J.S. Beck, *Nature*, 359, 1992, 710

[2] J.S. Beck, J.C. Vartuli, W.J. Roth, M.E. Leonowicz, C.T. Kresge, K.D. Schmitt, C.T-W. Chu, D.H. Olson, E.W. Sheppard, S.B. McCullen, J.B. Higgins and J.L. Schlenker, *J. Am. Chem. Soc.*, 114, 1992, 10834

[3] S. Ayyappan and N. Ulagappan, *Proc. Indian Acad. Sci. (Chem. Sci.)*, 108, 1996, 505

[4] S.D. Djajanti and R.F. Howe, *Stud. Surf. Sci. Catal.*, 105, 1997, 2067

[5] R.K. Rana, A.C. Pulikottil and B. Viswanathan, *Stud. Surf. Sci. Catal.*, 113, 1998, 211

[6] R.K. Rana and B. Viswanathan, *Catal. Lett.*, 52, 1998, 25

[7] D-H. Cho, T-S. Chang, S-K. Ryu and Y.K. Lee, *Catal. Lett.*, 64, 2000, 227

[8] J-Y. Piquemal, E. Briot, M. Vennat, J-M. Brégeault, G. Chottard and J-M. Manoli, *Chem. Commun.*, 1999, 1195

[9] J-Y. Piquemal, J-M. Manoli, P. Beaunier, A. Ensuque, P. Tougne, A-P. Legrand and J-M. Brégeault, *Micropor. Mesopor. Mater.*, 29, 1999, 291

[10] W. Zhang, J. Wang, P.T. Tanev and T.J. Pinnavaia, *Chem. Commun.*, 1996, 979

[11] R. Tsumara, S. Higashimoto, M. Matsuoka, H. Yamashita, M. Che and M. Anpo, *Catal. Lett.*, 68, 2000, 101

[12] S. Higashimoto, R. Tsumara, S.G. Zhang, M. Matsuoka, H. Yamashita, C. Louis, M. Che and M. Anpo, *Chem. Lett.*, 2000, 408

[13] S-T. Wong, H-P. Lin and C-Y. Mou, *Appl. Catal. A*, 198, 2000, 103

[14] J. Cui, Y-H. Yue, Y. Sun, W-Y. Dong and Z. Gao, *Stud. Surf. Sci. Catal.*, 105, 1997, 687

[15] Y. Yue, Y. Sun and Z. Gao, *Catal. Lett.*, 47, 1997, 167

[16] C-L. Zhang, S. Li, Y. Yuan, W-X. Zhang, T-H. Wu and L-W. Lin, *Catal. Lett.*, 56, 1998, 207

[17] P. Ferreira, I.S. Gonçalves, F.E. Kühn, M. Pillinger, J. Rocha, A. Thursfield, W-M. Xue, and G. Zhang, *J. Mater. Chem.*, 10, 2000, 1395

[18] S.D. Djajanti and R.F. Howe, *Stud. Surf. Sci. Catal.*, 97, 1995, 197

[19] H-G. Ang, K-S. Chan, G-K. Chuah, S. Jaenicke and S-K. Neo, *J. Chem. Soc., Dalton Trans.*, 1995, 3753

[20] M.V. Landau, L. Vradman, M. Herskowitz, Y. Koltypin and A. Gedanken, *J. Catal.*, 201, 2001, 22

[21] K. Zama, Y. Imada, A. Fukuoka and M. Ichikawa, *Appl. Catal. A*, 194-195, 2000, 285

[22] I.J. Shannon, T. Maschmeyer, R.D. Oldroyd, G. Sankar, J.M. Thomas, H. Pernot, J-P. Balikdjian and M. Che, *J. Chem. Soc., Faraday Trans.*, 94, 1998, 1495

[23] M. de Boer, R.G. Leliveld, A.J. van Dillen, J.W. Geus and H.G. Bruil, *Appl. Catal. A*, 102, 1993, 35

[24] T. Klimova, J. Ramírez, M. Calderón and J-M. Domínguez, *Stud. Surf. Sci. Catal.*, 117, 1998, 493

[25] M. Cheng, F. Kumata, T. Saito, T. Komatsu and Y. Tatsuaki, *Appl. Catal. A*, 183, 1999, 199

[26] J. Ramírez, R. Contreras, P. Castillo, T. Klimova, R. Zárate and R. Luna, *Appl. Catal. A*, 197, 2000, 69

[27] T. Halachev, R. Nava and L. Dimitrov, *Appl. Catal. A*, 169, 1998, 111

[28] A. Klemt, A. Taouli, H. Koch and W. Reschetilowski, *Stud. Surf. Sci. Catal.*, 127, 1999, 405

[29] K. Madhusudan Reddy, B. Wei and C. Song, *Catal. Today*, 43, 1998, 261

[30] T. Ookoshi and M. Onaka, *Chem. Commun.*, 1998, 2399

[31] C. Song and K. Madhusudan Reddy, *Appl. Catal. A*, 176, 1999, 1

[32] A. Wang, Y. Wang, T. Kabe, Y. Chen, A. Ishihara and W. Qian, *J. Catal.*, 199, 2001, 19

[33] T. Klimova, E. Rodríguez, M. Martínez and J. Ramírez, *Micropor. Mesopor. Mater.*, 44-45, 2001, 357

[34] M. Cheng, F. Kumata, T. Saito, T. Komatsu and T. Yashima, *Stud. Surf. Sci. Catal.*, 117, 1998, 485

[35] N.G. Kostova, A.A. Spojakina, K. Jiratova, O. Solcova, L.D. Dimitrov and L.A. Petrov, *Catal. Today*, 65, 2001, 217

[36] E. Vogt, J. van Dillen, J. Geus, J. Biermann and F. Janssen, in *"Proc. Int. Congr. Catal." (Editors: M.J. Phillips and M. Ternan)*, 4, 1988, 1976

[37] E.T.C. Vogt, M. de Boer, A.J. van Dillen and J.W. Geus, *Appl. Catal.*, 40, 1988, 255

[38] J.J.P. Biermann, F.J.J.G. Janssen, M. de Boer, A.J. van Dillen, J.W. Geus and E.T.C. Vogt, *J. Mol. Catal.*, 60, 1990, 229

[39] K.P. de Jong, *Stud. Surf. Sci. Catal.*, 63, 1991, 19

[40] A.J. van Dillen, J.W. Geus, L.A.M. Hermans and J. van der Meijden, in *"Proc. Int. Congr. Catal." (G.C. Bond, P.B. Wells and F.C. Tompkins, Eds.)*, 2, 1977, 677

[41] C-F. Cheng, D.H. Park and J. Klinowski, *J. Chem. Soc., Faraday Trans.*, 93, 1997, 193

[42] E.T.C. Vogt, *Ph.D. Thesis*, University of Utrecht, The Netherlands, 1988, Chapter 2.

[43] J.C.A.A. Roelofs, D.J. Lensveld, A.J. van Dillen and K.P. de Jong, *J. Catal.*, 203, 2001, 184

[44] A.C. Voegtlin, A. Matijasic, J. Patarin, C. Sauerland, Y. Grillet and L. Huve, *Micropor. Mater.*, 10, 1997, 137

5

The preparation of MCM-41 supported molybdenum catalysts with an AHM in HCl precursor solution

Abstract

A new method, involving an unusual molybdenum precursor, for the application of molybdenum inside the mesopores of all-silica MCM-41 was serendipitously discovered. The precursor, which is thought to be MoO_2Cl_2, was prepared by carefully adding ammonium heptamolybdate salt to a 1 : 1 mixture of demineralised water and hydrochloric acid. The resulting slightly yellow solution was impregnated onto powdered MCM-41 support material by the incipient wetness technique, followed by drying and calcination.

Thus prepared catalysts exhibit both high MoO_3 loadings, *i.e.* up to 20 wt%, and high dispersions, as evidenced by the absence of MoO_3 reflections in XRD. In addition, the unique hexagonal structure of the support material is fully retained, indicating framework stability towards the impregnated precursor solution. Textural analyses indicate that pore plugging does not occur, implying that molybdenum oxide is present as well-spread, incomplete layers inside the mesopores. A relatively small decrease of surface area, which was observed after catalyst preparation, could be fully ascribed to molybdenum weight loading of the materials.

Introduction

The invention of ordered mesoporous (support) materials in the early 1990's [1, 2] has resulted in a lot of research efforts to apply catalytically active phases inside the mesopores of these and related mesoporous materials. Environmental legislation has focused the attention especially on the development of catalysts for the abatement of sulphur compounds in transportation fuels; especially diesel. Combustion of sulphur compounds inside engines results in both the presence of polluting SO_2 (responsible for acid rain) in exhaust gases and increased emissions of solid particles (mainly soot). To decrease these emissions sulphur is removed from transportation fuels in refineries by various so-called hydrotreating processes. During hydrotreating hydrogen and a feedstock for transportation fuel are co-fed over (a) catalyst(s) resulting in a.o. the removal of sulphur from the feedstock with the concomitant formation of H_2S. Thus produced H_2S is removed from the product stream and subsequently converted into environmentally harmless elemental sulphur in a SuperClaus plant. Since industrial hydrotreating catalysts are molybdenum-based various methods to apply molybdenum inside the pores of mesoporous support materials have been studied during the last decade. An extensive overview of the literature on the preparation of molybdenum catalysts supported by mesoporous materials is presented in the introductory section of **chapter 4**.

The methods for molybdenum application can, somewhat ambiguously, be divided into two groups:

I. Methods which preserve the unique structural and textural properties of mesoporous support materials. Unfortunately these methods usually are either cost-intensive or difficult / laborious. In addition, molybdenum loadings of catalysts are generally low.

II. Impregnation with ammonium heptamolybdate (AHM). With this method high loadings of molybdenum can be achieved. Unfortunately, mesoporous support materials are not stable with respect to AHM, resulting in their destruction upon impregnation.

In order to combine the best of both methods, *i.e.* high molybdenum loadings as well as the preservation of the support structure, we explored a new approach to the preparation of (all-silica) MCM-41 supported molybdenum catalysts. Our method involved the use of a reduced Mo^{3+} precursor, which was impregnated onto the powdered support material by the incipient wetness technique. Upon drying and calcination MCM-41 supported MoO_3 catalysts with unprecedented high loadings and dispersions of the active phase were

obtained, with retention of the unique structural and textural properties of the support material. The results of these experiments have been compiled in **chapter 4**.

Despite the satisfactory results obtained with our new method we experienced a small drawback of the method during the practical execution of the experiments. In order to obtain a stable solution of the Mo^{3+} precursor an acidic environment is required. Moreover, chloride ions are needed to avoid re-oxidation of the molybdenum precursor during drying and the early stages of calcination. Therefore we used a 1 : 1 mixture of demineralised water and hydrochloric acid as a solvent for the molybdenum precursor. Upon preparation of the solvent mixture it was added to a weighted amount of AHM. Immediately after addition of the solvent mixture AHM was converted into a precipitate, which adhered tightly to the bottom and walls of the vessel. The formation of this precipitate was not a surprise, since it is well-known that hexavalent molybdate-precursors are converted into MoO_3 (or H_2MoO_4 at very low Mo^{VI} concentrations) at low pH values, as can be seen in figure 1. Nevertheless, thus formed precipitates seriously complicated handling of the suspensions prior to and during the first stages of the electrochemical reduction process. In order to alleviate these handling problems we explored alternative methods to prepare the starting suspensions. We hoped that an adaptation of the preparation process would result in the formation of a less coarse precipitate, which would not adhere to the vessel (or at least less tightly).

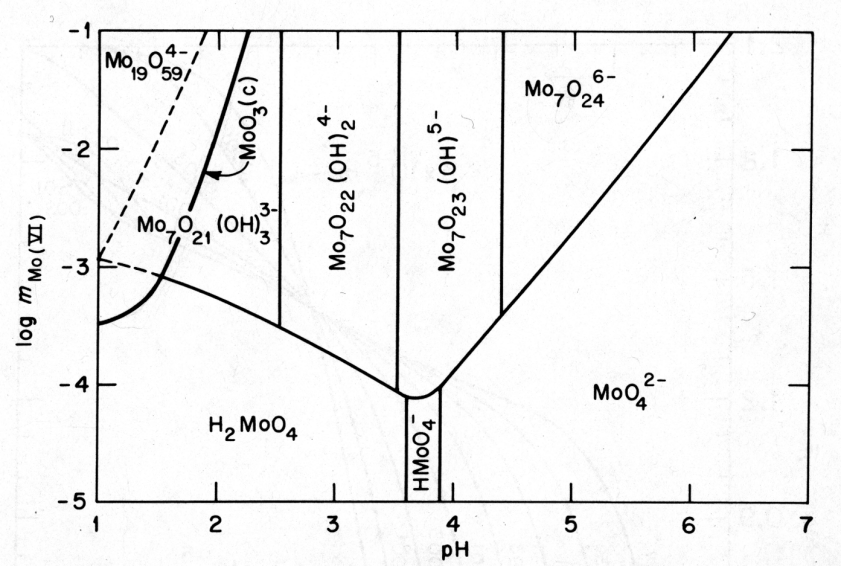

Figure 1: Diagram showing the hexavalent molybdenum species present in demineralised water as a function of the pH (diagram taken from ref. [3]). The curved thick line in the left part of the diagram is the solubility level of MoO_3.

Addition of only hydrochloric acid to AHM followed by the (very careful[1]) addition of water did not work. Also, dissolution of AHM in demineralised water followed by the addition of hydrochloric acid resulted in the formation of a strongly adhering precipitate. Adjustment of the addition rates of solvent (fast or slow) proved to be unsuccessful as well in all three cases (1 = solvent mix, 2 = water 1st and 3 = HCl 1st). Therefore we finally decided to change the mixing order of AHM and solvent: *i.e.* AHM was added to the 1 : 1 mixture of demineralised water and hydrochloric acid, instead of *vice versa*. To our great surprise in most cases a slightly yellow solution was obtained instead of a precipitate (for details: see experimental section).

Electrochemical reduction of solutions prepared by the dissolution of AHM in the 1 : 1 solvent mixture proved to be just as successful as reduction of the suspensions previously obtained, whilst the process was notably faster. Impregnation of thus obtained Mo^{3+} precursor solutions onto all-silica MCM-41 yielded the same excellent results as reported in chapter 4. Nevertheless, we were curious to know whether impregnation of the newly prepared precursor solution, containing hexavalent molybdenum species instead of trivalent Mo^{3+}, onto all-silica MCM-41 material would result in the destruction of the support material, as was the case upon impregnation with another hexavalent molybdenum precursor, *viz.* an aqueous AHM solution. To our surprise impregnation of the newly prepared molybdenum precursor did not result in the destruction of the MCM-41 support material. Both the structural and textural properties of MCM-41 were fully retained after drying and calcination and molybdena was present as highly dispersed layers inside the mesopores of the support, up to MoO_3 loadings as high as 20 wt%.

Experimental

Support synthesis

All-silica MCM-41 was prepared following a slightly adapted literature procedure [4]. First a synthesis gel was made starting from pyrogenic silica (Aerosil 380, Degussa), cetyltrimethylammoniumbromide (CTABr, Acros, 99+%), tetraethylammoniumhydroxide-solution (TEAOH, 20 wt% in water, Acros) and demineralised water. The molar composition of the synthesis gel

[1] Addition of water to a concentrated (strong) acid generates a lot of heat, which can cause splashing of acid out of the vessel in an uncontrolled manner! Therefore this order of addition should actually always be avoided.

was 1 SiO_2 : 0.27 CTABr : 0.19 TEAOH : 40 H_2O. TEAOH-solution was diluted with demineralised water and CTABr was dissolved at ambient temperature. Subsequently SiO_2 was added over a period of about one hour and the resulting synthesis gel was aged at room temperature for 24 hours under stirring. Subsequently the highly viscous gel was transferred to a teflon-lined autoclave. This autoclave was placed in an oven and the synthesis gel was aged hydrothermally at 150°C under autogeneous pressure for 3 days. The resulting white product was worked up by repeated washing with demineralised water and filtration, after which it was dried in air for 12 hours at 120°C (heating rate = 1°C min^{-1}). Subsequently template was removed by calcination in air for 6 hours at 550°C (heating rate = 1°C min^{-1}).

Catalyst preparation

Molybdenum precursor solutions were prepared by carefully dissolving required amounts of AHM (Acros, *p.a.*) into 1 : 1 mixtures of demineralised water and concentrated hydrochloric acid (37%, Merck, *p.a.*). It should be noted that AHM has to be added relatively slowly in order to prevent the precipitation of coarse MoO_3: *i.e.* AHM is slowly added until a "cloudy" white product starts to form within the yellow solution. At that moment AHM addition is stopped until the white "clouds" have disappeared. Fortunately, dissolution of the white products is usually very fast, *i.e.* within a few seconds or a few tens of seconds at most. This procedure of AHM addition and dissolution is repeated until the required molybdenum concentration is achieved. Generally, preparation of approximately 100 ml of precursor solution takes only a few minutes. Violent stirring of the precursor solution during AHM additions significantly helps to speed up the dissolution process. Finally, to optimise stirring preparation vessels should ideally be equipped with baffles.

Thus obtained molybdenum precursor solutions were impregnated onto powdered all-silica MCM-41 *via* the incipient wetness technique. Prior to impregnation MCM-41 was evacuated for at least 15 minutes at room temperature. Impregnations were carried out in static vacuum on approximately 1 gram of support material. After impregnation the materials were dried at 120°C for 12 hours and calcined at 450°C for 6 hours, all in air (heating rates: 1°C min^{-1}). Molybdena loadings of thus prepared catalysts were 5, 10, 15 and 20 % by weight, calculated as:

$$\{ g\ MoO_3\ /\ (g\ MCM\text{-}41 + g\ MoO_3) \} * 100\%$$

Characterisation techniques

Nitrogen physisorption

Textural analyses of the samples were performed on a Micromeritics ASAP 2400 apparatus. Measurements were carried out at -196°C. Prior to analysis the samples were outgassed *in vacuo* at 300°C. Surface areas were calculated using standard BET and t-plot theory; pore volumes and pore size (distributions) were calculated according to BJH theory.

XRD

The structural integrity of the MCM-41 supported catalysts after impregnation was determined with a Philips PW 1820 powder diffraction system using Cu Kα radiation. The presence or absence of crystalline silica and / or molybdenum phases was determined with an Enraf Nonius PDS 120 powder diffraction system using Co Kα_1 radiation.

TEM

Electron micrographs were obtained with a Tecnai 20F transmission electron microscope from Philips, equipped with a tungsten field emission gun operated at 200 keV. A small amount of sample material was powdered in a mortar, suspended in a small amount of ethanol and dispersed further in an ultrasonic bath. Next a small droplet of the resulting suspension was applied onto a thin holey carbon film supported by a copper grid.

Results and discussion

Catalyst preparation

X-ray diffractograms of the catalysts after drying and calcination display at least three well-resolved reflections at low angles, which can be assigned to the hexagonal mesoporous structure of the MCM-41 support material, as can be seen in figure 2. Therefore these diffractograms indicate that the support material has successfully resisted the impregnation treatment with a hexavalent molybdenum precursor compound. These findings were corroborated by TEM measurements, which also showed that the support

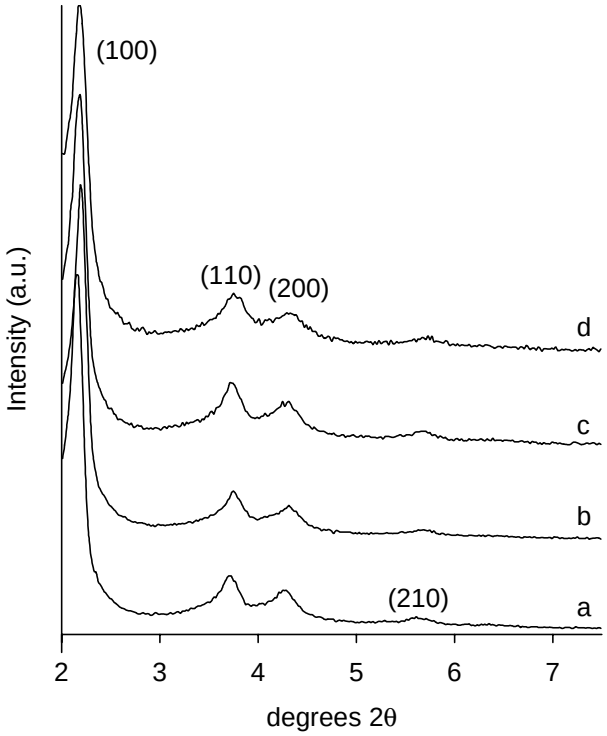

Figure 2: X-ray diffractograms of MCM-41 supported molybdena catalysts prepared with AHM in HCl precursor solutions, showing the reflections originating from the hexagonal mesoporous support structure. a = 5 wt% MoO_3, b = 10 wt%, c = 15 wt% and d = 20 wt%.

framework of the resulting catalysts was still intact after catalyst preparation. Some representative micrographs can be seen in figures 3 and 4. The stability of the support material towards a solution of AHM in HCl is opposed to the behaviour displayed towards another hexavalent molybdenum precursor compound, *viz.* AHM in aqueous solution, since it was shown previously in chapter 4 that impregnation with molybdate precursors resulted in the destruction of the support material. Clearly, dissolution of (poly)molybdate anions in hydrochloric acid results in the formation of another type of hexavalent molybdenum precursor compound (*vide infra*), with a different chemical reactivity towards the amorphous silica pore walls of the support material.

Next to the stability of the support material towards the hexavalent molybdenum precursor its stability towards the highly acidic impregnation solution is also remarkable. Iler collected data on the solubility of amorphous silica at a variety of different conditions, including pH [5]. It was shown that amorphous silica is soluble in acidic solutions, although (equilibrium) concentrations of dissolved, monomeric silica are relatively low, especially at room temperature [6]. Moreover, despite the fact that dissolution of

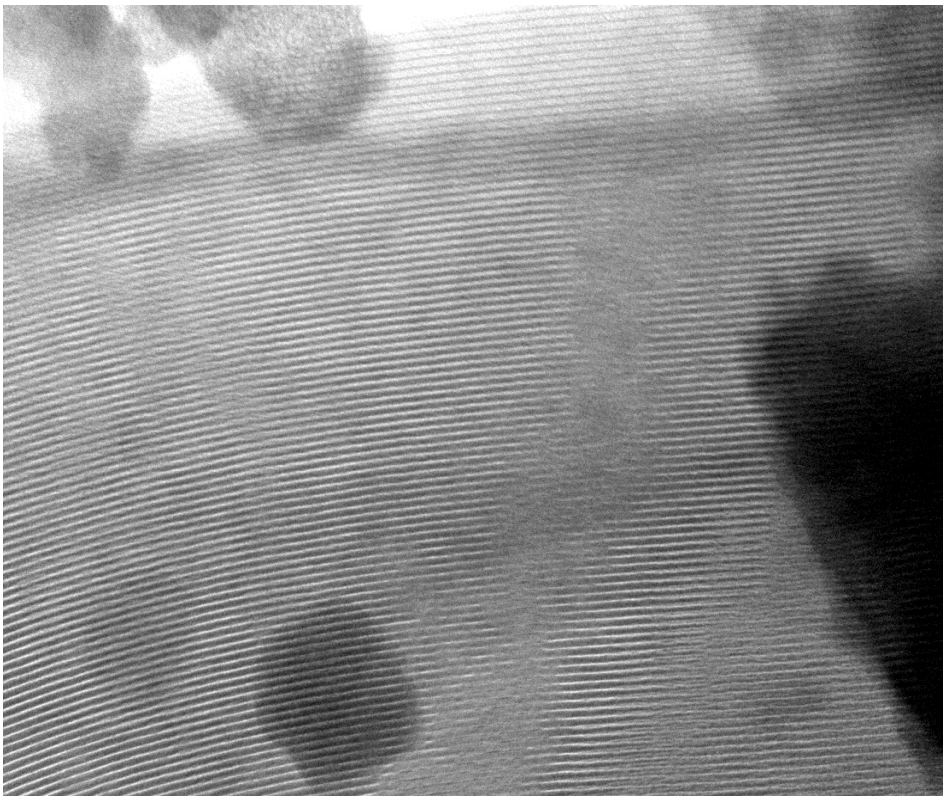

Figure 3: TEM image showing the ordered support structure in the 20 wt% catalyst.

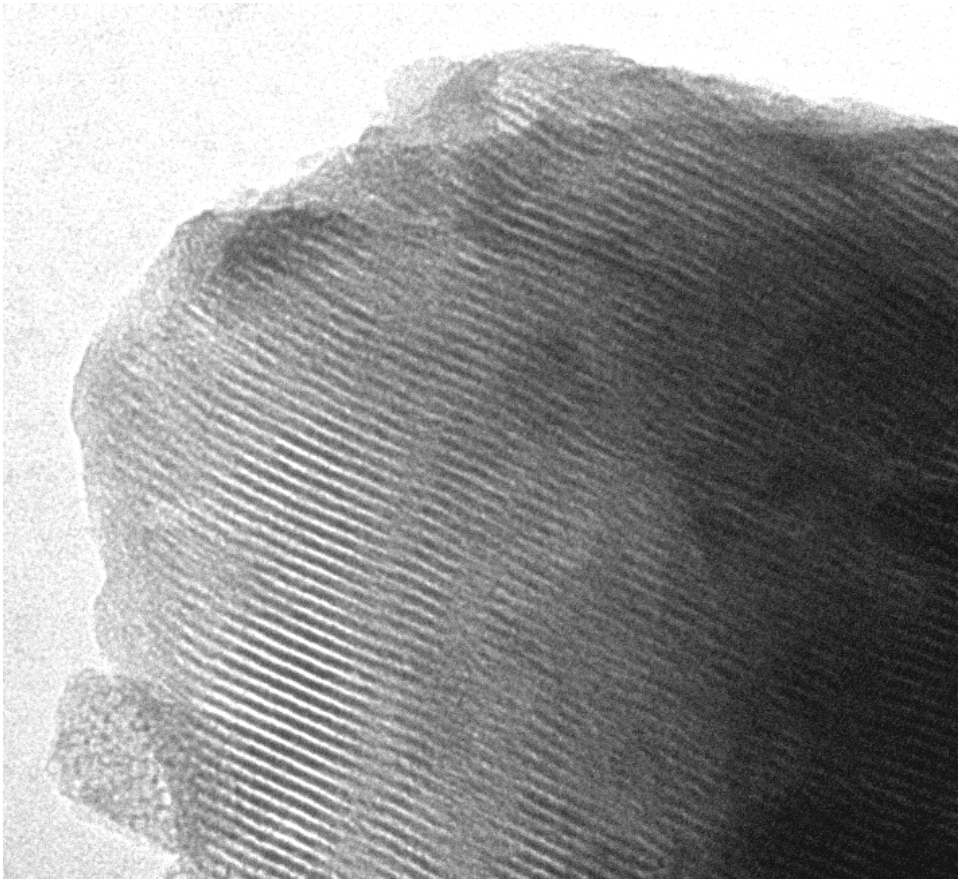

Figure 4: Another TEM image showing the ordered support structure in the 20 wt% catalyst.

amorphous silica is thermodynamically possible the kinetics for this process are slow in acidic media (*i.e.* below a pH level of 3), due to the absence of sufficient amounts of hydroxyl ions, which serve as a "dissolution catalyst" [7]. Since dissolution occurs at the silica surface, correlations between the dissolution rate and the silica surface area have been drawn up, indicating that amorphous silicas with high surface areas display higher rates of dissolution [8]. Therefore, although silica dissolution is slow in acidic media, it might be expected that the very high surface area of MCM-41 in combination with the very thin amorphous pore walls facilitates dissolution of the support material. Nevertheless, our MCM-41 support material was found to be stable towards the highly acidic impregnation solutions.

X-ray diffraction was also used to establish whether large crystalline particles / aggregates of MoO_3 had formed after the drying and calcination treatments. The absence of reflections other than those of the MCM-41 support structure indicates that large, crystalline molybdenum phases are not present in the catalysts. TEM investigations corroborate this finding, since no other phase than the mesoporous support material was observed. This means that the dispersion of molybdena over the support material is high. Since the "external" surface area of MCM-41 amounts to a mere 10 $m^2\ g^{-1}$ [9], this finding implies that molybdena has to be dispersed over the very large internal surface area, *i.e.* molybdena is present inside the mesopores of the support (as intended). However, since the pore diameter of the MCM-41 support material is rather small (*viz.* 2.85 nm) molybdena nanoparticles might have formed, due to the relatively weak interaction between MoO_3 and silica, thus giving rise to pore blocking of the support material. Nevertheless, results obtained from nitrogen physisorption measurements indicate that up to molybdena loadings of at least 15 wt% pore blocking does not occur, since the very high surface area and pore volume of the support material have been retained upon catalyst preparation, as demonstrated by the data given in table 1. The decreases of surface areas and pore volumes relative to the parent MCM-41 material can be fully attributed to weight loading of the catalysts. A somewhat larger than expected decrease of pore volume and average pore diameter for the 20 wt% catalyst might be attributed to pore blocking, although the values reported for the surface area (calculated according to both the BET and t-plot method) contradict this assumption. In view of the error margin of the technique, approximately 5 %, it is reasonable to assume that pore blocking occurs to a very small extent only for the 20 wt% catalyst, if at all.

Table 1: Results of textural analyses of the parent MCM-41 support material and molybdena-loaded catalysts.

sample	BET surface area (m^2 g^{-1})	t-plot surface area (m^2 g^{-1})	pore volume (ml g^{-1})	average pore diameter (nm)
parent MCM-41	994	963	0.96	2.85
5 wt% MoO_3/MCM-41	950	918	0.97	2.75
10 wt% MoO_3/MCM-41	913	901	0.94	2.70
15 wt% MoO_3/MCM-41	874	873	0.92	2.65
20 wt% MoO_3/MCM-41	830	834	0.76	2.55

For matter of completeness the measured nitrogen isotherms for the parent MCM-41 support material and the resulting catalysts are shown in figure 5. It is seen that the characteristic capillary condensation step is retained for all catalyst samples, as was already apparent from the data in table 1. However, upon increasing molybdena loadings the capillary condensation step shifts towards lower values of p / p_0, indicating that narrowing of the mesopores occurs due to the presence of layers of well-spread molybdena inside the mesopores. Calculations learn that the amount of molybdenum oxide is too small to completely cover the walls of the mesopores and as a result incomplete layers of molybdenum oxide will be

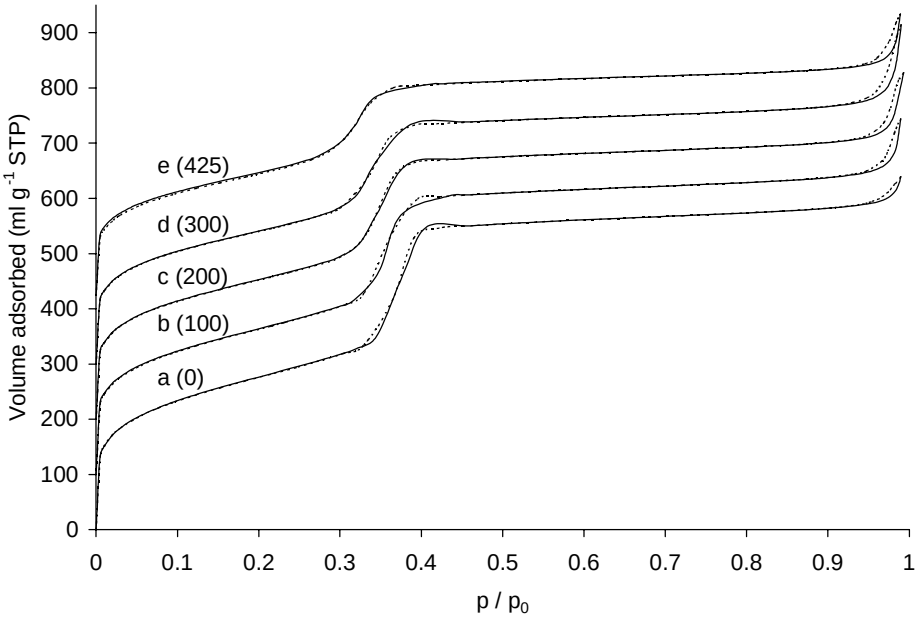

Figure 5: Nitrogen isotherms of parent MCM-41 and molybdena-loaded catalysts, prepared by impregnation of an AHM in HCl precursor solution. a = parent MCM-41 (0), b = 5 wt% MoO_3/MCM-41 (100), c = 10 wt% MoO_3/MCM-41 (200), d = 15 wt% MoO_3/MCM-41 (300) and e = 20 wt% MoO_3/MCM-41 (425). The numbers in parentheses indicate the onset of the isotherms. The continuous lines present adsorption data, whereas the dotted lines present desorption data.

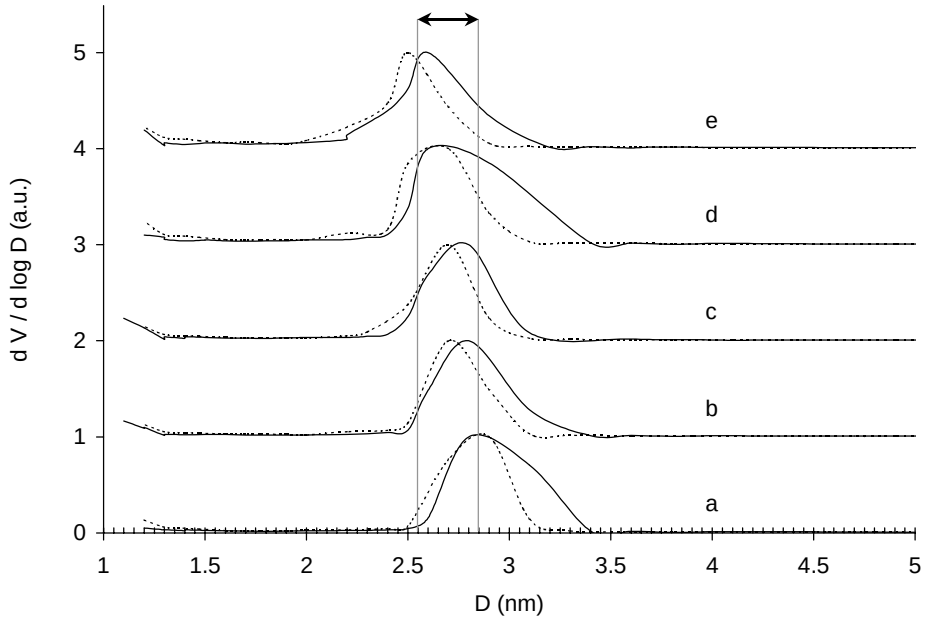

Figure 6: Pore size distributions of parent MCM-41 support material and molybdena-loaded catalysts. a = parent MCM-41, b = 5 wt% MoO_3/MCM-41, c = 10 wt% MoO_3/MCM-41, d = 15 wt% MoO_3/MCM-41 and e = 20 wt% MoO_3/MCM-41. Solid lines present adsorption data, dotted lines present desorption data.

present. Pore size distribution plots of the parent MCM-41 support material and the molybdena-loaded catalysts are displayed in figure 6. It is seen that molybdena loading results in a decrease of the average pore diameter. Since it was mentioned above that there is not enough molybdenum oxide to completely cover the pore walls, the decrease of the average pore size of the MCM-41 support material must be ascribed to the presence of a well-spread molybdenum oxide layer in the mesopores. The presence of relatively large amounts of molybdenum oxide near the pore openings can be explained by the occurrence of a flow of solvent towards the pore openings during drying of the catalysts after impregnation. If the interaction between the silica pore walls and the impregnated molybdenum precursor compound is limited part of the precursor will be entrained with the solvent flow during the drying step and as a result deposition of precursor material near the pore openings occurs (*vide infra*). Similar results were obtained for MCM-41 supported MoO_3 catalysts prepared by impregnation with a reduced Mo^{3+} precursor, as described in chapter 4: EDX analyses (after calcination) showed an enrichment of molybdena at the pore openings. It is very likely that the same mechanisms have been operative during drying of the MCM-41 support material impregnated with the "new" precursor. Upon calcination the precursor

compound (completely) converts into MoO_3, which will redisperse inside the mesopores due to spreading phenomena. It should be noted that spreading of MoO_3 over silica surfaces generally is not very successful, but the very large surface area of MCM-41 significantly alleviates this constraint, thus giving rise to the high molybdena dispersion of the prepared catalysts. Nevertheless, after calcination the mesopore openings of the MCM-41 support material apparently remain somewhat enriched in molybdena. This feature might however be beneficial from a catalytic point of view since it alleviates the necessity of reactant diffusion deep into the mesopores.

Molybdenum precursor

As mentioned in the introductory section, the formation of a *solution* of molybdenum precursor out of AHM and a 1 : 1 mixture of demineralised water and hydrochloric acid was somewhat surprising. The yellow colour of the solution instigated us to review the list of known inorganic molybdenum compounds [10] in order to determine the exact nature of the "new" molybdenum precursor. In view of the colour, the solubility, the chemicals present in the solution, *viz.* molybdenum oxo-ions as well as chloride ions, the valency of Mo (*viz.* 6+) and stability considerations the most likely candidate for the precursor compound is MoO_2Cl_2. Unfortunately, data on solutions of molybdenum compounds were not provided. Nevertheless, further literature research corroborated the assumption of the formation of MoO_2Cl_2. Cotton and Wilkinson desribe the formation of polymeric oxy-anions of hexavalent molybdenum (such as heptamolybdate ions) in weakly acidic solutions [11]. In "very strong acidic solution of hydrochloric acid (> 6 mol l^{-1})" these oxy-polyanions depolymerise to generate "a species which appears to be MoO_2Cl_2" [12]. In a later edition of their work Cotton and Wilkinson characterise the species formed upon the dissolution of MoO_3 in HCl to be $[MoO_2Cl_2(H_2O)_2]$ and $[MoO_2Cl_4]^{2-}$ [13]. An HCl concentration of 6 mol l^{-1} predominantly yields $[MoO_2Cl_2(H_2O)_2]$, whereas an increase of the concentration of HCl to 12 mol l^{-1} predominantly yields $[MoO_2Cl_4]^{2-}$ [13]. Furthermore, the dissolution of MoO_3 in hydrochloric acid has been described by Mellor [14], Rollinson [15] and Mackay and Mackay [16]. Here it should be noted that the synthesis of MoO_2Cl_2 usually involves the reaction of gaseous chlorine compounds (such as Cl_2 or HCl) with MoO_3 or MoO_2 at elevated temperatures, either in the presence or absence of O_2, instead of the dissolution of MoO_3 in concentrated hydrochloric acid. Thus generated, solid

MoO_2Cl_2 is reported to rapidly hydrolyse when it is contacted with water [17 - 19], due to the following equilibrium [17]:

$$MoO_2Cl_2 + H_2O \leftrightarrows MoO_3 + HCl \quad (1)$$

It follows, that at sufficiently high concentrations of HCl the MoO_2Cl_2 compound is the thermodynamically stable species [19].

In view of the above-described literature results it is possible to understand the processes occurring during the preparation of our precursor solution. When AHM is added slowly to the hydrochloric acid solution (6 mol l^{-1}) the heptamolybdate oxy-anions depolymerise and form MoO_2Cl_2. A too fast addition of AHM apparently results in the formation of very fine-grained MoO_3 or molybdic acid ($MoO_3 \cdot 2H_2O$, the white clouds), which redissolves very rapidly due to the equilibrium given above. As a result a stable hydrochloric acid solution of MoO_2Cl_2 is obtained. In this solution also some $[MoO_2Cl_4]^{2-}$ might be present, albeit to a small extent only [13]. It should be mentioned here that, in view of the literature described above, the suspensions we first obtained by adding solvent to AHM, instead of *vice versa*, should, from a thermodynamic point of view, also have been converted into solutions containing MoO_2Cl_2. Such a transformation was not observed, however. We reason that this finding can be explained by a kinetically very slow redissolution process of MoO_3, which is further inhibited by a low surface area from which dissolution has to take place (due to the coarse nature of the obtained precipitates).

Upon catalyst preparation *via* incipient wetness impregnation with this MoO_2Cl_2-precursor the characteristic features of the ordered mesoporous MCM-41 support material are completely retained (*vide supra*). With another hexavalent molybdenum precursor solution, *viz.* aqueous AHM, notably different results were obtained (as described in chapter 4): the mesoporous support structure collapsed and a microporous material was obtained instead. Therefore, the different structures and concomitant chemical reactivity of both types of precursor compound must explain the observed differences. In the case of impregnation with an aqueous AHM solution, which has not been pH-adjusted, $Mo_7O_{24}^{6-}$ isopoly-anions will be present in solution. From literature it is well known that these (poly)molybdate anions are able to provoke an interaction with silica, resulting in the formation of heteropoly-anions [20], which ultimately yield α-crystobalite, a crystalline silicondioxide compound, as observed by Arnoldy [21]. Although the destruction of the MCM-41 support material was apparent, we did not observe any α-crystobalite. As a result of

the high thermodynamic potential of silica in the amorphous pore walls reaction with heptamolybdate anions occurs, (presumably) resulting in the formation of the heteropoly-anion of silicomolybdic acid *via* reaction (2), although the formation of other heteropoly-anions can not be excluded at this stage. Therefore further research is advocated to elucidate the exact nature of the species formed.

$$12\ Mo_7O_{24}^{6-} + 7\ SiO_2 + 22\ H_2O \leftrightarrows 7\ SiMo_{12}O_{40}^{4-} + 44\ OH^- \qquad (2)$$

It should be noted that the amount of AHM admitted inside the mesopores during impregnation is too small for reaction (2) to occur stoichiometrically and the presence of silicomolybdic acid ($H_4SiMo_{12}O_{40}{\cdot}xH_2O$) has not been observed with x-ray diffraction. Therefore, we suggest that after formation, the $SiMo_{12}O_{40}^{4-}$ compound decomposes, yielding amorphous silica:

$$SiMo_{12}O_{40}^{4-} + 24\ OH^- \leftrightarrows 12\ MoO_4^{2-} + "SiO_4^{4-}" + 12\ H_2O \qquad (3)$$

In this equation SiO_4^{4-} denotes the anion of silicic acid, $Si(OH)_4$. Next to this anion a multitude of other silicate species can be generated. However, at the prevailing pH-levels all these silicate species will condense to yield amorphous silica. Thus formed amorphous silica will have a notably lower thermodynamic potential than the amorphous silica initially present in the pore walls. After reaction (3) the generated molybdate anions (MoO_4^{2-}) are able to interact again with the remaining pore walls, either as MoO_4^{2-} or $Mo_7O_{24}^{6-}$, formed by the following reaction:

$$7\ MoO_4^{2-} + 8\ H_3O^+ \leftrightarrows Mo_7O_{24}^{6-} + 12\ H_2O \qquad (4)$$

The conversion of amorphous silica with a high thermodynamic potential into amorphous silica with a lower thermodynamic potential is the driving force for the processes described above. As a result of reactions (3) and (4) molybdate (poly)anions become continuously available for reaction with the MCM-41 support material. It follows that the molybdate (poly)anions serve as homogeneous dissolution catalysts, which are regenerated after each cycle. Unfortunately it is generally not possible to bypass this destructive catalytic action of the impregnated precursor by adjustment of the pH of the impregnated solution. At pH-levels higher than 7 the MCM-41 support structure dissolves due to the mineralising effect of OH^- ions present in the solution. Moreover, MoO_4^{2-} formed from $Mo_7O_{24}^{6-}$ by the reverse of reaction

(4) would probably also still be able to bring about the decomposition of MCM-41 *via* the reverse of reaction (3). A decrease of the pH will give rise to the formation of other isopoly-anions of molybdenum (*cf.* figure 1), which will show similar reactivity towards MCM-41 as $Mo_7O_{24}^{6-}$. In addition, a too large pH-decrease, brought about by any acid apart from HCl, will result in the precipitation of MoO_3 from the precursor solution, due to the following reaction:

$$Mo_7O_{24}^{6-} + 6\ H_3O^+ \quad \leftrightarrows \quad 7\ MoO_3\ (s) + 9\ H_2O \qquad (5)$$

From the above discussion it follows that (poly)molybdate precursors are not suitable for the preparation of silica-supported catalysts, especially when MCM-41 is the support material of choice. Only upon reaction with HCl a molybdenum species is formed from $Mo_7O_{24}^{6-}$, which does not give rise to the unfavourable interactions described by reactions (2) and (3). Apparently, the generated MoO_2Cl_2 species is not able to provoke Si-leaching from the framework. This finding might be related either to a decreased chemical interaction of the precursor with the pore walls or to the incapability of the MoO_2Cl_2 complexes to convert into heteropoly-anionic structures upon interaction with silica (or both). Therefore, it is not (yet) clear whether the preservation of the support structure is thermodynamically (possibility of the formation of heteropoly-anionic complexes starting from MoO_2Cl_2 instead of isopoly-anionic heptamolybdate) or kinetically (interaction of the MoO_2Cl_2 complexes with the pore walls ór the *rate* of formation of the heteropoly-anionic structures) controlled, in the case of catalyst preparation with a solution of AHM in 6 mol l^{-1} hydrochloric acid.

Finally, the behaviour of the dissolved complex upon drying is considered. Since there will probably be no substantial electrostatic or hydrogen bonding interactions between the MoO_2Cl_2 compound and the silica pore walls the precursor will be entrained with the solvent flow during drying. The implications of this process have been previously discussed (*vide supra*). In addition, it should be noted that upon drying of an aqueous hydrochloric solution an HCl concentration of approximately 20.2 wt% will be reached, corresponding to the azeotropic composition of a binary H_2O-HCl mixture. This behaviour implies that the composition of the impregnated solution during drying is very close to the initial composition (approximately 18.5 wt% HCl). This means that only a small decrease of pH will occur during drying and as a result the MoO_2Cl_2 species initially present after impregnation will not convert

into other (potentially detrimental) molybdenum compounds (*e.g.* $Mo_7O_{24}^{6-}$, MoO_3 or $MoO_2Cl_4^{2-}$) during the drying process.

Conclusions

A new method for the preparation of all-silica MCM-41 supported molybdena catalysts has been developed. This method relies on the incipient wetness impregnation of an unusual molybdenum precursor, *viz.* a solution of AHM in a 1 : 1 mixture of demineralised water and hydrochloric acid. Upon addition of AHM to the solvent mixture depolymerisation of heptamolybdate anions occurs and MoO_2Cl_2 complexes are formed. The very high concentration of HCl in thus generated solutions prevents hydrolysis of the complexes towards MoO_3. Upon impregnation of these precursor solutions onto MCM-41, followed by drying and calcination, the characteristic ordered structure of the support material is fully retained, in contrast to results obtained upon impregnation with another hexavalent molybdenum precursor, *viz.* an aqueous solution of AHM. Therefore, the chemical interactions between MCM-41 and molybdenum precursor compound are notably different for MoO_2Cl_2 and heptamolybdate isopoly-anions. Another remarkable feature is the stability of the MCM-41 support material towards the highly acidic nature (6 mol l^{-1} HCl) of the impregnated precursor solutions.

Combined characterisation results indicate that the dispersion of molybdenum oxide over MCM-41 is very high. An implication of this finding is that molybdena must almost completely be situated inside the mesopores of the support material. Nevertheless, despite the frequently encountered weak interactions between MoO_3 and silica, textural analyses indicate that plugging of the mesopores by molybdenum oxide nanoparticles does not occur, implying that molybdena is present as incomplete monolayers, which have well-spread over the large mesopore surface area. A small decrease of the pore diameter upon molybdena loading is observed, which might be attributed to a slight enrichment of molybdena at the pore openings. Nevertheless, this new method of catalyst preparation yields all-silica MCM-41 supported molybdena catalysts with (comparatively) very high MoO_3 loadings (*viz.* up to 20 wt%), combined with a very high dispersion of the active phase. Moreover, the structural integrity of the MCM-41 support material is completely retained with this method. Similar results have thus far only been obtained when a reduced Mo^{3+} complex is used as a precursor during catalyst preparation (**chapter 4**). However, the method disclosed here is notably simpler from a practical viewpoint.

Acknowledgements

Ad Mens is kindly thanked for performing the nitrogen physisorption measurements. Hans Meeldijk and Professor Geus are kindly thanked for characterisation of the described materials with TEM.

Literature

[1] C.T. Kresge, M.E. Leonowicz, W.J. Roth, J.C. Vartuli and J.S. Beck, *Nature*, 359, 1992, 710

[2] J.S. Beck, J.C. Vartuli, W.J. Roth, M.E. Leonowicz, C.T. Kresge, K.D. Schmitt, C.T-W. Chu, D.H. Olson, E.W. Sheppard, S.B. McCullen, J.B. Higgins and J.L. Schlenker, *J. Am. Chem. Soc.*, 114, 1992, 10834

[3] C.F. Baes and R.E. Mesmer: *"The Hydrolysis of Cations"*, published by John Wiley & Sons, Inc., New York, USA, 1976, chapter 11.2.1

[4] C-F. Cheng, D.H. Park and J. Klinowski, *J. Chem. Soc., Faraday Trans.*, 93, 1997, 193

[5] R.K. Iler: "*The Chemistry of Silica*", published by John Wiley & Sons, Inc., New York, USA, 1979, chapter 1

[6] R.K. Iler: "*The Chemistry of Silica*", published by John Wiley & Sons, Inc., New York, USA, 1979, chapter 1, p. 40-47

[7] R.K. Iler: "*The Chemistry of Silica*", published by John Wiley & Sons, Inc., New York, USA, 1979, chapter 1, p. 62-65

[8] R.K. Iler: "*The Chemistry of Silica*", published by John Wiley & Sons, Inc., New York, USA, 1979, chapter 1, p. 65-73

[9] A.C. Voegtlin, A. Matijasic, J. Patarin, C. Sauerland, Y. Grillet and L. Huve, *Micropor. Mater.*, 10, 1997, 137

[10] *CRC Handbook of Chemistry and Physics*, published by CRC Press, Inc., Boca Raton, Florida, USA, table "Physical Constants of Inorganic Compounds"

[11] F.A. Cotton and G. Wilkinson: "*Advanced Inorganic Chemistry - A Comprehensive Text*", 2nd Edition, published by Interscience Publishers (John Wiley & Sons), New York, USA, 1966, p. 937

[12] F.A. Cotton and G. Wilkinson: "*Advanced Inorganic Chemistry - A Comprehensive Text*", 2nd Edition, published by Interscience Publishers (John Wiley & Sons), New York, USA, 1966, p. 940

[13] F.A. Cotton and G. Wilkinson: "*Advanced Inorganic Chemistry*", 5th Edition, published by Interscience Publishers (John Wiley & Sons), New York, USA, 1988, p. 829

[14] J.W. Mellor: "*A Comprehensive Treatise on Inorganic and Theoretical Chemistry*", Volume XI, published by Longmans, Green and Co. Ltd., London, UK, 1931, p. 619

[15] C.L. Rollinson, in "*Comprehensive Inorganic Chemistry*" (J.C. Bailar, H.J. Emeléus, R. Nyholm and A.F. Trotman-Dickenson, editors), published by Pergamon Press, Oxford, UK, 1973, p. 732

[16] K.M. Mackay and R.A. Mackay: "*Introduction to Modern Inorganic Chemistry*", 4th Edition, published by Blackie & Son Ltd., Glasgow / London, UK (USA, Canada and Mexico: Prentice Hall), 1989, p. 247

[17] J.W. Mellor: "*A Comprehensive Treatise on Inorganic and Theoretical Chemistry*", Volume XI, published by Longmans, Green and Co. Ltd., London, UK, 1931, p. 632

[18] F.A. Cotton and G. Wilkinson: "*Advanced Inorganic Chemistry - A Comprehensive Text*", 2nd Edition, published by Interscience Publishers (John Wiley & Sons), New York, USA, 1966, p. 959

[19] J.H. Canterford and R. Colton: "*Halides of the Second and Third Row Transition Metals*", published by Interscience Publishers (John Wiley & Sons), London, UK, 1968, p. 223

[20] F.A. Cotton and G. Wilkinson: "*Advanced Inorganic Chemistry*", 5th Edition, published by Interscience Publishers (John Wiley & Sons), New York, USA, 1988

[21] P. Arnoldy, *Ph.D. Thesis*, University of Amsterdam, The Netherlands, 1985, chapter 5

6

Catalytic characterisation of bulk and silica-supported molybdena catalysts

an explorative study

Abstract

The catalytic oxidation of ethane was used as a test reaction to probe the dispersions of a number of molybdena catalysts. MCM-41 supported catalysts, which exhibited a high dispersion of MoO_3, were shown to be highly active, although the selectivity towards ethene (oxidative dehydrogenation) was very low. Kinetic parameters showed that the catalysts did not suffer from internal diffusion limitations. Values for the apparent activation energy were centred around 110 kJ mol^{-1}, indicating that a redox mechanism is operative. Moreover, the high dispersions of MoO_3/MCM-41 suggest that catalysis proceeds *via* a pseudo-redox mechanism, in which structural defects constitute the active sites. Catalyst preparation with MoO_2Cl_2 yielded MoO_3/MCM-41 with a larger amount of active sites than with Mo^{3+} as a precursor. A linear correlation of the number of active sites with molybdena loading indicates that the dispersion of MoO_3/MCM-41 remains invariably high up to 25 wt% MoO_3.

Bulk molybdena and Aerosil-200 supported catalysts of lower dispersion were shown to be less active, although higher selectivities for ethene were obtained. Catalyst preparation with MoO_2Cl_2 resulted in the formation of large platelets of MoO_3 separate from the Aerosil-200 support.

Introduction

In the previous chapters two newly developed methods for the preparation of molybdena catalysts supported by mesoporous all-silica MCM-41 have been described. Various characterisation techniques (*viz.* nitrogen physisorption, x-ray diffraction and transmission electron microscopy) revealed that molybdena had formed incomplete monolayers inside the mesopores of MCM-41, thus exhibiting a high dispersion, without damaging the unique support structure. The considerable interaction between MoO_3 and the support, yielding monolayers of active phase, contrasts with the normally encountered weak interaction between molybdena and silica supports, resulting in the formation of large crystallites of the active phase. Therefore, it is very interesting to study the catalytic properties of our MCM-41 supported MoO_3 catalysts and to compare the results with molybdena catalysts of lower dispersions. In addition, it is very important to assess whether internal diffusion limitations occur within the MCM-41 mesopores during catalysis.

It is well known that MoO_3-based catalysts can be used for the selective oxidation of various organic compounds. Generally a high selectivity is obtained because lattice oxygen is the active species in the catalytic reaction. Lattice oxygen is less reactive than oxygen radicals, which can also be generated on a catalytic surface. During the catalytic reaction lattice oxygen is consumed and thus surface vacancies are created in the MoO_3 lattice, which can be replenished by gas-phase molecular oxygen. This mechanism, which has been well-documented in literature, is referred to as the Mars - Van Krevelen mechanism.

In view of the above-mentioned facts we have decided to study the catalytic properties of our MoO_3/MCM-41 catalysts in the oxidative dehydrogenation of ethane. During this reaction ethane is dehydrogenated to ethene and hydrogen reacts with oxygen to produce water. The release of water instead of hydrogen makes this reaction exothermic and thermodynamically favourable:

$$2\ C_2H_6 + O_2 \rightarrow 2\ C_2H_4 + 2\ H_2O \qquad \Delta H°_{298} = -116\ kJ\ mol^{-1}C_2H_6$$

Ethane is a chemical of a relatively low value, whereas ethene is an interesting feedstock for a wide number of processes and products. Therefore the selectivity (and yield) of the oxidation reaction should be as high as possible. Unfortunately, combustion of ethane (or produced ethene) can also occur, which results in a large temperature increase due to the exothermicity

of oxidation reactions. If ethane is totally combusted to CO_2 and water the enthalpy of reaction ($\Delta H°_{298}$) amounts to no less than -1,470 kJ $mol^{-1}{}_{C_2H_6}$. Partial combustion to CO and water still gives an enthalpy change as high as -1,047 kJ mol^{-1}. Nevertheless, the latter reaction is preferred as a side-reaction, as CO finds widespread application in various chemical processes, whereas CO_2 is useless. Due to the exothermicity of both the selective oxidation and combustion reactions heat is produced during catalysis. This heat is able to bring about the thermal dehydrogenation of ethane to ethene and hydrogen, an endothermic reaction:

$$C_2H_6 \rightarrow C_2H_4 + H_2 \qquad \Delta H°_{298} = +138 \text{ kJ } mol^{-1}{}_{C_2H_6}$$

Thus far, only a very limited number of publications have appeared dealing with the catalytic oxidative dehydrogenation of ethane over silica-supported molybdena catalysts. Ward *et al.* studied this reaction in a multi-pass fixed bed reactor with nitrous oxide (N_2O) as the oxidising species [1]. The main conclusion from this study was that hexavalent molybdenum ions (initially present in MoO_3) were partially reduced to Mo^{5+} and Mo^{4+} species, as evidenced with EPR and XPS. Moreover, more than one type of Mo^{5+} species was supposed to be generated during the catalytic experiments, although only one of the different Mo^{5+} species was thought to catalyse the oxidative dehydrogenation reaction. Additionally, it was found that water vapour produced during the reaction has an inhibiting effect on the catalytic activity. Subsequently, Yang and Lunsford also used molecular oxygen (next to N_2O) to study this reaction in a conventional single-pass fixed bed reactor [2]. Low ethane conversions allowed these authors to determine activation energies for the reactions using different oxidising agents. With molecular oxygen as the oxidising species a notably higher apparent activation energy for the selective dehydrogenation reaction was obtained than for the reaction with N_2O, *viz.* 98 *vs.* 77 kJ mol^{-1}. Finally, Blaauw also studied the oxidative dehydrogenation of ethane, both over silica-supported and bulk MoO_3 catalysts [3]. Experiments were executed with a molar C_2H_6 to O_2 ratio of 2 : 1, *i.e.* in a net reducing environment. It was found that the activities and selectivities of the studied catalysts depended mainly on the concentration of oxygen defects at the surface of the MoO_3 phase. A high concentration of surface defects induced a partial reduction of the catalytic surface, giving rise to an increased catalytic activity. Unfortunately, the high activity was found to be accompanied by a low selectivity towards ethene. Calculated apparent activation energies were in

the order of 100 kJ mol^{-1}, indicating that ethane oxidation proceeds *via* a redox mechanism.

Experimental

Catalyst preparations

The procedures described in chapters 4 and 5 were employed to prepare molybdena catalysts supported by all-silica MCM-41. Molybdena catalysts supported by Aerosil-200 (Degussa) have been prepared by incipient wetness impregnation with solutions of ammonium heptamolybdate (AHM, Acros, *p.a.*) dissolved either in demineralised water or a 1 : 1 mixture of demineralised water and concentrated hydrochloric acid (37%, Merck, *p.a.*) (see chapter 5). In order to obtain bodies of Aerosil-200 suitable for impregnation the support was suspended in demineralised water, filtered over a Büchner funnel and dried overnight at 60°C. Subsequently the dry filter cake was gently crushed in a mortar and the sieve fraction of 0.5 -1 mm was used for incipient wetness impregnations. Prior to impregnation the support material was degassed for 15 minutes at room temperature. Impregnations were carried out in a static vacuum. After impregnation the materials were dried for 12 hours at 120°C (ramp: 1°C min^{-1}) and subsequently calcined for 6 hours at 450°C (ramp: 1°C min^{-1}), all in air. A bulk MoO_3 catalyst was prepared by careful addition of a diluted ammonia (Merck, *p.a.*) solution in demineralised water to an Mo^{3+} solution in hydrochloric acid, prepared by electrolysis (see chapter 4). Addition of NH_3 *via* injection below the surface of the liquid resulted in the homogeneous deposition precipitation (HDP) of $Mo(OH)_3$ (brown colour), which was washed (with demineralised water) and filtered numerous times in order to remove ammonium chloride. Next the precipitate was dried (6 hours at 120°C, ramp: 1°C min^{-1}) and calcined (6 hours at 450°C, ramp: 1°C min^{-1}), both in air.

Characterisation with electron microscopy

Some selected catalyst samples were characterised with a Tecnai 20F transmission electron microscope from Philips, equipped with a tungsten field emission gun operated at 200 keV. With this microscope it is possible to obtain both bright-field and dark-field TEM images as well as local elemental compositions of the catalysts with EDX. To study the catalysts a small amount of sample material was powdered in a mortar, suspended in a small amount

of ethanol and dispersed further in an ultrasonic bath. Next a small droplet of the resulting suspension was applied onto a thin holey carbon film supported by a copper grid.

Catalytic characterisation

The catalytic properties of various molybdena catalysts were studied using the oxidative dehydrogenation of ethane as a test reaction. The catalytic experiments were executed at the Department of Combinatorial Catalysis of Akzo Nobel Catalysts in Amsterdam (The Netherlands). Catalyst samples were powdered and loaded into quartz fixed bed reactors with an internal diameter of 3 mm. These reactors were placed in an oven and heated to the desired temperatures. The catalyst samples (exactly 30 mg) were continuously flushed with a 1 ml min^{-1} (STP) flow of a mixture of nitrogen and oxygen (Air Liquide, zero grade), resembling synthetic air (*i.e.* 18% O_2). Into this gas mixture small (8 µl) pulses of ethane were injected. Effluent gases were analysed with an Agilent Technologies 6890 gas chromatograph, operated at 35°C and equipped with a Hewlett Packard PLOT column (Al_2O_3, 30 m, internal ∅ = 0.53 mm) and a flame ionisation detector, implying that only hydrocarbons could be detected. From the GC-data conversions (X) and selectivities towards ethene (S) were calculated with the following formulae:

$$X = \{ ([C_2H_6]_{in} - [C_2H_6]_{out}) / [C_2H_6]_{in} \} * 100\%$$

$$S = \{ [C_2H_4] / ([C_2H_6]_{in} - [C_2H_6]_{out}) \} * 100\%$$

The catalytic behaviour of most catalysts was studied isothermally at 550°C for 1 hour. During this time 10 pulses of ethane were fed to the reactor. In addition, Arrhenius plots were obtained from measurements between 350 and 425°C (ramps: 3°C min^{-1}).

Results and discussion

First of all, the catalytic behaviour of a number of 20 wt% catalysts as well as that of bulk MoO_3 was studied. With these experiments the influence of the support and of the preparation method could be investigated. Figure 1 shows the results of the catalytic experiments performed at 550°C. Both conversion levels and selectivities towards ethene are presented. It should be

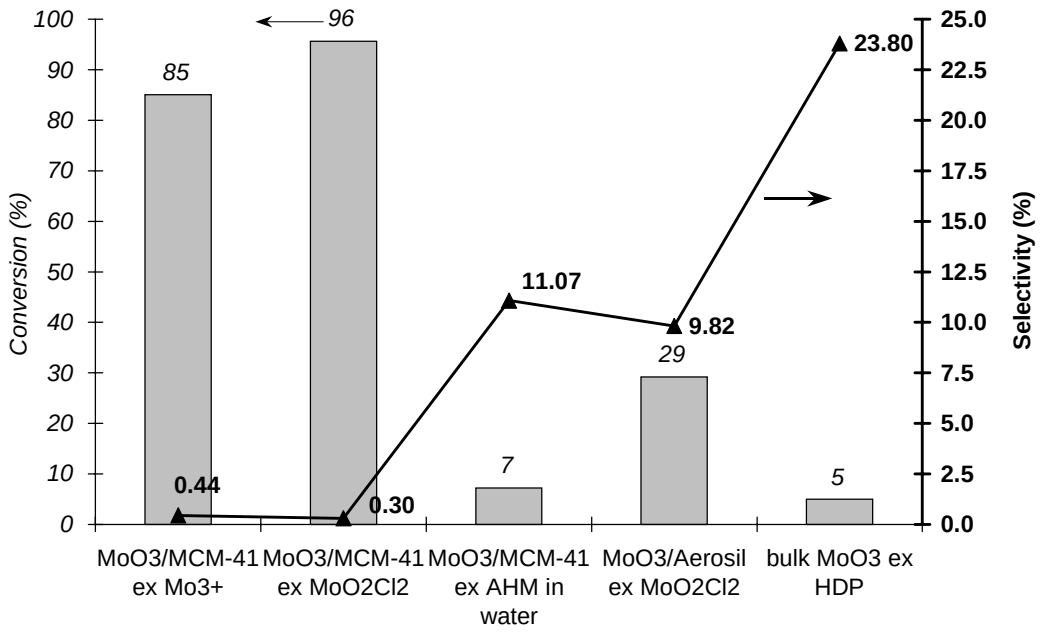

Figure 1: Catalytic behaviour at 550°C of 20 wt% molybdena catalysts and bulk MoO_3. Bars indicate conversion levels (left y-axis) and the black line indicates the selectivity towards C_2H_4 (right y-axis).

noted that selectivities can be compared properly only if the conversion levels are (almost) similar. Therefore, the selectivities in figure 1 can only be used as a qualitative indication of catalyst behaviour. It is seen that the catalysts supported by intact MCM-41 show considerably higher conversion levels than the other catalysts. In chapters 4 and 5 it was demonstrated that MoO_3/MCM-41 catalysts prepared by impregnation with a *suitable* precursor, *viz.* Mo^{3+} or MoO_2Cl_2, displayed a very high dispersion of the active phase, which was situated inside the mesopores of the support material. Clearly, a high dispersion of molybdena induces a high conversion of ethane. It should be noted that catalytic activity usually increases with the dispersion of the active phase, although in this case this assumption is not straightforward.

In this chapter it will be demonstrated that catalysis proceeds *via* a redox mechanism (as evidenced by the high apparent activation energy for the reaction, around 110 kJ mol^{-1}, *vide infra*). The active phase involved in the most well-known redox mechanism, *i.e.* the Mars - Van Krevelen mechanism, is a three-dimensional oxide lattice. The compound to be oxidised takes up oxygen from the lattice, while gas-phase molecular oxygen replenishes the removed lattice oxygen species. Literature has related the catalytic performance of oxidic active phases, such as MoO_3 [3] and V_2O_5 [4, 5], to the concentration of surface defects. Since the redox mechanism does not

proceed uniformly on the oxidic surface, but exclusively on defect sites, the mechanism is referred to as the "*pseudo-redox" mechanism*. Blaauw has documented that this pseudo-redox mechanism is not restricted to three-dimensional MoO_3 lattices [3]. Specially prepared silica-supported molybdena catalysts containing exclusively monolayers of the active phase exhibited an apparent activation energy of about 100 kJ mol^{-1} for the oxidative dehydrogenation of ethane. The apparent activation energies exhibited by three-dimensional MoO_3 and by monolayers of molybdenum oxide being equal indicates that the reaction of ethane on the monolayers also proceeds *via* a redox mechanism. The active phase of our MoO_3/MCM-41 catalysts is not crystalline MoO_3, but a well-spread molybdena layer, not completely covering the very large surface area of the MCM-41 support. Consequently, it is to be expected that the same pseudo-redox mechanism is operative with our MCM-41 supported catalysts. The high levels of conversion of ethane shown in figure 1 indicate that the molybdena monolayers on our MoO_3/MCM-41 catalysts prepared from Mo^{3+} and MoO_2Cl_2 precursor solutions possess high concentrations of structural defects.

Next the catalytic behaviour of the bulk MoO_3 catalyst prepared by homogeneous deposition precipitation of $Mo(OH)_3$ *ex* Mo^{3+} will be discussed. Blaauw has previously reported that upon calcination of thus generated $Mo(OH)_3$ a bulk MoO_3 material with a comparatively large concentration of defects is generated [3]. Hence bulk MoO_3 *ex* $Mo(OH)_3$ shows notably higher conversion levels (*i.e.* 10^2 times higher) than a commercial MoO_3 material. Nevertheless, the conversion of ethane over the catalyst prepared from $Mo(OH)_3$ is very low on a catalyst weight basis, as can be seen in figure 1. The explanation for this finding is that the specific surface area (S_{BET}) of this catalyst is very low, *viz.* 2.9 m^2 g^{-1}, implying that, although the defect *concentration* is high, the *absolute number* of defects per unit weight of catalyst is very low. The selectivity of this bulk MoO_3 catalyst towards ethene, on the other hand, was the highest for all catalysts measured. Although this behaviour could also be attributed to a difference in conversion levels, it should be noted that the observed trend (*i.e.* an increase of selectivity at decreasing conversion levels) has been reported before by Blaauw [3].

The molybdena catalyst supported on Aerosil-200 appears to have an intermediate activity, as can be seen in figure 1. However, when a rough estimate for the MoO_3 surface area is made, it follows that the activity of this catalyst is rather close to that of the bulk MoO_3 catalyst. This finding suggests that the MoO_3 phase of the Aerosil-supported catalyst displays a notable bulk character. Indeed, various characterisation techniques indicate that the

molybdena dispersion of this catalyst is low. X-ray diffraction yields a pattern with sharp peaks that can be ascribed to MoO_3 (not shown). Bright-field TEM observations also indicate that molybdena is to a very large extent present as a bulk material. Moreover, the observations show that molybdena is not present as large particles on the surface of Aerosil-200, but that very large and thin platelets of MoO_3, separate from the support, have formed during the catalyst preparation procedure, as can be seen in figures 2, 3 and 4. The platelets were found to extend over several hundreds of nanometers. For matter of completeness it should be mentioned that these platelets have never been observed with the MCM-41 supported catalysts. Dark-field images of the platelets indicate that the platelets are crystalline. Figures 4 and 5 show representative examples of a bright- and dark-field image. Subsequently taken electron diffraction patterns, one of which is shown in figure 6, exhibit very well resolved diffraction spots. Although the afore-mentioned techniques all demonstrate the presence of bulk or bulk-like MoO_3 it could very well be possible that next to the platelets an (appreciable) amount of molybdena had also spread over the surface of the support. To determine whether (and to what extent) molybdena was present on the particles of the Aerosil-200 support EDX was used. The results indicated that almost no molybdenum was present on the support, thus corroborating the low dispersion of active phase inferred previously from the catalytic measurements. From these results it is concluded that the molybdenum precursor used for preparation of the catalyst, *viz.* a solution of MoO_2Cl_2 in 6 mol l^{-1} HCl, did not give rise to a strong interaction with the support. It is envisaged that as a result homogeneous nucleation of platelets of (a precursor of) MoO_3 has occurred in the bulk of the solution during drying of the impregnated particles of support material.

The last catalyst included in figure 1 is the "MCM-41 supported" catalyst prepared *via* incipient wetness impregnation with an aqueous AHM precursor solution. The fact that the activity of this catalyst is similar to that of the bulk catalyst could indicate that the dispersion of the active phase is very low. However, x-ray diffraction did not show any features of MoO_3 or other crystalline molybdenum phases. It follows that a low dispersion presumably is not the only explanation for the observed behaviour. In chapter 4 it has been demonstrated that impregnation of MCM-41 with an aqueous solution of AHM results in a collapse of the mesoporous support framework. Therefore it is supposed that most of the precursor has become encapsulated by amorphous silica during the collapse of the MCM-41 framework. In addition, nitrogen physisorption measurements indicate that during the destruction all

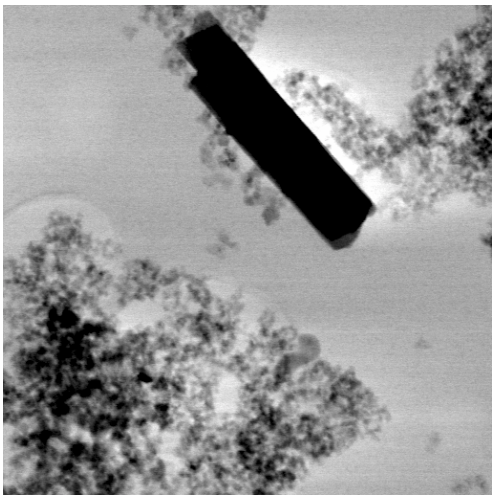

Figure 2: Bright-field STEM image showing platelets of MoO_3, next to (much) smaller particles of the Aerosil-200 support.

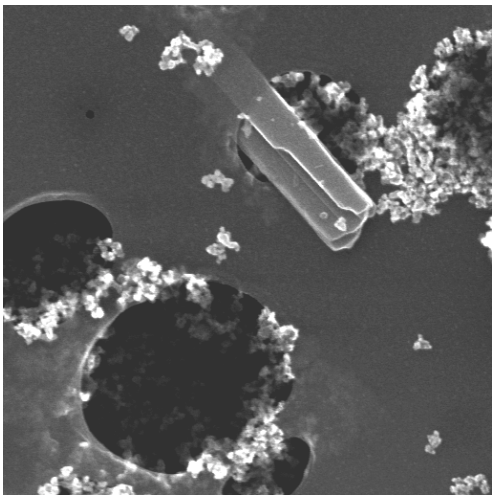

Figure 3: Secondary electron image of the MoO_3 platelets of figure 2, showing morphological features.

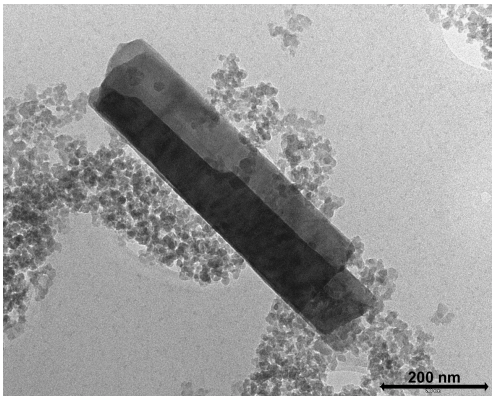

Figure 4: Close-up bright-field TEM image of the MoO_3 phase of figure 2. It is seen that there are three platelets of MoO_3 situated on top of each other.

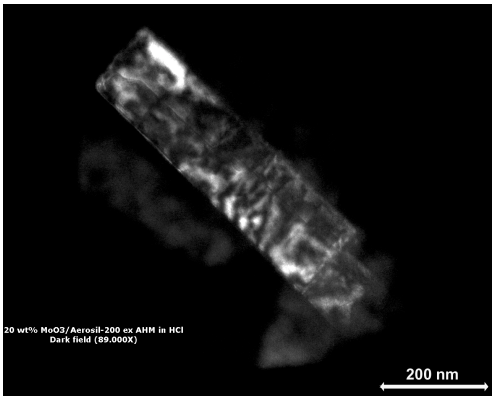

Figure 5: Dark-field TEM image of the MoO_3 platelets. The white parts demonstrate the crystalline nature of the platelets.

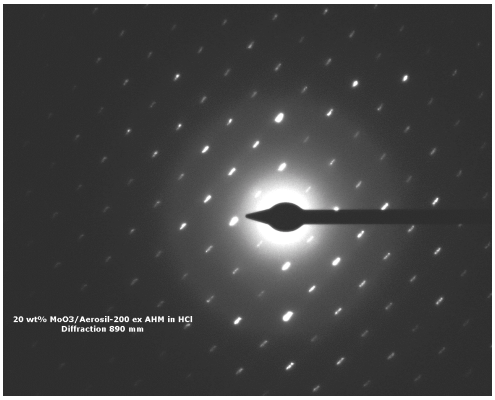

Figure 6: Electron diffraction pattern of the three platelets of figure 4. Every diffraction spot consists of three contributions

mesopores have disappeared and that a considerable amount of micropores has been generated instead. Therefore, transport of ethane towards molybdena that has not become encapsulated by amorphous silica has to occur *via* these micropores. As a result the transport will be slow, resulting in internal diffusion limitation. Both explanations mentioned above provide evidence for the observed low conversion of ethane over this catalyst, as the accessibility of molybdena is strongly decreased by the collapse of the MCM-41 support structure. In view of these results this catalyst will not be discussed any further in the remainder of this chapter.

The catalysts were studied further in the temperature range between 350 and 425°C in order to obtain information about the reaction mechanism and the number of active sites present and to assess whether diffusion limitation occurs when MCM-41 is used as a support for a catalytically active component. To this end Arrhenius plots were constructed, assuming first order kinetics in ethane, *i.e.*:

$$- d [C_2H_6] / d t = k * [C_2H_6]^{1.00} * [O_2]^{0.00} * [H_2O]^{0.00} \quad (1)$$

with: k = rate constant

Formally this assumption of first order kinetics in ethane is not valid, as it has been shown previously that water produced during the catalytic reaction has an inhibiting effect on the conversion (*i.e.* there is a negative reaction order in water), both for the oxidative dehydrogenation of ethane [1] and the deep oxidation of methane [6, 7]. However, in our experiments ethane is not fed continuously to the reactor, but only as one 8 µl pulse every six minutes. As a result the vapour pressure of water inside the catalyst bed will be almost zero during the reaction and water is therefore not expected to affect the kinetics of ethane oxidation significantly during our experiments.

Equation (1) can be converted into:

$$\ln \ln \{ 1 / (1 - x) \} = - (E_{act,\ app} / R) * (1/T) + \ln k_0 \quad (2)$$

in which:

$$k = k_0 * \exp (-E_{act,\ app} / RT) \quad (3)$$

with: x = fractional conversion (value between 0 and 1)
$E_{act, app}$ = apparent activation energy
R = gas constant
T = temperature (in K)
k_0 = pre-exponential factor

In an Arrhenius plot ln ln {1 / (1-x)} is plotted against 1/T. When the same reaction mechanism is operative over the entire temperature range, it should be possible to draw a straight line through the data points. It follows that the slope of the line equals - $E_{act, app}$ / R. It is frequently observed that the slope of the curve starts to decrease at increasing temperatures, although this decrease of catalytic activity is not accompanied by a change of reaction mechanism. Three processes can be responsible for this behaviour:

1. irreversible deactivation of the catalyst, *e.g.* by the accumulation of (side-) products (*e.g.* coke) at the surface of the active phase, resulting in blocking of the catalytically active sites (*e.g.* [3]).
2. a decrease of the adsorption coefficient of reactants at increasing temperatures, which also gives rise to lower reactant concentrations at the surface of the catalyst.
3. diffusion limitation of reactants and / or products to / from the surface of the active phase.

Next to the determination of the apparent activation energy of the reaction studied, the Arrhenius plot can also be used to obtain information on the number of active sites on the catalyst, since k_0, the pre-exponential factor, is a good measure for this number. A value for ln k_0 is obtained by extrapolating (the straight part of) the Arrhenius curve to 1/T = 0.

Figure 7 presents Arrhenius plots of four MCM-41 supported molybdena catalysts. It is seen that straight lines can be fitted satisfactorily through the data points. For the Aerosil-supported and bulk molybdena catalysts conversion levels were far too low to yield reliable Arrhenius curves in the temperature range studied (*viz.* 350 - 425°C). From the slope of the lines drawn through the data points values for $E_{act, app}$ were calculated, which are presented in table 1. From the high values of $E_{act, app}$ it follows that the catalytic reaction proceeds *via* a redox-type of mechanism. As stated before the molybdena dispersion of the MCM-41 supported catalysts is very high and no crystalline MoO_3 could be detected in the samples. Blaauw established that the conversion levels of ethane over molybdena could be appropriately correlated with the defect concentration of the molybdena active phase, both

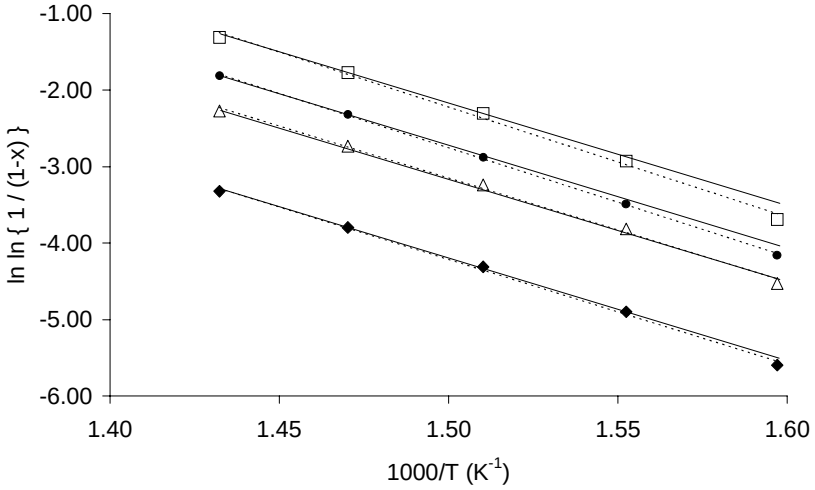

Figure 7: Arrhenius plots, measured between 350 and 425°C, of the following catalysts: ◆ 5 wt% MoO_3/MCM-41 *ex* Mo^{3+}, △ 10 wt% MoO_3/MCM-41 *ex* Mo^{3+}, • 20 wt% MoO_3/MCM-41 *ex* Mo^{3+}, □ 20 wt% MoO_3/MCM-41 *ex* MoO_2Cl_2. Dashed lines are best fits through the data points; full lines are fits constructed with $E_{act,\ app}$ = 113 kJ mol^{-1}.

for catalysts displaying high and low MoO_3 dispersions [3]. Because of the high values for $E_{act,\ app}$ and the absence of a crystalline MoO_3 phase it is very likely that with our catalysts catalysis will take place at defect sites too. Therefore we think that the elementary steps occurring during catalysis can most suitably be described by a pseudo-redox mechanism in which defects act as the catalytically active sites (*vide supra*).

The Arrhenius plots were also used to determine the approximate amounts of active sites on the catalysts studied. To this end an average value for $E_{act,\ app}$ of 113 kJ mol^{-1} was used to fit straight lines through each series of data points. These lines are included in figure 7. It is seen that there is a satisfactory agreement between the measured data points and the fits. From the extrapolations of these lines to 1000/T = 0 values for the pre-exponential factors could be derived. These values have also been included in table 1 and

Table 1: Activation energies and pre-exponential factors for a number of selected catalysts.

catalyst	$E_{act,\ app}$ (kJ mol^{-1})	k_0 #
5 wt% MoO_3/MCM-41 *ex* Mo^{3+}	110	$1.02*10^7$
10 wt% MoO_3/MCM-41 *ex* Mo^{3+}	107	$2.95*10^7$
15 wt% MoO_3/MCM-41 *ex* Mo^{3+}	113	$2.64*10^7$
20 wt% MoO_3/MCM-41 *ex* Mo^{3+}	114	$4.35*10^7$
25 wt% MoO_3/MCM-41 *ex* Mo^{3+}	113	$4.77*10^7$
20 wt% MoO_3/MCM-41 *ex* MoO_2Cl_2	113	$7.87*10^7$

Calculated from Arrhenius curves fitted through the data points with $E_{act,\ app}$ = 113 kJ mol^{-1} (full lines in figure 7).

have been plotted as a function of catalyst loading in figure 8. The line fitted through the data points in figure 8 indicates that there is a good[1] linear correlation between catalyst loading and k_0, despite the influence of the 10 wt% catalyst, which exhibits a relatively high value of k_0. The linear correlation proves that the dispersion of the molybdena active phase remains invariably high, irrespective of catalyst loading. This feature should be attributed to the very high surface area of the MCM-41 support material, which enables molybdena to be present as well-spread monolayers inside the mesopores, even at the highest MoO_3 loadings.

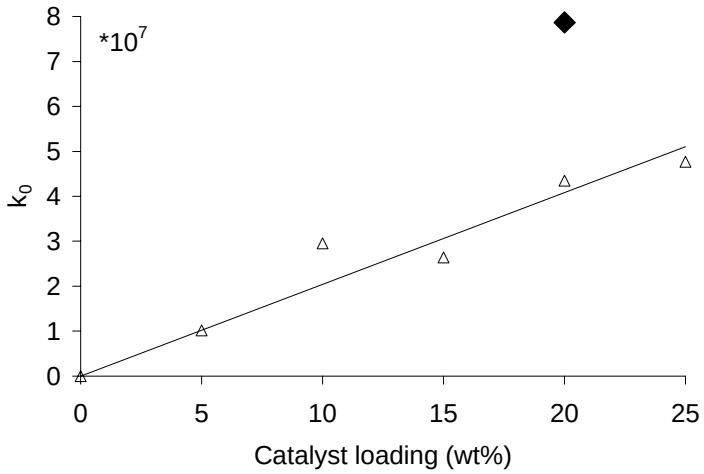

Figure 8: k_0 as a function of catalyst loading for: △ the MoO_3/MCM-41 *ex* Mo^{3+} series and ◆ 20 wt% MoO_3/MCM-41 *ex* MoO_2Cl_2.

When the two 20 wt% MoO_3/MCM-41 catalysts prepared *via* incipient wetness impregnation with different molybdenum precursors are compared it is seen that there is a large difference in the number of active sites on these catalysts. This difference was not noted previously with other characterisation techniques. The most probable explanation for this finding is that the interaction of the MoO_2Cl_2 precursor with the all-silica MCM-41 support differs from that of the Mo^{3+} precursor, which results in a higher precursor dispersion after catalyst preparation with MoO_2Cl_2. This higher dispersion is retained

[1] It should be noted that only a limited number of data points were used to construct the Arrhenius curves and that a small adjustment of the slope of the curves has a rather pronounced effect on the value of k_0 (since extrapolation of the curves to 1000/T = 0 gives the value of **ln** k_0). Therefore, in view of this rather strong dependency an optimisation of the value of $E_{act,\ app}$ with which the data points are fitted and an increase of the number of measurements could result in a better correlation between catalyst loading and k_0. However, such an optimisation has not been pursued here. Still, despite these constraints the correlation shown in figure 8 can be regarded as reliable.

upon calcination. This explanation implies that with MoO_2Cl_2 more mono- and oligomolybdate species are obtained after calcination, whereas with Mo^{3+} more polymolybdate material is formed. Another (more tentative) possibility is that active phases with different defect concentrations are obtained with different precursors. Both explanations account for the fact that with other techniques no differences between catalysts prepared *via* the two different methods are apparent. A spectroscopic characterisation of the catalysts will probably provide more insight into this matter.

Here, it should be noted that catalyst preparation with another all-silica support, *viz.* Aerosil-200, and MoO_2Cl_2 as a precursor gave rise to a notably different result, as a catalyst with a very low MoO_3 dispersion was obtained with Aerosil-200 as a support (*vide supra*), in contrast to MCM-41. This difference should mainly be attributed to the special nature of the MCM-41 support, which presents a much larger surface area for interaction with the MoO_2Cl_2 precursor than Aerosil-200. In addition, we allude to the possibility that the confinement of the precursor inside the mesopores of MCM-41 prevents the generation of sufficiently large, stable nuclei necessary for the formation of the platelets observed after catalyst preparation with an Aerosil-200 support. Further research is advocated to verify this assumption.

Finally, the possible occurrence of diffusion limitations with our MCM-41 supported catalysts was also assessed. The high values for the apparent activation energies for the oxidation of ethane, included in table 1, indicate that our MCM-41 supported molybdena catalysts are not subject to internal diffusion limitation, as such a situation would have resulted in notably lower values for $E_{act,\ app}$. This conclusion is corroborated by the Arrhenius curves, since it can be seen in figure 7 that these curves do not deviate from linear behaviour at increasing temperatures, which also implies that internal diffusion limitation does not occur at temperatures up to 425°C.

Conclusions

In this chapter the influence of MoO_3 dispersion on catalytic behaviour was investigated for a large number of catalysts with different molybdena dispersions. To this end use was made of the catalytic oxidation of ethane, which proved to be a valuable test reaction.

MCM-41 supported MoO_3 catalysts exhibiting a high dispersion were found to be highly active for ethane oxidation, although selectivities towards ethene were low. A kinetic characterisation revealed that oxidation proceeded *via* a redox-type mechanism. However, since MoO_3 supported by MCM-41

does not exhibit a three-dimensional lattice from which oxygen can be removed, the catalytic reaction is thought to take place at defect sites of the active phase. Therefore catalysis is assumed to proceed *via* a so-called pseudo-redox mechanism.

A determination of the pre-exponential factor, which is a measure for the number of active sites, for the MCM-41 supported catalysts indicated that there is a linear relationship between molybdena loading and the number of active sites for catalysts prepared with Mo^{3+} as a precursor. This finding implies that up to MoO_3 loadings as high as 25 wt% the dispersions do not decrease. A catalyst prepared with MoO_2Cl_2 as a precursor showed a notably larger number of active sites, which indicates that the precursor affects either the dispersion of the resulting MoO_3 active phase or its defect concentration or both.

From Arrhenius curves and the high values of $E_{act,\ app}$ it was concluded that the MCM-41 supported catalysts do not suffer from internal diffusion limitations, which is an attractive feature. Nevertheless, it should be noted that the oxidation of ethane was only a (valuable) test reaction, since the instability of the all-silica MCM-41 framework towards steam will most likely exclude the application of this type of catalysts in oxidation catalysis.

Non-MCM-41 supported catalysts with lower dispersions of the molybdena active phase showed a considerably lower activity in the oxidation of ethane, although the selectivity towards ethene was notably higher. Due to the limited activity kinetic data could not be determined for these catalysts. Nevertheless, other characterisation techniques indicated that an Aerosil-200 supported catalyst prepared with MoO_2Cl_2 as a precursor exhibited large platelets of MoO_3 after calcination. This observation implies that although successful for the preparation of MCM-41 supported catalysts, this precursor does unfortunately not yield catalysts with high molybdena dispersions when silica with a (relatively) low surface area is used as a support.

Acknowledgements

Professor Geus is very kindly acknowledged for the supervision of the research presented in this chapter and for making the beautiful TEM images. Dr. Robert Jonker and Pieter Schreuder are kindly thanked for enabling and performing the catalytic experiments at the Department of Combinatorial Catalysis of Akzo Nobel's Catalysts Division. Ad Mens and Vincent Koot are kindly thanked for characterisation of the catalysts.

Literature

[1] M.B. Ward, M.J. Lin and J.H. Lunsford, *J. Catal.*, 50, 1977, 306

[2] T-J. Yang and J.H. Lunsford, *J. Catal.*, 63, 1980, 505

[3] R.J. Blaauw, *Ph.D. Thesis*, Utrecht University, The Netherlands, 1997, chapter 2

[4] J. van de Berg, A.J. van Dillen, J. van der Meijden and J.W. Geus, in: *Surface Properties and Catalysis by Non-Metals* (J.P. Bonnelle *et al.*, eds.), 1983, 493

[5] J. van de Berg, *Ph.D. Thesis*, Utrecht University, The Netherlands, 1984

[6] J.C. van Giezen, F.R. van den Berg, J.L. Kleinen, A.J. van Dillen and J.W. Geus, *Catal. Today*, 47, 1999, 287

[7] J.C. van Giezen, *Ph.D. Thesis*, Utrecht University, The Netherlands, 1997, chapters 3 and 4

Summary, Conclusions and Recommendations

This thesis describes the use of MCM-41 as a support material for heterogeneous catalysts. MCM-41 is an ordered, mesoporous material displaying a honeycomb-like arrangement of narrow mesopores (diameter ~ 3 nm), which are separated by very thin (~ 1 nm) pore walls composed of amorphous silica. Both the synthesis and properties of MCM-41 are described in some detail in **chapter 2**. The very interesting physical properties of this material, *viz.* large surface area and pore volume as well as mesoporosity, make MCM-41 suited for application as a support material for heterogeneous catalysts. Unfortunately, as a result of the very thin pore walls the stability of MCM-41 towards certain (solutions of) precursors of the catalytically active phase is very limited. However, this feature makes MCM-41 ideally suited to serve as a model mesoporous support material for fundamental research aimed at the development of highly dedicated methods for the application of precursors of active phases onto a wide variety of mesoporous supports.

In view of some interesting anticipated applications the preparation of MCM-41 supported heterogeneous nickel and molybdenum catalysts has been pursued in this thesis. The main research objective was the development of relatively simple and reproducible preparation methods, which preserve the interesting properties of the MCM-41 support material and which yield catalysts with high dispersions of active phase. Another point of interest was to assess whether diffusion limitations occur when the resulting materials are used as catalysts.

The application of nickel / nickel oxide inside the mesopores of all-silica MCM-41 is described in **chapter 3**. It is shown that incipient wetness impregnation with a common nickel nitrate precursor yields catalysts with a low dispersion of active phase after drying and calcination. It is anticipated that there is only a weak interaction between the nickel precursor and the support material and as a result a considerable amount of nickel nitrate is entrained with the flow of solvent during drying following impregnation, giving

rise to the deposition of large crystallites of nickel nitrate outside the mesopores of MCM-41. Recent research indicates that subsequent calcination treatments of catalysts *ex* nitrate could also contribute to the observed low dispersions. Therefore further research is advocated to study the influences of both drying and calcination on the dispersion of the resulting catalysts in more detail. Despite the unfavourable processes occurring during drying and calcination a small amount of nickel nitrate is retained inside the mesopores and as a result thus prepared catalysts exhibit a broad particle size distribution with large particles next to the MCM-41 support and very small nanoparticles situated inside the mesopores.

The use of aqueous solutions containing nickel ions chelated by citrate ligands yields Ni(O)/MCM-41 catalysts of a notably higher dispersion, containing exclusively small nanoparticles, which are situated inside the mesopores of MCM-41. The beneficial effect of the nickel precursor on the dispersion of the resulting catalysts is attributed to the film-forming abilities of the impregnated nickel citrate solution during drying. A large viscosity increase of the impregnated precursor solution upon drying inhibits redistribution of nickel citrate. Moreover, the chelating ligands interact with the silica pore walls *via* hydrogen bonding, thus further immobilising the precursor compound. As a result a thin film of nickel citrate has formed on the mesopore surface after drying. During a subsequent calcination treatment the thin film breaks up and citrate ligands combust without destroying the structure of the support material, thereby yielding NiO/MCM-41 catalysts with a high dispersion of nickel oxide nanoparticles confined exclusively inside the mesopores.

In **chapter 4** a new method, involving a reduced Mo^{3+} precursor, has been developed for the preparation of MoO_3 catalysts supported by all-silica MCM-41. Solutions containing Mo^{3+}-chloride complexes are obtained by electrochemical reduction of suspensions containing a hexavalent molybdenum precursor in a 1 : 1 mixture of water and hydrochloric acid. The Mo^{3+} precursor solutions are impregnated onto MCM-41 *via* the incipient wetness technique. After drying and calcination the resulting catalysts exhibit a very high dispersion of MoO_3, which is present as (incomplete) monolayers inside the mesopores of the MCM-41 support. This behaviour is opposed to the normally encountered weak interaction between silica and molybdena and its precursors, which results in MoO_3/SiO_2 catalysts of notably lower dispersions. It should be stressed that the favourable properties of the MCM-41 support material are completely retained upon catalyst preparation

with Mo^{3+}. Moreover, molybdena loadings of the resulting catalysts are high, *viz.* up to 25 wt% MoO_3.

Although satisfactory results were obtained with the new preparation method described in chapter 4, another method, making use of a hexavalent molybdenum precursor species, is presented in **chapter 5**. The precursor is obtained by dissolution of ammonium heptamolybdate (AHM) in a 1 : 1 mixture of water and hydrochloric acid. A thus prepared solution contains MoO_2Cl_2 as the precursor species. Incipient wetness impregnation of the MoO_2Cl_2 solutions onto all-silica MCM-41 also yields MoO_3/MCM-41 catalysts with unprecedented high loadings and dispersions of molybdena, which is present as (incomplete) monolayers inside the mesopores of the support material. Also with this precursor the unique structure of the support material is retained. These results, obtained with MoO_2Cl_2, strongly deviate from the behaviour displayed by MCM-41 towards another hexavalent molybdenum precursor, which is very commonly used for catalyst preparation, *viz.* an aqueous solution of AHM. With AHM complete destruction of the ordered mesoporous support material occurs, resulting in the formation of a non-ordered microporous material. An explanation for the findings is presented, which takes into account the reactivity of both types of precursor towards silica. Further research is recommended to elucidate the exact reaction mechanism by which AHM and silica react and the species that are involved in this mechanism.

Finally, in **chapter 6** the catalytic properties of the prepared MoO_3/MCM-41 catalysts are tested in the oxidation of ethane. MCM-41 supported molybdena catalysts show much higher levels of conversion than reference catalysts with equal molybdena loadings, but which exhibit notably lower MoO_3 dispersions. From a kinetic evaluation of catalyst performance it is suggested that catalysis takes place *via* a pseudo-redox mechanism in which structural defects constitute the active sites. Apparent activation energies are in the order of 110 kJ mol^{-1}, indicating that internal diffusion limitations do not occur. This finding was corroborated by the fact that constructed Arrhenius plots were linear up to 425°C. Values for the pre-exponential factor, derived from the Arrhenius plots, increase linearly with MoO_3 loadings up to 25 wt%, indicating that molybdena dispersions are invariably high for all catalysts tested, although catalyst preparation with MoO_2Cl_2 yields a considerably higher value for k_0 than catalyst preparation with Mo^{3+} (at equal molybdena loadings). A spectroscopic investigation is recommended to explain the observed difference.

Furthermore, it is interesting to note that catalyst preparation with a solution of MoO_2Cl_2 precursor is not successful with all-silica support materials exhibiting notably lower surface areas than MCM-41. Homogeneous nucleation is thought to bring about the formation of large platelets of MoO_3 and as a result thus-prepared catalysts display low dispersions and concomitant low conversion levels.

Summarising, the development of new methods for the application of nickel and molybdenum precursors inside the mesopores of MCM-41 has been successful. The resulting catalysts displayed high dispersions of active phase, while the unique structure of the support material was completely retained. Moreover, diffusion limitations during catalysis did not occur.

For future work a number of interesting research questions remain, relating to the topics described in this thesis. From a fundamental point of view it is interesting to know whether nickel and molybdenum can be applied together onto MCM-41, with a high dispersion and retention of the support structure. Furthermore, the possibility of the generation of nickel- or cobalt-promoted MoS_2 inside the mesopores of MCM-41 remains illusive and future research can provide insight into this matter. Also, in view of the results presented in chapter 6 spectroscopic investigations of the catalysts (*e.g.* with EPR and Raman spectroscopy and ideally combined with catalysis results) will provide a more detailed picture of the structure of MoO_3 inside the mesopores of MCM-41. Finally, the MCM-41 supported nickel catalysts prepared with a citrate precursor could prove to be valuable materials for fundamental studies on nanoparticles, *e.g.* with (S)TEM-EELS measurements.

Samenvatting, Conclusies en Aanbevelingen

Dit proefschrift beschrijft het gebruik van MCM-41 als dragermateriaal voor heterogene katalysatoren. MCM-41 is een mesoporeus materiaal met een geordende structuur. De mesoporiën, met een diameter van ongeveer 3 nm, liggen gerangschikt als in een honingraat en worden van elkaar gescheiden door zeer dunne wandjes van amorf silica (ongeveer 1 nm dik). Zowel de synthese als de eigenschappen van MCM-41 worden in **hoofdstuk 2** beschreven. De interessante texturele eigenschappen, zoals een groot specifiek oppervlak en porievolume, alsmede de mesoporositeit, maken MCM-41 zeer geschikt als dragermateriaal voor heterogene katalysatoren. Door de dunne poriewandjes is MCM-41 echter niet bestand tegen sommige precursoroplossingen die gebruikt worden tijdens katalysatorbereiding. Het feit dat MCM-41 vaak "instort" tijdens katalysatorbereiding maakt het wel bij uitstek geschikt om als standaardmateriaal te dienen voor fundamenteel onderzoek dat er op gericht is om aangepaste katalysatorbereidingsmethoden te ontwikkelen voor mesoporeuze materialen.

In verband met enige verwachte toepassingen is er voor gekozen de bereiding van MCM-41 gedragen heterogene nikkel- en molybdeen-katalysatoren te bestuderen. Het hoofddoel hierbij was de ontwikkeling van (relatief) eenvoudige en reproduceerbare katalysatorbereidingsmethoden, die voorkomen dat MCM-41 instort en waarmee hoge beladingen van actieve fase verkregen kunnen worden. Verder is bestudeerd of diffusielimitering optreedt tijdens katalytische toepassing van de gemaakte materialen.

Het aanbrengen van nikkel / nikkeloxide in de mesoporiën van all-silica MCM-41 wordt beschreven in **hoofdstuk 3**. Droge impregnatie met een nikkelnitraatprecursor resulteert na drogen en calcineren in katalysatoren met een lage dispersie. Waarschijnlijk is er slechts een geringe mate van interactie tussen het dragermateriaal en nikkelnitraat, waardoor tijdens drogen een aanzienlijke hoeveelheid nikkelnitraat meegevoerd wordt met het oplosmiddel. Het gevolg hiervan is dat er grote nikkelnitraatkristallieten buiten

de mesoporiën van MCM-41 neerslaan. Recent onderzoek heeft laten zien dat processen die optreden tijdens het calcineren van katalysatoren ex nitraat ook kunnen bijdragen aan het verlagen van de dispersie van de actieve fase. Daarom wordt vervolgonderzoek naar de precieze invloed van drogen en calcineren op de dispersie aanbevolen. Ondanks de nadelige droog- en calcinatie-effecten, blijft een gedeelte van het geïmpregneerde nikkelnitraat achter in de mesoporiën van MCM-41, zodat uiteindelijk een katalysator met een brede deeltjesgrootteverdeling verkregen wordt: in de mesoporiën bevinden zich zeer kleine nanodeeltjes, terwijl buiten de poriën grote kristallieten gevormd zijn.

Het gebruik van een waterige oplossing van nikkelcitraat resulteert na impregneren, drogen en calcineren in MCM-41 gedragen nikkelkatalysatoren met een aanzienlijk hogere dispersie. Er worden alleen nikkeloxide nanodeeltjes gevormd, die zich uitsluitend in de mesoporiën bevinden. De gunstige invloed van de nikkelprecursor moet toegeschreven worden aan de filmvormende eigenschappen tijdens drogen. Door een grote viscositeit-toename wordt herverdeling van de precursor tegengegaan, terwijl de chelerende liganden de nikkelcomplexen aan de poriewanden binden d.m.v. waterstofbruggen. Hierdoor wordt tijdens drogen een dunne film van nikkelcitraat op het mesoporieoppervlak afgezet. Tijdens calcineren worden de chelerende citraatliganden verbrand zonder dat de structuur van het MCM-41 dragermateriaal instort. Het gevolg is dat een materiaal verkregen wordt dat uitsluitend nanodeeltjes in de mesoporiën bevat.

Voor de bereiding van all-silica MCM-41 gedragen molybdeenoxide-katalysatoren is in **hoofdstuk 4** een nieuwe methode ontwikkeld, waarbij gebruik gemaakt wordt van een gereduceerde Mo^{3+} precursor. Suspensies van een zeswaardige molybdeenprecursor in een 1 : 1 oplossing van zoutzuur en water worden electrochemisch gereduceerd, waardoor oplossingen met Mo^{3+}-chloride complexen worden verkregen. Deze oplossingen zijn gebruikt voor droge impregnatie van MCM-41. Na drogen en calcineren is molybdeen-oxide hoogdispers aanwezig in de mesoporiën van het dragermateriaal, waar het incomplete monolagen gevormd heeft. Deze resultaten zijn tegengesteld aan de normaal waargenomen zwakke interactie tussen silica en molybdeen-oxide, welke meestal aanleiding geeft tot MoO_3/SiO_2 katalysatoren met een lage dispersie. Verder dient nadrukkelijk vermeld te worden dat het MCM-41 materiaal niet instort met de hier ontwikkelde bereidingsmethode en dat de molybdeenoxidebelading van de bereide katalysatoren zeer hoog is, nl. 25 gewichtsprocent MoO_3.

Hoewel met de bereidingsmethode uit hoofdstuk 4 zeer bevredigende resultaten verkregen werden, wordt in **hoofdstuk 5** een andere, eenvoudigere methode beschreven, waarbij gebruik gemaakt wordt van een zeswaardige molybdeenprecursor. De precursor wordt verkregen door ammoniumheptamolybdaat (AHM) op te lossen in een 1 : 1 mengsel van zoutzuur en water en bestaat uit MoO_2Cl_2-complexen. Door droge impregnatie van all-silica MCM-41 met deze precursoroplossingen worden wederom MoO_3/MCM-41 katalysatoren met hoge molybdeenoxidebeladingen en -dispersies verkregen. Ook met deze methode stort de MCM-41 structuur niet in en worden incomplete monolagen van molybdeenoxide afgezet in de mesoporiën van de drager. De resultaten die behaald worden met de zeswaardige MoO_2Cl_2-precursor staan in schril contrast met resultaten verkregen na droge impregnatie met een andere veelgebruikte zeswaardige molybdeenprecursor, nl. AHM. Met AHM stort de structuur van het geordende, mesoporeuze MCM-41 volledig in en wordt een ongeordend microporeus materiaal gevormd. Voor deze verschillen wordt een verklaring gegeven, waarbij de reactiviteit van beide precursors t.o.v. silica in ogenschouw wordt genomen. Verder onderzoek wordt aanbevolen om het precieze reactiemechanisme van AHM met silica op te helderen en om te bestuderen welke verbindingen bij de reacties betrokken zijn.

Tenslotte worden in **hoofdstuk 6** de katalytische eigenschappen van verscheidene molybdeenoxidekatalysatoren getest d.m.v. de oxidatie van ethaan. MCM-41 gedragen molybdeenoxidekatalysatoren vertonen veel hogere conversies dan referentiekatalysatoren met een zelfde molybdeen-oxidebelading, maar met lagere dispersies. Een kinetische beschouwing laat zien dat katalyse waarschijnlijk verloopt via een pseudo-redoxmechanisme, waarin defecten in de structuur van de actieve fase de actieve sites vormen. Schijnbare activeringsenergieën liggen rond 110 kJ mol^{-1}, hetgeen een aanwijzing is dat er geen interne transportbelemmering plaatsvindt. Dezelfde conclusie werd getrokken uit het rechte verloop van de Arrheniuscurven tot 425°C. Met de Arrheniuscurven werden ook pre-exponentiële factoren, k_0, bepaald. Het blijkt dat k_0 recht evenredig toeneemt met de molybdeenoxide-belading van de MoO_3/MCM-41 katalysatoren, zodat gesteld kan worden dat de dispersie van de actieve fase onveranderlijk hoog is tot en met een molybdeenoxidebelading van 25 gewichtsprocent. Katalysatorbereiding met MoO_2Cl_2 levert overigens een aanzienlijk hogere waarde voor k_0 op dan bereiding met Mo^{3+} (bij eenzelfde molybdeenoxidebelading). Een verklaring

hiervoor zou verkregen kunnen worden na verder onderzoek van de katalysatoren met spectroscopische technieken.

Verder is gebleken dat katalysatorbereiding met MoO_2Cl_2 niet succesvol is als een all-silica dragermateriaal met een aanzienlijk lager specifiek oppervlak wordt gebruikt. Er worden namelijk grote molybdeenoxide-plaatjes gevormd, waarschijnlijk door homogene kieming in de precursor-oplossing. Het gevolg hiervan is dat de dispersie en ethaanconversie van deze katalysatoren laag is.

Samenvattend kan gesteld worden dat de ontwikkeling van nieuwe bereidingsmethoden voor het afzetten van nikkel en molybdeen in de meso-poriën van MCM-41 succesvol is gebleken. De gemaakte katalysatoren vertonen een hoge dispersie van de actieve fase en de structuur van het dragermateriaal stort niet in. Tevens is gebleken dat tijdens katalyse geen transportbelemmeringen optreden.

Voor toekomstig werk aan de beschreven materialen blijft echter een aantal interessante onderzoeksvragen over. Zo is het interessant om te onderzoeken of het mogelijk is om nikkel en molybdeen samen, met een hoge dispersie, op MCM-41 af te zetten zonder dat de dragerstructuur instort. Daarnaast dient de mogelijke vorming van nikkel- of cobaltgepromoteerd MoS_2 in de mesoporiën van MCM-41 onderzocht te worden. Verder geven de resultaten uit hoofdstuk 6 aanleiding tot een spectroscopische karakterisering van de MCM-41 gedragen molybdeenoxidekatalysatoren (bijvoorbeeld met ESR of Raman-spectroscopie), zodat meer inzicht in de structuur van de molybdeenoxidefase verkregen wordt. Tenslotte zijn de nikkelkatalysatoren bereid met een nikkelcitraatprecursor interessante materialen voor fundamenteel onderzoek aan nanodeeltjes, bijvoorbeeld met (S)TEM-EELS.

Dankwoord

Hoe een dankwoord goed te beginnen? Toen ik voor hoofdstuk 5 uitzocht wat voor molybdeenprecursor ik nou eigenlijk precies gemaakt had, stuitte ik op een boek van J.W. Mellor [1], dat begon met deze prachtige woorden:

Dedicated
TO THE
PRIVATES IN THE GREAT ARMY
OF WORKERS IN CHEMISTRY
THEIR NAMES HAVE BEEN FORGOTTEN
THEIR WORK REMAINS

Hoewel het zeer te betwijfelen valt of het werk beschreven in dit proefschrift de tand des tijds zal doorstaan, wil ik middels dit dankwoord de gelegenheid te baat nemen alle "soldaten" die in de oorlog mee hebben gevochten zéér hartelijk te bedanken voor alle geleverde inspanningen en het enthousiasme waarmee vaak ten strijde werd getrokken. Opdat jullie níet vergeten worden!

Ten eerste wil ik, nu op minder militaristische wijze, mijn co-promotor Jos van Dillen bedanken voor de zeer prettige begeleiding en vele steun gedurende de afgelopen jaren. Beste Jos, waarschijnlijk zul je wel eens (?) gek van me zijn geworden, maar altijd weer wist je het onderzoek / mij in goede banen te leiden. Jouw prachtig flegmatieke manier van doen en laten hielp daarbij zeer. Het was een groot voorrecht om je als co-promotor te hebben. Het ga je goed! (Maar blijf uitkijken voor plotseling overstekende uitlaten).

Mijn promotor, Krijn de Jong, wil ik bedanken voor de geboden mogelijkheid het hier beschreven onderzoek uit te kunnen voeren. De grote

mate van vrijheid hierbij stelde me in staat me vooral bezig te houden met mijn geliefde onderwerp van katalysatorbereiding, waarvoor mijn dank. En hoewel we het redelijk vaak niet met elkaar eens waren, waardeer ik de manier waarop we e.e.a. toch afgerond hebben zeer. Vooral jouw niet aflatende enthousiasme zal ik niet snel vergeten.

Professor Geus, hoewel u al jaren actief bent in de katalyse, heeft het me veel deugd gedaan dat u ook zelf wel eens de rol van katalysator speelt. U heeft de activeringsenergie voor het gereedkomen van dit proefschrift nl. aanzienlijk verlaagd. Heel hartelijk bedankt voor alle bemoeienissen op katalysegebied, het vele TEM-werk en de vele prettige discussies over o.a. chemie en sport!

Twee mensen die op deze plaats in de opsomming niet mogen ontbreken, o.a. vanwege hun vele steun en hulp bij het onderzoek, zijn Jules "jajajajaja…..absolute topper!!!" Roelofs [2] en Ellart "toedeledoki!" de Wit. Jules, hartelijk bedankt voor de vele bemoedigende woorden door de jaren heen, je vriendschap en je (vele) pogingen mij enig relativeringsvermogen bij te brengen. Verder mag ook je rol als gangmaker bij vele activiteiten, zowel binnen als buiten de vakgroep, niet onvermeld blijven. Hoewel ik soms wens dat je me nooit backgammon geleerd had, hoop ik dat we samen nog veel leuke dingen zullen doen (zolang het maar niet nog meer prullaria voor aan de muur oplevert). Ellart, jij was de laatste echte ontzwavelaar en in die hoedanigheid heb ik veel van je geleerd. Ik kon altijd op je terugvallen bij problemen met de opstelling en / of LabView en je had ook altijd een bemoedigend woord klaar als ik het weer eens niet zag zitten. Mijn dank is groot.

Twee personen aan wie ik ook zeer veel te danken heb, zijn "m'n grote jongen en m'n kleine meid". Oftewel mijn hoofdvakstudenten Gerbrand Mesu en Jeannette Smulders. Hoewel twee hoofdvakstudenten in 4½ jaar misschien wat weinig lijkt, prijs ik me zeer gelukkig dat uitgerekend jullie twee bij mij wilden afstuderen. Jullie inzet en betrokkenheid waren nl. voortreffelijk en hebben geleid tot een aantal zeer waardevolle bijdragen aan dit proefschrift. Kers op de taart was dat jullie daarnaast ook nog eens twee zeer fijne persoonlijkheden zijn, zodat ik ontzettend heb genoten van de samenwerking. Jeannette, ik wil je ook nog speciaal bedanken voor onze gezamenlijke wandelingen: ik heb Jules zelden zo jaloers gezien! Af en toe een etentje en we blijven mailen! Houdoe. Gerbrand, zelfs na je periode bij mij had je nog niet genoeg van universitair onderzoek en dus werd je collega-

AIO. Dat vond ik zeer aangenaam, maar nog mooier is dat we een vriendschap voor het leven gekregen hebben. Bedankt voor je vele steun en diepzinnige gesprekken van de afgelopen jaren! Ik ben blij dat je naast me wilt zitten tijdens de verdediging van dit boekje.

In het kader van diverse practica heb ik ook nog een aantal andere studenten mogen begeleiden. In chronologische volgorde waren dat Adri (A_3) van Laak & Alwies van der Heijden (A&A), Mayken Wadman & Joke Ferwerda en Birgit Wieczorek & Marcel Peterse. Dames en heren, door jullie enthousiasme en inzet werden het steeds drie zeer plezierige weken. Het practisch werk was nogal eens lastig, omdat jullie vaak de eer te beurt viel om een hele nieuwe syntheseroute uit te proberen. Maar die probeersels hebben uiteindelijk toch maar mooi geleid tot twee hoofdstukken in dit proefschrift.

Verder wil ik ook nog mijn "adoptiestudent" bij Akzo Nobel, John Sitters, bedanken voor de prettige samenwerking en het mij wegwijs maken in de wereld van de inzwaveling. John, veel succes gewenst bij het afronden van het werk.

Twee prachtige scripties werden geschreven door Marjoleintje Toebes en Bas Tappel. Ik heb er heel veel van geleerd en ik dank ook jullie voor de plezierige wijze waarop e.e.a. tot stand kwam.

Een groot aantal uitstekende studenten, alsmede goede begeleiding zijn echter niet genoeg om een onderzoek succesvol uit te kunnen voeren. Het karakteriseren van de gemaakte materialen is zo mogelijk nog lastiger en ik ben dan ook veel mensen dankbaar voor het uitvoeren van een heleboel metingen, alsmede het op orde houden / brengen van de apparatuur die daarvoor noodzakelijk is. De meest in het oog springende techniek is natuurlijk electronenmicroscopie en ik dank alle mensen die hier bij betrokken zijn geweest. Henk Pluijgers, bedankt voor het in perfecte staat houden van de microscopen en de sympathieke manier waarop je me vaak te hulp schoot achter de CM-10. Cor van der Spek, jij maakte een begin met de karakterisering van de Ni(O)/MCM-41 materialen en al gauw bleek dat deze helaas niet erg stabiel waren in de electronenbundel. Toch kreeg je het voor elkaar een aantal schitterende foto's te produceren, waarvoor dank. Een zo mogelijk nog moeilijkere taak was weggelegd voor Sandra Kemp tijdens het onderzoeken van MoO_3/MCM-41, dat nog instabieler was. Sandra, ik bewonder je doorzettingsvermogen tijdens de vele, vele uren achter de microscoop. Zelfs een brandje in het Kruyt kon je er niet van weerhouden de

monsters te onderzoeken. Hulde! Tenslotte wil ik in dit rijtje Hans Meeldijk bedanken voor het toepasbaar maken van de low-dose techniek, waardoor de materialen een stuk beter geanalyseerd kunnen worden, alsmede voor het uitvoeren van een groot aantal uiterst waardevolle EDX metingen. Hans, ik dank je en ik hoop dat je in de toekomst nog veel meer mooie MCM-plaatjes zult maken.

Marjan Versluijs-Helder wil ik bedanken voor het mogelijk maken van vele XRD metingen, met name bij kleine hoeken, die vele belangrijke ~~spectra~~ diffractogrammen opgeleverd hebben. Ik was al berucht vanwege m'n experimentele muizenval, maar ik hoop dat jij nog lang plezier zult hebben van m'n andere "high-tech solution" [3]. Vincent Koot bedank ik voor de TPR analyses, Tom Visser en Fouad Soulimani voor hun hulp bij de verkennende Raman experimenten en Fred "het ochtendzonnetje" Broersma voor TGA metingen. Leon Coulier, bedankt voor de XPS analyses van NiO/MCM-41.

Pieter Schreuder en Robert Jonker van Akzo Nobel ben ik zeer veel dank verschuldigd voor de katalytische metingen uit hoofdstuk 6. Katalyse leek lange tijd het breekpunt van het onderzoek te worden, maar dankzij jullie prachtige faciliteiten zijn de monsters toch nog gemeten, hetgeen overigens nog mooiere resultaten opleverde dan waar ik vooraf van had durven dromen. Heren, bedankt voor alle moeite, de plezierige samenwerking en één weekje creatief boekhouden. Ook dank ik Eelco Vogt voor het mogelijk maken van e.e.a. en het mij bekend maken met enige industriële mores.

Zéér veel technische ondersteuning heb ik mogen ontvangen vanuit de werkplaats en electronica. Evert, Henk en Victor, hartelijk bedankt voor alle inspanningen die jullie geleverd hebben tijdens het uitvoeren van diverse reparaties en jullie hulp met de opstelling. Jullie werk is voor mij ontzettend belangrijk geweest (en ik denk niet alleen voor mij). Het spijt me dan ook zeer dat jullie niet meer zo nauw bij de vakgroep betrokken zijn als voorheen, want de samenwerking met jullie vond ik altijd zowel zeer nuttig als aangenaam!

Twee mensen, die ik hierboven nog niet genoemd heb, wil ik speciaal bedanken voor hun ongelooflijke inzet en waardevolle bijdragen aan dit proefschrift. John Raaymakers, het doet me zeer verdriet dat ik jou alleen nog maar postuum kan bedanken voor de fantastische ondersteuning op vele gebieden. Ik geloof niet dat ik ooit eerder iemand heb ontmoet die zich belangeloos zo verschrikkelijk uit de naad werkte voor andere mensen als jij. Hartelijk bedankt voor de vele metingen en de soms compleet onnavolgbare

manier waarop je daarbij te werk ging. Je verbazing toen je voor de eerste keer een MCM-41 gemeten had, zal ik nooit meer vergeten. Ad Mens, ik ben je zeer dankbaar voor de vele stikstofphysisorptie en XPS metingen die je uitgevoerd hebt en bovenal voor het beschikbaar stellen van zoiets simpels als een voedingskastje (anders had dit dankwoord al na hoofdstuk 3 gestaan…). Verder was het ook zeer plezierig dat je altijd te vinden was voor een praatje over het een of ander. Ad, je bent een bovenste beste.

Ook zonder (andere) ondersteunende diensten begin je als AIO niet veel. Daarom wil ik Dymph Savenije, Monique Lamers, Thea Pozzi en Thea van Oosten naast de gezelligheid bedanken voor het afwerken van veel formaliteiten en papierwerk. Dymph, veel plezier met je nikkelcitraat (wees blij dat het geen 20 m^3 is). Monique, leuk dat er soms mensen zijn met dezelfde muziekvoorkeur; veel plezier met luisteren naar Heather en succes met de kruiden.

Jan, Ingrid en Aloys van de AV-Dienst bedank ik voor het maken van vele mooie posters en het regelmatig verbeteren van de lay-out hiervan. Het was altijd prettig om bij jullie langs te gaan en wat ouwe koeien uit de sloot te halen (ik zal geen namen noemen). Met name de foto uit midden jaren '80 was een topper! Aloys, speciale dank voor het maken van de prachtige omslag van dit boekje.

Ook bedank ik alle heren van de glasblazerij, en met name Wim "kwartsblazer" Nieuwenhuis, voor het vervaardigen van vele prachtige apparaten en de plezierige atmosfeer waarin dat gebeurde. Met name de electrolysevaatjes waren kunststukjes waarmee ik zeer verguld was.

En uiteraard bedank ik Fred "het ochtendzonnetje" Broersma ook: voor alle chemicaliën en kwalitatief uitermate tevredenstellende discussies (en af en toe bijna een klomp voor m'n harses). ;-))

Verder wil ik al mijn (ex-)collega-AIO's, studenten en leden van de vaste staf bedanken. Jullie waren en zijn onontbeerlijk voor een goede sfeer op de werkvloer en wat dat betreft lieten jullie je vaak van je beste kant zien. Bedankt voor de gezelligheid, collegialiteit, (vieze) moppen, uitjes, hulp waar nodig en vele legendarische koffiepauzes (**om half vier!!!**) en borrels [4].

Een paar collega's wil ik echter toch nog wat persoonlijker bedanken voor hun betrokkenheid:

Lieve Marije, allereerst bedankt voor het mij bekend maken met Tori. Het schrijven van een proefschrift is een stuk aangenamer met *Scarlet's Walk* vrijwel continu op de achtergrond. Verder wil ik je bedanken voor je empathie en een aantal goede gesprekken. Ik vond het fijn je als collega te hebben en hoop dat we in de toekomst samen af en toe "mooie dingen" blijven doen.

Lieve Marjolein, een naam van een bloem en dan ook nog altijd fleurig en opgewekt zijn! Als een beetje bleu meisje kwam je lang geleden een mooie scriptie voor mij schrijven. Daarna werd je een zeer gewaardeerde collega, met wie ik het zeer fijn samenwerken vond en die niet (meer) op haar mondje gevallen is. Ik bewonder je vanwege je altijd positieve instelling en wens je veel succes en sterkte bij het afronden van je eigen onderzoek. Dankjewel voor alle gezelligheid. (En als ik je nog eens kan helpen met het bekijken van ehh… XRD metingen moet je het maar even laten weten, want dat doe ik graag!)

Lieve , ehh…, Beste Ad, Adje^{E}, Monsieur Moustache, "papa-Ad", jij was vaak een beetje een mentor voor me. Je maakte me wegwijs in de wereld van de anorganische synthese en wilde me altijd met raad en daad terzijde staan. Je was ook bijna [5] altijd goedgeluimd en in voor een vriendelijk praatje. Hartelijk dank voor de fijne samenwerking. Door het waarschijnlijk duurste kopje koffie uit de geschiedenis van de vakgroep verneukte je wel bijna "m'n eerste keer", maar de hete nachten in Grenoble maakten heel veel goed! En nu ik het toch over Grenoble heb: Moniek, ook jij bedankt voor alle gezelligheid. De hele afdeling R&D vond het fijn jou als buurvrouw te hebben.

Lieve Daphne, in de loop der tijd ben je een soort zusje voor me geworden. Ik dank je voor de vele lol die we samen gehad hebben, maar ook voor de intieme gesprekken die we af en toe gevoerd hebben. We voelen dingen vaak op dezelfde manier aan, waardoor je een grote steun voor me bent. Ik hoop dat we in de toekomst zo close blijven en dat we nog veel leuke dingen zullen doen. Ik wens je alle goeds toe.

Eigenlijk zou ik nog wel meer mensen kunnen (moeten) bedanken, maar het dankwoord wordt nu toch wel aan de erg lange kant, dus heb ik maar besloten een aantal zaken / personen, soms leuk, soms niet, uit de afgelopen 4½ jaar samen te vatten onder een kopje curiosa. Degenen die menen zich aangesproken te moeten voelen: bedankt!

Curiosa

De Christelijke Agrarische Hogeschool in Dronten (een less-favoured area, inderdaad ja), Analytisch Chemisch Meten, de traditionele Chinese keuken, Eco-Magic, ESRF, Hongaarse communicatie-technieken,

Diederik K. ("IK BEN ALTIJD LIEF!!!") [6]:

De Labtops (een prachtige traditie in wording), Miss Piggy, NCCCCC enz., een Neanderthaler, de Teammaster en de Tourpool waren vaak een bijzondere aanvulling op het "gewone" AIO-leventje.

Tenslotte wil ik nog een aantal mensen bedanken die minder bij het onderzoek betrokken waren, maar die wel degelijk bijgedragen hebben aan een plezierige periode.

Herr Micha Müller, alias de-man-die-het-voor-elkaar-kreeg-zijn-huis-in-de-hens-te-steken-tijdens-het-ophangen-van-een-schilderijtje, je bent een typisch geval van een ruwe bolster met een blanke pit. Je hebt altijd in no-time de lachers op je hand en weet iedereen op te vrolijken. Ik heb je echter ook leren kennen als iemand bij wie je je hart kunt uitstorten en ik dank je zeer voor je steun in moeilijke periodes. Als ik al je memorabele acties hier moet gaan beschrijven kost me dat minstens vijf bladzijden, dus dat zal ik niet doen, maar ik wil je nog wel bedanken voor de vele leuke dingen die we gedaan hebben (voetbal, concerten, cabaret en nog veel meer). Nu alleen nog wat beter scoren in de Teammaster. Forza!

Emiel, ondanks je tekortkomingen (FC Zwolle-supporter en *organisch* chemicus) ben je een goeie gast. Bedankt voor je regelmatige interesse voor het "zand met gaatjes" en je vriendschap. Ik wens jou en Monica veel succes

met de afronding van jullie promotieonderzoek. Ben benieuwd wat het in Twente bestuder'n van 't afzett'n van monolag'n gaat oplever'n. En voor de komende jaren veel sterkte gewenst met de reizen naar Almelo, Oss, Sittard en Volendam. ;-))

Een andere voetbalsupporter in hart en nieren, Patrick Loffeld, wil ik ook hartelijk bedanken voor zijn vriendschap. Gelukkig heb jij weer meer verstand van voetbal en gaan we daarom regelmatig samen naar de lokale FC. Ook de vele etentjes, spelletjes, onnavolgbare discussies, avondjes uit en het aanleggen van een tuin zal ik niet snel vergeten. Hopelijk blijven we dat ook in de toekomst regelmatig doen (behalve die tuin, alsjeblieft!)

In dit rijtje voetballiefhebbers mag Jan Ebskamp zeker niet ontbreken. Jan, je maakte mijn verblijf op het practicum door jouw aanwezigheid een stuk draaglijker. Bedankt voor de vele aangename discussies over wielrennen, voetbal en andere zaken en het consequent deelnemen aan alle Tourpools.

Na 7½ pagina dankwoord heb ik nu bijna iedereen gehad, maar er is nog één iemand die ik uitzonderlijk hartelijk wil bedanken voor de afgelopen jaren: Ries Janssen, trouwe kamergenoot. Hoe je het in vredesnaam uitgehouden hebt weet ik niet, maar het was mij altijd een genoegen als je er was. Door je rust, gevoel voor humor, steun en vriendschap vond ik het altijd zeer prettig werken op de afdeling R&D. Hoewel het jammer was dat je wel eens vals speelde met computerspelletjes en postersessies, ben je d'r één uit duizenden! Ik hoop dat we samen nog heel veel plezier zullen beleven en ben blij dat je mijn tweede paranimf wilt zijn.

Dennis

[1] J.W. Mellor: "*A Comprehensive Treatise on Inorganic and Theoretical Chemistry*", Volume XI, published by Longmans, Green and Co. Ltd., London, UK, 1931

[2] Ook wel bekend als "Backgammonkoning de Eerste", alias fotorobje.

[3] Party, party bij de XRD!!!

[4] Hoewel ik nog steeds wacht op die ene beloofde **Belgische** bierborrel…..

[5] Alleen niet op Schiphol……? Raar maar waar.

[6] Legendarische uitspraak vlak voor een hoofdvaktentamen.

Curriculum Vitae

Op 4 mei 1974 werd ik geboren te Vlaardingen. Ik was een wolk van een baby en de vlag ging uit. Na de fröbel-, kleuter- en lagere school succesvol te hebben doorlopen begon ik in 1986 met de VWO-opleiding aan de Rijksscholengemeenschap te Oud-Beijerland (of all places…). In 1993 mocht ik na 7 jaar eindelijk het gewenste diploma in ontvangst nemen, waarna ik na lang wikken en wegen besloot Scheikunde te gaan studeren. Ik koos er voor dat te gaan doen in de mooiste stad *in het haartsie van het laand: Utereg me stadje*. Na 1 jaar mocht ik het propaedeuse-diploma in ontvangst nemen en dat deed ik dan ook. Verderop in de studie koos ik als (kleine) bijvakken Anorganische Chemie en Organometaalchemie, om vervolgens af te studeren met als hoofdvak Heterogene Katalyse. Eind augustus 1998 ontving ik mijn doctoraaldiploma. Met genoegen, en dat was wederzijds. Vervolgens werd mij gevraagd mijn verblijf aan de Universiteit Utrecht nog wat te verlengen om onderzoek te doen naar de bereiding van MCM-41 gedragen heterogene katalysatoren. Aangezien dit mij zeer interessant leek, heb ik deze kans met beide handen aangegrepen. Het onderzoek voerde ik van 1-12-1998 tot 1-1-2003 uit binnen de Sectie Anorganische Chemie en Katalyse, onder de bezielende leiding van Dr. Jos van Dillen, Prof. Dr. Ir. John Geus en Prof. Dr. Ir. Krijn de Jong. De meeste resultaten die verkregen zijn in deze periode worden in dit proefschrift beschreven.

…
'O ja?' zei de wolf. 'Zou dat het zijn? Ik dacht dat het kwam door de kool en de geit.'
'Wat? Wat gebeurde er dan met een kool en een geit?'
'Ik heb een keer een kool opgegeten', zei de wolf.
'Een kool? Maar wolven eten toch geen kool?'
'Nee, dat is zo. Maar deze kool zat in een geit. Hij was verpakt in een geit.'
'Aha, je bedoelt dat je een geit hebt opgegeten?'
De wolf knikte. ' Heel lang geleden…', zei hij zacht en hij keek Pluk aan met schaamte in z'n ogen.
'Praten we niet meer over…', zei Pluk.
…

[Uit: *Pluk van de Petteflet, "De heen- en weerwolf"*, Annie M.G. Schmidt]